Modeling of local bond behavior and meso-scale 3D discrete analysis of corroded RC structures

（腐食したRC構造の局所付着モデルの開発
と
三次元メソスケール離散解析）

ジラディロック　パンヤウット

A dissertation submitted to
University of Tokyo
In partial fulfillment on the requirements for
The Degree of Doctor Philosophy

Supervisor
Associate Professor Kohei Nagai

Department of Civil Engineering
University of Tokyo
Tokyo, Japan

August 2018

ABSTRACT

Nowadays, many reinforced concrete structures are exposed to the marine environments which result in chloride ion penetration, subsequently decreasing in structural capacity due to the corrosion. The main problem is we don't know the residual capacity of the deteriorated structure. Therefore, an estimation of internal damage and residual capacity of corroded reinforced concrete is important for maintenance and predicting service life of the structures.

This research aims to develop the numerical system to predict the structure behaviors and residual capacity after the corrosion damage take place based on Rigid Body Spring Model (RBSM).
In this study, first the simulation scheme is divided into two section, the corrosion damage simulation and mechanical loading simulation. The original RBSM model of author's research group already have the ability to predict the structure performance and predict the local damage appropriately. However, the function for introduced the corrosion damage into the model had not been developed yet by the time that the author started this research. Hence, the originality of this research is to develop the simulation model of corrosion behavior in reinforced concrete based on meso-scale 3D discrete and adapt that function into the RBSM program.

The corrosion behaviors that were considered in this study including the non-uniformity of the corrosion pattern, the rebar reduction, the rust expansion and the bond deterioration. By developing these functions one by one and implement into RBSM model, the numerical model for simulating the residual capacity and behavior of corroded RC structure can be achieved.

Firstly, the non-uniform corrosion pattern was considered in RBSM simulation. In reality or even under control condition in experiment room, the corrosion is formed up non-uniformly along the rebar. In RBSM simulation, the rebar reduction area, the expansion of rust and other corrosion behaviors are modeled vary in each location along the rebar location. In this research, the rebar corrosion profile every 5 mm obtained by X-ray photogram technique of previous corroded beam experiment are used as an input information to verify the applicability of the final corrosion model.

Next, the expansion corrosion damage simulation is developed based on expansive strain model. In reality, once the corrosion occurs, it will create the voluminous rust product at the interface between rebar and concrete. As a result, the increment of internal pressure will damage the adjacent concrete. This behavior was simulated in RBSM by expansive strain model. By gradually give the initial strain at the interface between rebar and concrete, the simulation model will calculate the additional stress based on given expansive strain. By this method, the expansion of corrosion product can be simulated in the same manner as reality. However, the relationship between expansive strain at interface and corrosion degree are varied based on environment condition. For example, under fast corrosion i.e. corrosion acceleration test, the corrosion product will form up as liquidity, while the slow corrosion process i.e. in real structure, the corrosion product will form up as solid form which crate more damage to surrounded concrete. Hence, in this study, the inverse method has been used to develop the constitutive model for corrosion expansion. In RBSM simulation, the model with the same dimension, covering depth and material properties is modeled. Then, the expansive strain model gradually gives at the interface for introducing the expansion

damage until the same damage crack width as reality appears in simulation. By this method, the constitutive model for corrosion can be achieved.

In reality, the bond of RC structure consists with mechanical bond from interlocking between rebar and concrete and friction bond at the interface. While the bond in RBSM are represented by the response of normal spring and shear spring at interface between element. When the corrosion take place not only the formation of corrosion product that changes the rebar surface property, the rebar also deformed its shape due to the corrosion. However, in RBSM simulation, the rebar is modeled as rigid body which the shape cannot be deformed. Hence, the equivalent modification of shear spring and normal spring at interface need to be performed for represent the changing of mechanical bond and chemical bond. In this study, the constitutive models of bond deterioration were well developed based on the designed experiment program. The changing of the chemical bond and mechanical bond was extracted from the experiment results and was used for developed the modification factors in shear spring and normal spring. The concrete specimens reinforced with round bar and deformed bar were subjected to the corrosion acceleration test to generate the different corrosion percentage on the reinforcement. The corrosion acceleration electrical current-time were varied in each specimen for obtaining different corrosion percentage. (0, 3, 5,3 and 12.3% in round bar reinforcement and 0, 10.5 and 23.1% in deformed bar specimen). To eliminate the effect of corrosion cracking concrete, the specimen with non-crack concrete were prepared. After the pull-out test on cracked concrete specimen, the cover concrete was removed. The same corroded rebars were used as reinforcement in casting of new specimen. The pull-out tests were performed on non-crack concrete specimen. The pull-out capacity of different corrosion percentage and different type of reinforcement (round bar and deformed bar) were analyzed. The new constitutive model of shear spring and normal spring were proposed based on the changing of maximum pull-out capacities at different corrosion degree.

Finally, the member scale simulations were simulated for verification the applicability of numerical model. By combining all corrosion functions into the program, the corroded beam simulations were simulated by using the real corrosion profiles from previous experiment. The beams simulation with non-uniform corrosion and uniform corrosion are simulated to study the effect of spatial corrosion profiles. Also, the effect of corrosion at the anchorage zone was studied by intentionally set the corrosion profiles at anchorage zone and shear span zone. By introducing the initial damage from corrosion by corrosion models, the stiffness reduction and lower loading capacities of corroded beam were simulated well. The local failure behavior like local cracking, local strain distribution of rebar shows a good agreement with the input corrosion profiles. In conclusion, the numerical model can simulate the stiffness reduction, residual capacity and failure pattern appropriately comparing with the experimental results.

ACKNOWLEDGEMENTS

First of all, I would like to express my heartfelt gratitude to my advisor, Associate Professor Kohei Nagai, for the continuous support of my Doctoral study and related research, for his immense knowledge and great motivation. His guidance always assisted me in all the difficult time of research. This research could not be complete without the kind support from him, supervisor who endured the countless failures and mistakes, and guide me with great patience and kindness.

I would like to give my sincere gratitude to Professor Mitsuyoshi Akiyama, who kindly allow the author used his valuable important experimental results for developing the simulation model. This research would not be complete without those precious data.

The author is grateful to Professor Toshiharu Kishi, Professor Ishida Tetsuya and Professor Tomonori Nagayama, the co-supervisor, for all of their valuable comments and great recommendation in developing the programing in this research.

Living in Japan and conducting research in this laboratory are made easier by the guidance of my foreign senior students, Mr. Liyanto Eddy, who always gives a kind support when the author was in trouble. Thanks are due to Mrs. Tarekegne Biruktawit Taye, foreign labmate, who came to this country at the same time with me and was sharing both happy and difficult time of studying in Japan.

The author would like to express his thanks to his precious brother, Pakawut JIRADILOK, who always give a good mental support during the difficult time in PhD life, and be a good consultant for mathematic problem.

The author would like to take this opportunity to express his gratitude to all of the Department faculty members, FSO staff and civil engineering office staff for their help and support in all documentary matter and.

The government of Japan is acknowledged for awarding the author a MEXT scholarship amongst other many potential candidates to pursue his Doctoral's studies in Japan.

Thankful acknowledge is given to my best friends, senior and junior in Japan, Chananun Chai mongkhol, Pipat Methavanitpong, Punyawat Rojanawisan and Sumet Supprasert, who always come to support mad cheer me up when I was in trouble. Their kindness will remain in my good memory.

Finally, the author thanks his family, father, mother, sister and brothers for the encouragement, support and attention. They tell him what he need to hear, not what he want to hear, always be there for him in the good and bad times.

TABLE OF CONTENTS

Chapter1
Introduction

1.1 Background and statement of problem

Nowadays, there are many reinforced concrete structures that exposed to the marine environments, like the structure in the coastal area and splash zone, which result in chloride ion penetration into the structures, subsequently decreasing in structural capacity due to the corrosion. When the reinforced steel contact with the chloride ion, the reinforce corrosion occur resulting in cracked, spalled, delaminated covering concrete, and the durability of the structure is severely decreased. This phenomenon gradually decreases the structural capacity overtime.

Figure 1.1 spalling of concrete in corroded RC structure [9]

Figure 1.2 Different level of corroded reinforcing bar and corrosion crack from expansion of corroded bar [10,11]

The major problem of the corroded structure is that it is difficult to know to residual capacity after corrosion take place. Due to the corrosion, the material properties of concrete and rebar become different from the original design. So, the mechanical performance of the corroded structure is different from no corrosion structure.

The corrosion damage on RC structure has been investigated through experimental and analytical studies by many research group. One major degradation process of reinforced concrete structure is the corrosion of the steel reinforcement. Not only the reduction of the reinforcing bar's mechanical strength itself, but the internal pressure from the formation of corrosion product is also a reason of deterioration. The increment of the expansion pressure may result in the high tensile stress in the surrounded concrete, cracking and spalling of covering concrete, respectively. Figure 1.3 shows the cycle of corrosion process in RC structure member. [1,2,3,4,5,8]

Normally, these local behaviors gradually deteriorate the structure performance. However, corrosion something can increase the structure capacity. For example, it has been reported that small amount of corrosion can increase shear capacity at the interface due to the surface roughness [5,6,7], or in some corrosion pattern, instead of lower RC beam capacity, the corrosion changed the beam shear carrying behavior from truss action become tied arch action which results in increment of shear capacity of RC beam. [16] Hence, the study of corrosion at local scale is quite difficult and complicate issue. These complex behaviors need to be clarified for of comprehensive assessment of structure performance. [1,2,3,4,5,8,16]

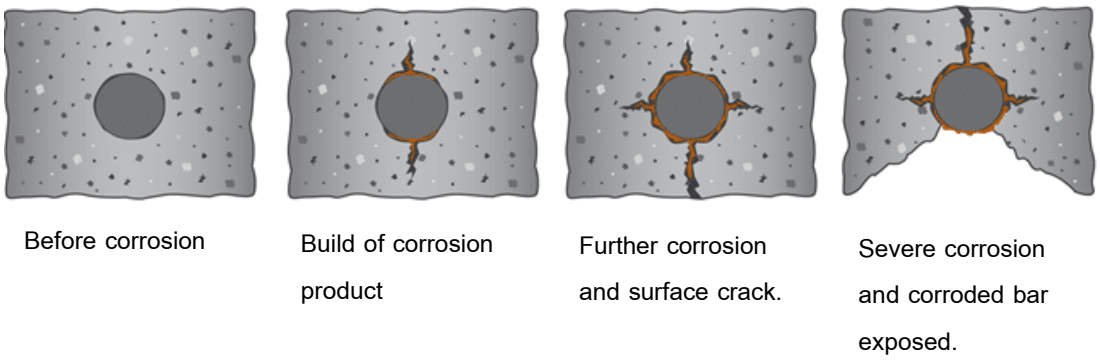

Figure 1.3 Corrosion cycling in reality [17]

Then, in term of structure analysis, there are several difficulties for analysis the behavior of corroded structure, especially, the corrosion effect at the meso scale. The analysis of structure performance can separate the numerical model into two stages, the induced damage from corrosion stage and the loading mechanism stage. Figure 1.4 and figure 1.5 show the influent factors that affect corroded RC behavior.

During the corrosion, the changing of mechanical bond at the interface is the combination between rust expansion, cracking development and confinement from surrounded concrete. Before the crack occurs, the stress at in interface increase as the corrosion degree increase due to the formation of corrosion product and confinement from the concrete. Afterward, once the crack occurs, the stress confinement will decrease due to the damage of surrounded concrete and the leaking of the corrosion product through to the crack spacing. These complicate behaviors which occur simultaneously need to be consider for structure analysis.

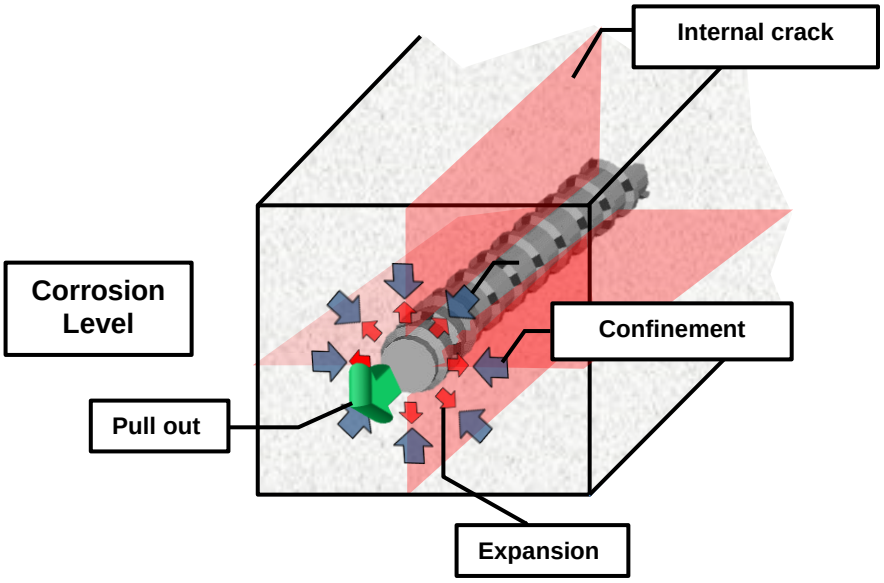

Figure 1.4 Corrosion influent factor on RC loading mechanism

Then, for the analysis during mechanical loading, the stress transfer between rebar and concrete is also changed due to the corrosion effect. The calculation need to consider the changing of mechanical bond and chemical bond, remaining stress from rust expansion, changing of effective rebar cross-section area and so on. The discontinuity, slipping or separation at interface can easier occurs due to the reduction of mechanical bond from loss of rebar's knot shape and damage of concrete. The reduction of effective cross-section area can lead to yielding failure of reinforcement. On the top of that, the initial corrosion cracking damage may lead to a different failure pattern of the macro structure. In this sense, it is very tough to consider all effect in calculation. Hence, the development of the numerical model that induced each parameter one by one should be appropriate approach for corroded structure behavior simulation.

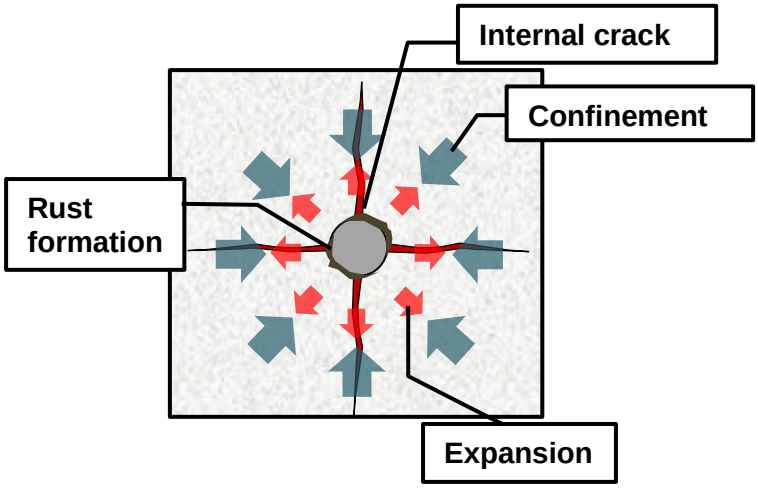

(a) cross-section view of corroded reinforcement steel

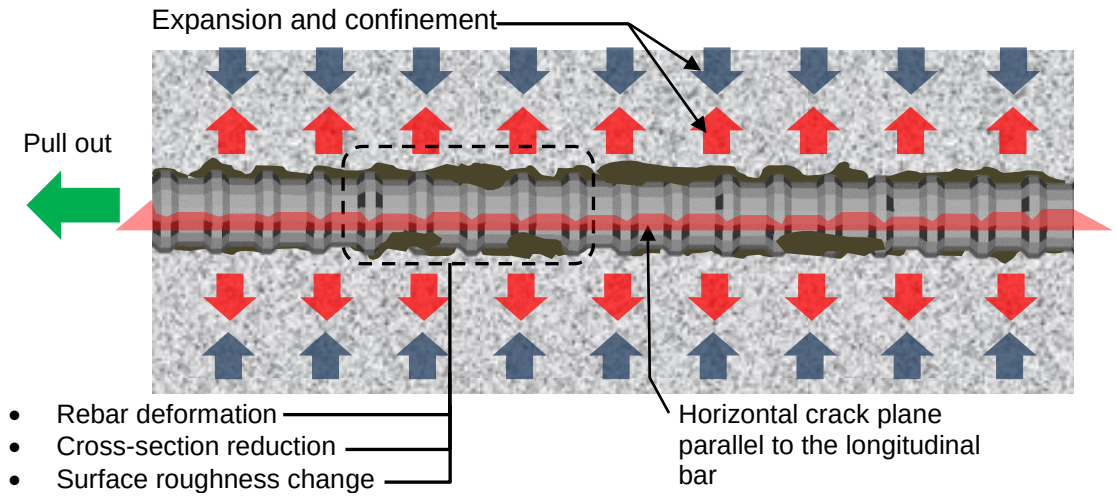

(b) Longitudinal view of corroded reinforcement steel

Figure 1.5 Influent parameter that effect corroded RC behavior

Nowadays, there are many research studies about the structural performance of corroded RC member with corroded reinforcement steel using FEM analysis. Generally, when the concrete is using together with good arrangement of steel reinforcement, the structure response can assume to be homogeneous material at macro scale. In this sense, the FEM which calculate the force as average response is perfectly suitable with structure analysis. However, in corrosion problem, the important topic is focusing on the local damage at mesoscale (or corrosion cracking) which can affect the macroscopic behavior. The direction and location of crack is very important. In this case, the crack should be treated as a single discrete element which the size, direction and location are precise calculated. In order to simulate the local cracking damage from corrosion appropriately, FEM, which is an average response model, need many special modification, like very fine meshing, fixed crack plane by implanted discrete element, or crack queuing algorithm [12-13]. Generally, the finer mesh is, the higher stress concentration will be developed near the crack tips. So, FEM need very fine mesh to define the geometry of the mesoscopic structure. Moreover, nonlinear analysis has to be carried-out by the calculation procedure where the load is applied in discrete increment. Due to the average response in FEM analysis, at one increment step, they may be many elements having developed stress exceed than cracking limits, and thus many elements may crack simultaneously due to the average response in FEM analysis. So, it is difficult to simulate the cracking in the same manner as the real behavior by FEM. Figure 1.6 shows the simulation of corrosion crack formation using FEM by T. Kukrit in 2004. In this numerical model, by using fine meshing and low shear resistance interface element.

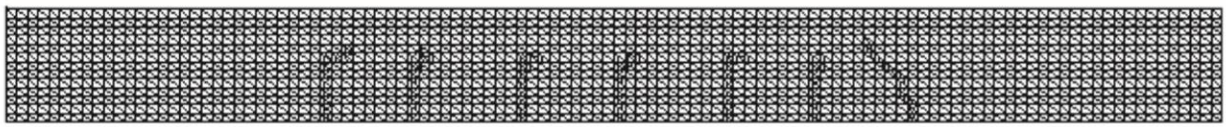

(a) Very fine meshing in FEM for cracking simulation (A.K.H. Kwan et al., 2015) [12,13]

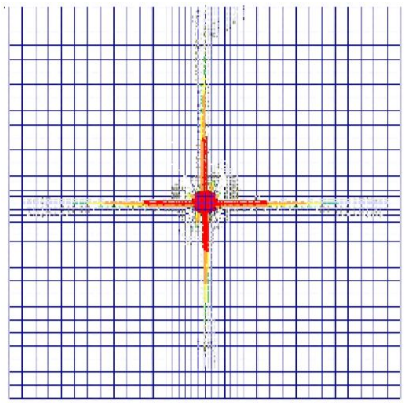

(b) Corrosion crack simulation by FEM

Figure 1.6 Numerical crack propagation by FEM

Then, once again after the local corrosion damage problem, the residual capacity of the corroded structure need to be known. Which means, the loading mechanism should be performed. In this sense, the FEM analysis have to manage the calculation of two type of element which is with single discrete crack element and the average response element for non-corroded zone which is overlapped in corrosion zone. It is very difficult to calculate property between two systems. However, it can be done by prepare the artificial crack in at the corrosive crack location. In 2004, Kukrit et al.[14] has develop an FEM simulation for corroded RC beam with corrosion cracking. In this simulation, the artificial crack plane with discrete element are set in advance on FEM beam model. Even, this study's result showed a good agreement with the corroded experiment beam, but it need to know the location, direction and size of corrosion crack in advance for setting the artificial crack in the numerical model.

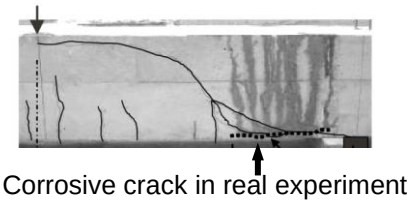

(a) Corrosion crack and loading crack in experiment [19]

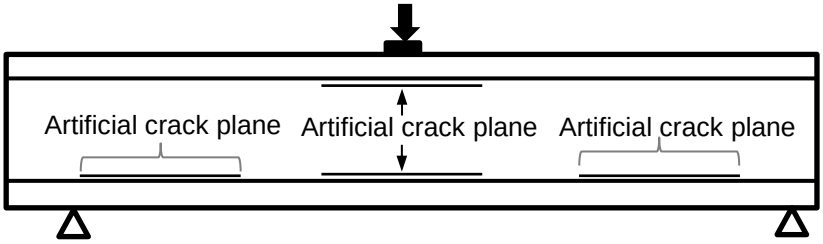

(b) Artificial crack plane in FEM analysis

Figure 1.7 Setting of artificial corrosion damage in FEM

Another issue is that the crack treatment is FEM is quite different from the reality. Normally, the crack In typical FEM is treated by a smeared crack concept which assumed many micro crack in the cracked concrete element. Though, in the reality, the crack is a separation of concrete or rebar and quite similar to the discrete element concept. However, at the normal RC structure analysis which

concrete can be assumed as homogenous material, this concept is show no problem in calculation. Nevertheless, in corrosion problem, the local corrosion damage is a complex behavior that can affect the macro structure behavior. The direction and location of corrosion crack can lead to a different failure pattern[15]. The smeared crack concepts may not appropriate in this problem.

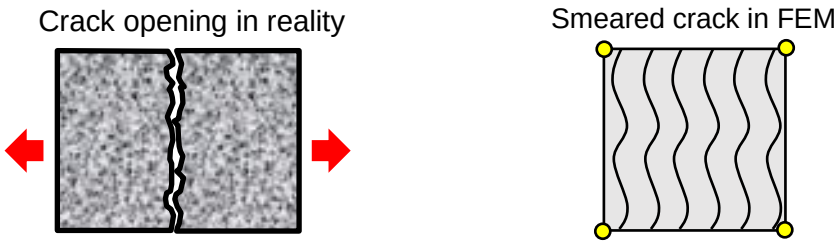

Figure 1.8 Crack in reality and smeared crack in FEM

A number of research by FEM treat corrosion cracking at interface between steel bar and concrete as flat bond element which parallel to the longitudinal bar as shown in figure1.9. The bond stress and changing sue to the slipping between rebar and concrete. By the concept, the separation or the bond reduction due to corrosion can be simulated.

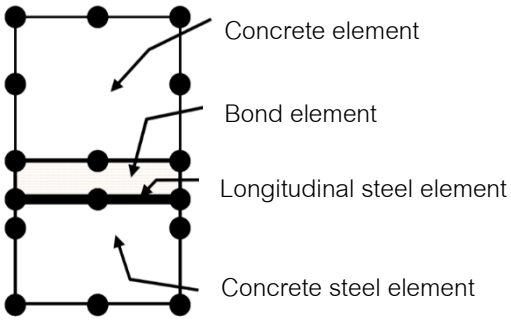

Figure 1.9 Outline of bond element in FEM

However, this concept only simulates the damage of corrosion in the parallel direction to the longitudinal reinforcement direction. Therefore, in some situation, simulation results cannot simulate the changing of stiffness in corroded beam appropriately. For example, in case of research conducted by S. Lim in 2016, even the FEM analysis can simulate the changing of capacity of corroded RC beam at different corrosion degree, but the model cannot simulate the changing of stiffness or the softening behavior of corroded appropriately comparing with the experimental results [15].

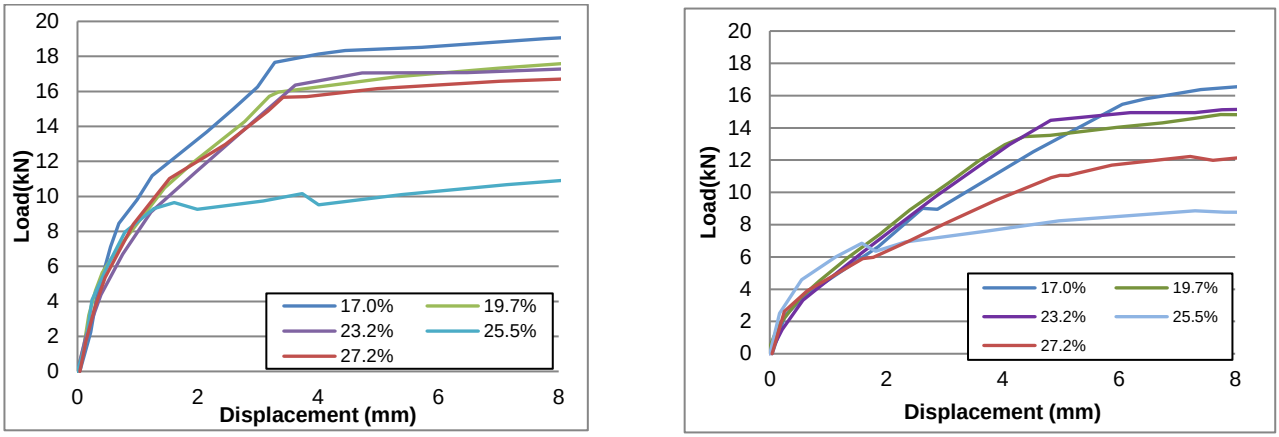

(a) Load-displacement of corroded beam by FEM (b) Load-displacement from experiment

Figure 1.10 Load-displacement relationship of corroded beam loading from FEM and experiment

The different in stiffness between simulation and real corroded beam may occur because of several reason. First possibility is the shape and direction of corrosion crack. In FEM analysis, the element mashing is set to be isometric rectangular shape, so the crack will follow this trial. That make the crack in FEM is flat and parallel to the longitudinal bar. Even using the bond element or discrete element for artificial crack, the crack is assumed to be perfectly flat and parallel to the longitudinal rebar. (Figure 1.11) Then, when we consider the mechanism of RC structure, for example, pulled-out test simulation on corrosion crack concrete specimen. Theoretically, if the rebar is treated as a line or truss element and the concrete is treat as normal FEM, the corrosion cracking which is parallel to the longitudinal bar will have no effect on pull out behavior.

However, in the reality, the crack is not flat due to the shape of rebar and existing of aggregate. (Figure1.12) So, when the corrosion expansion occurs, the expansion force is not just normal to the rebar direction, but it also has a diagonal force due to the shape of deformed bar. The existing of aggregate also change the crack propagation direction. So, it may crate the micro crack in the normal direction to the longitudinal direction of rebar. Then, when the mechanical loading is applied, this micro crack may lead to the early opening of the transverse crack in force direction e.g. the flexural in beam. The stiffness of corroded beam is lowering comparing with the non-corroded beam. Another reason is the remaining stress at interface and interface treatment in FEM analysis. When the corrosion occurred, the rust product will form up at the interface between rebar and concrete. This voluminous product creates the internal stress at the interface between rebar and concrete. This remaining stress may affect the structural behavior during the loading mechanism. In typical FEM analysis for corrosion, the interface element in FEM, which is set as an artificial crack by interface bond element or discrete element with modification of material properties, cannot represent the effect of remaining stress.

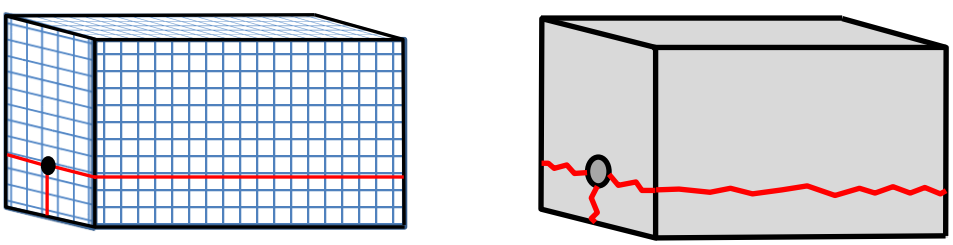

Figure 1.11 flat crack treatment in FEM and zig-zag crack in reality.

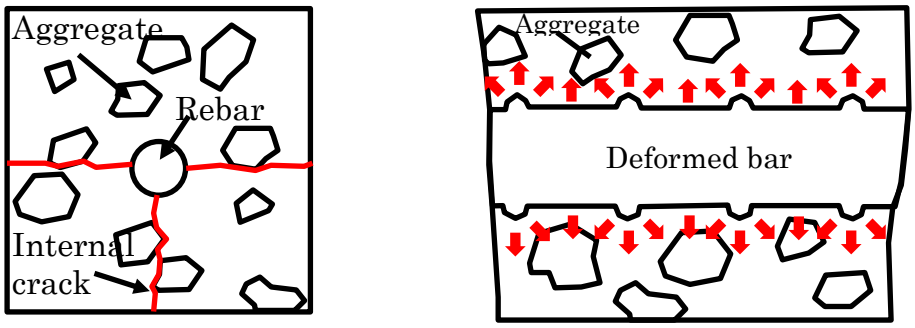

Figure 1.12 Existing of aggregate and deform bar in reality.

Moreover, in these researches by FEM, the range of study was focusing on the flexural failure or simple shear failure member like RC beam or column. Actually, only by hand calculation with knowing the average corrosion percentage, the residual capacity of these structures can be calculated and give a similar result with the simulation model. However, it would be difficult to simulate the cracking of corroded RC structure in such a complex zone like beam-column joint or anchorage part. In this case, the corrosion cracking cannot be simply treated as a single discrete plane.

In this sense, the discrete analysis model at meso-scale may be more appropriate choice because the calculation of crack can be done automatically by the model characteristic. The model doesn't need to manage the difficulty between two element systems (discrete crack element and smeared crack element). With the random mashing and constitutive model at meso scale, the crack propagation can be treat in the same manner as the real concrete. Moreover, the crack from expansion damage can be simulate automatically as a model nature without using artificial crack plane. And, the effect of remaining expansive stress from expansion can be consider during the loading mechanism. Based on these reasons, the discrete analysis model may be a proper choice for assessment of the corrosion cracking problem and residual capacity of corroded structure.

1.2. Purpose of research

For corrosion problem, to determine the internal behavior of corroded structure by experimental method would take a lot of time and cost. In this sense, simulation seems to be a useful tool for simulating the behavior of the structure.

Hence, the purpose of this research is to develop the numerical model for revealing the internal behavior and residual capacity of existing corroded structure. In field of retrofitting and maintenance, knowing residual capacity will make it easier for deciding an action whether the retrofitting or demolishing will be done.

In order to simulate the local failure behavior of corrosion damage. The system has several requirements such as, the 3D analysis because the corrosion damage occurs in three dimension, the meso-scale analysis because the corrosion cracking always happen at meso scale, and the discrete analysis because it is important to simulate the local damage accurately such as the crack propagation of the cracking location. Base on these requirement, 3D mesoscale discrete analysis should appropriate for these problems. So, in this study, the author decided to use Rigid Body Spring Model(RBSM) as a based model for develop the numerical model for predict the residual capacity and internal behavior of corroded RC structure.

Theoretically, the mechanical behavior or local failure behavior like crack of concrete covering which results from swelling rusted rebar can directly simulated by RBSM simulation. Comparing with Finite Element Method, one of the key notions of RBSM is its random geometry based on Voronoi meshing diagrams, so that the locations and direction of crack propagation do not need to be anticipated and adaptive re-meshing is not need. (Bolander and Le,1999) In RBSM, analytical model is meshed into polyhedral shape whose faces are interconnected by a set of spring, 2 shear and 1 normal. Take benefit from this concept, the local behavior such as rust expansion can directly simulated by given the expansive strain at interface between rebar and concrete. For the crack propagation of specimen under mechanical loading, RBSM is suitable model for this approach. Previous studies of RBSM simulation show the capability in prediction of fracture of reinforced concrete structure. However, the original RBSM does not have a function to simulate the corrosion behavior. Thus, in this study, the author has considered the real corrosion behaviors such as steel weight loss, knot shape deformation, bond deterioration, and developed the constitutive model for represent those behavior is developed one by one and implement those function into the original Rigid Body Spring Model.

In this study, the impact of corrosion expansion, steel cross-section effective area and bond deterioration are investigated. The constitutive models are developed for represent these effects in numerical model. The necessary information for bond deterioration constitutive model are obtained from the electrical accelerated corrosion experiments and pull out test of different corrosion percentage specimens. Experiment program were originally designed for extract the necessary information of corrosion effect on bond and surface properties for development the equivalent interface model under corrosion stage.

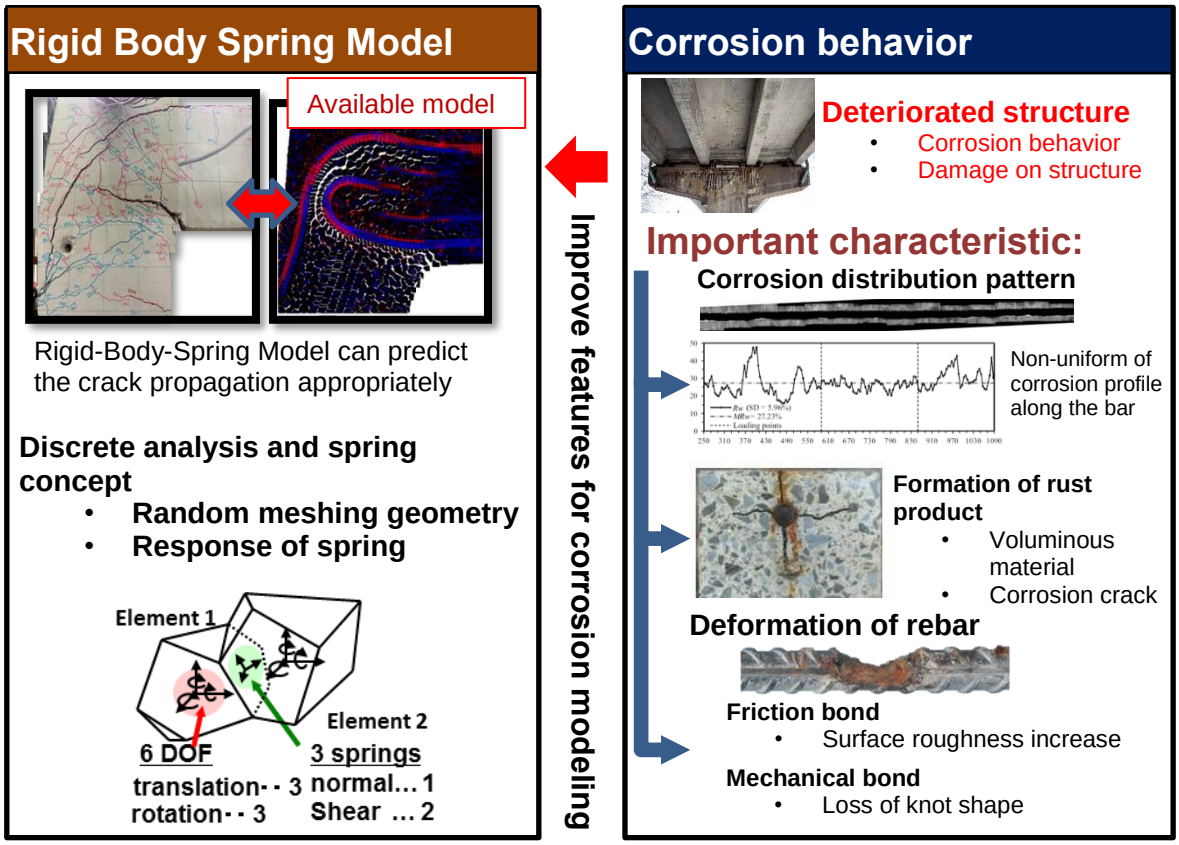

Figure 1.13 Concept of combination of RBSM with corrosion model

This numerical model predicted the residual performance provides support for retrofitting process, inspection and verification of existing corroded structure. Moreover, the structure performance of each retrofitting method can be evaluated and selected for the most appropriate and economic method.

1.3 Literature review

1.3.1 Effect of stirrups arrangement on failure of beam column joint with mechanical anchorages by discrete model, L. EDDY and K. NAGAI, The University of Tokyo, 2015

Liyanto Eddy and Kohei Nagai, the University of Tokyo, have been developing the 3 dimensional numerical discrete analysis model, RBSM. In their recent study, RBSM simulation has been used for simulating the experiment of beam-column joint with complex rebar arrangement. This research was conducted in order to reduce the reinforcement bar congestion in beam column joint. A 3 dimensional meso-scale discrete analysis is used to investigate the effect of the stirrups arrangement on the failure of beam column joint with mechanical anchorages through the comparison with the experimental results. Several cases of rebar arrangement with various stirrup locations have been simulated. The results show that when no stirrup is provided along the anchorages or stirrups are provided at the end of the anchorages, brittle failure occurs at the top surface of beam column joint. On the other hand, when stirrups are provided along the anchorages flexural/ductility failure occurs. Based on experimental results and simulation results, E. Liyanto and team proposed that stirrups along anchorage are needed to prevent the local failure, anchorage failure, in beam column joint with mechanical anchorage by providing confinement effect along the anchorage.

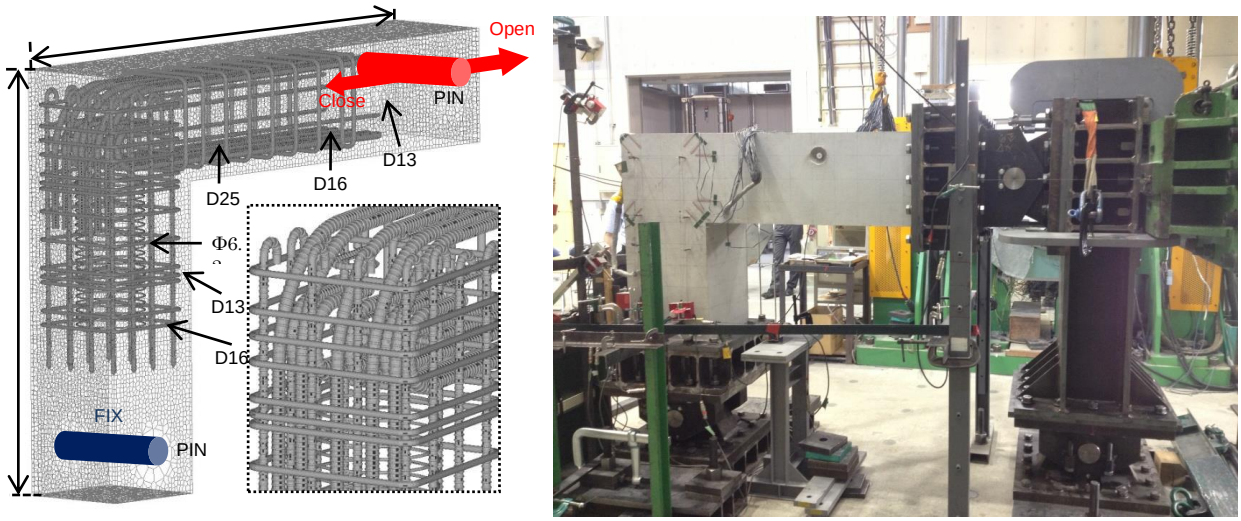

(a) **(b)**

Figure 1.14 (a) RBSM Simulation model by L. Eddy and K. Nagai, 2015
(b)Experiment by JR railway

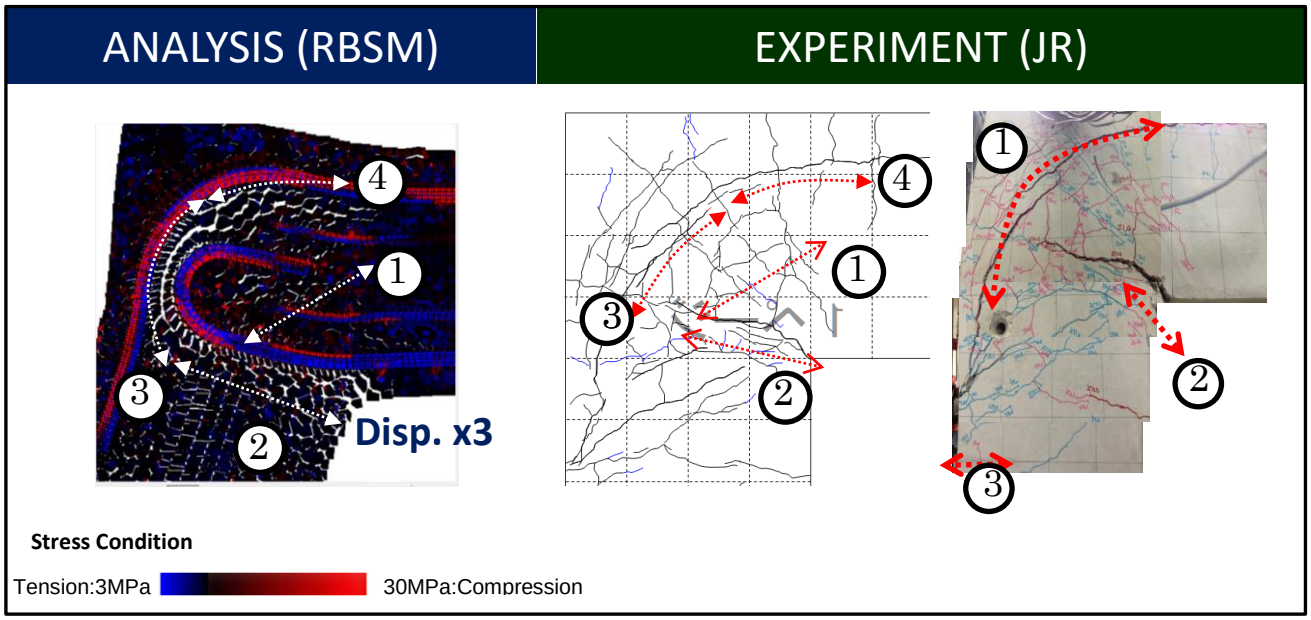

Figure 1.15 Comparison of Simulation result with Experimental result
[E.Liyando et al. 2015, JR railway]

In this paper, RBSM can simulate the complicate rebar arrangement in the same pattern as real specimen as shown in Figure 1.14. The crack propagation and direction in simulation results gave a same tendency with that of the experiment as shown in Figure 1.15, and These show that RBSM is an effective tool for simulating and prediction of the local fracture behavior of reinforced concrete structure. Therefore, in this Thesis, RBSM is chosen for simulating the crack propagation in concrete under loading.

1.3.2 Assessment of the structural performance of corrosion-affected RC members based on experimental study and probabilistic modeling, S. Lim, 2016 [15]

In 2016, Sopokhem Lim and team have conducted the experiment about corrosion acceleration on RC beam for studying the effect of spatial corrosion on structural behavior. Several corroded RC beam experiments were conducted to study different amount and different pattern of corrosion. After the corrosion acceleration test, the digital camera and X-ray technique were used to measure the corrosion profile along the rebar. By measuring the alignment from central line of rebar before and after corrosion at different angles, the residual cross-section of rebar can be calculated. Figure 1.18 show the steel weight loss profile along the rebar of beam specimen with stirrup and without stirrup by X-ray technique.
Then, the corroded beams were subjected to the mechanical loading test the find the residual capacity. The FEM simulation were conducted and compared with the experimental results to confirm the necessity of non-uniform corrosion in prediction of corroded beam simulation.
Figure 1.16 show the beams dimension with and without stirrup used in his study.

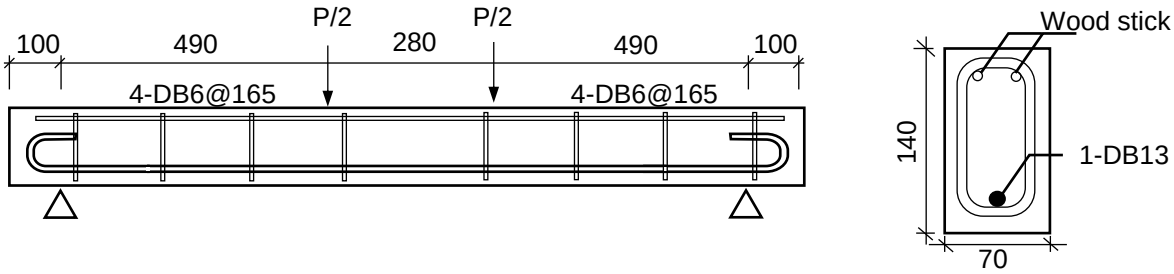

Figure 1.16 Dimension of beam in corrosion acceleration experiment

In his study, He conducted two set of simulation for each beam. First simulation is the simulation with uniform corrosion pattern that have the same average corrosion degree as the experiment, second simulation is the non-uniform corrosion pattern that the corrosion pattern was calculated by using Gumbel distribution function based on scale factor and location factor from the experimental results.

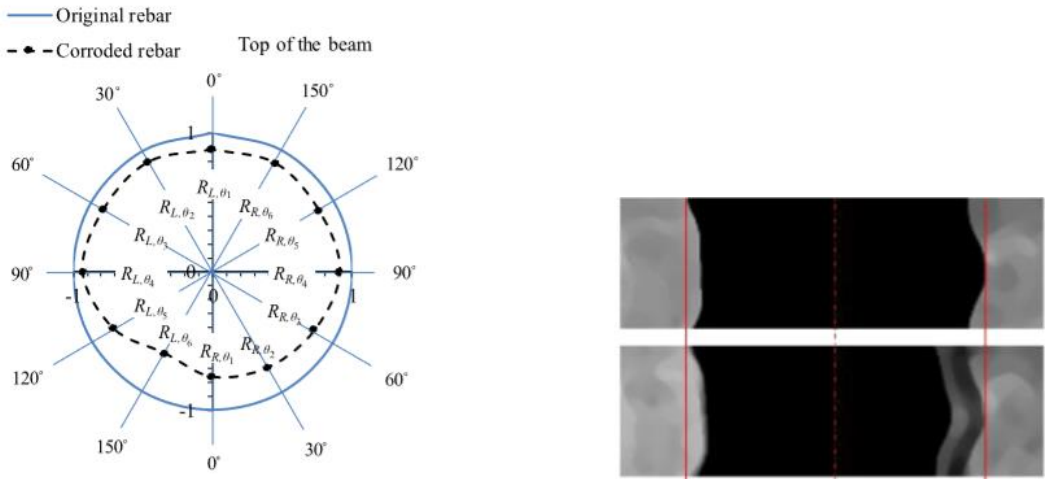

(a) Construction of residual steel cross-section area

(b) Alignment of non-corroded and corroded rebar

Figure 1.17 (a) construction of the residual steel cross section area (b) X-ray photo of rebar before and after corrosion.

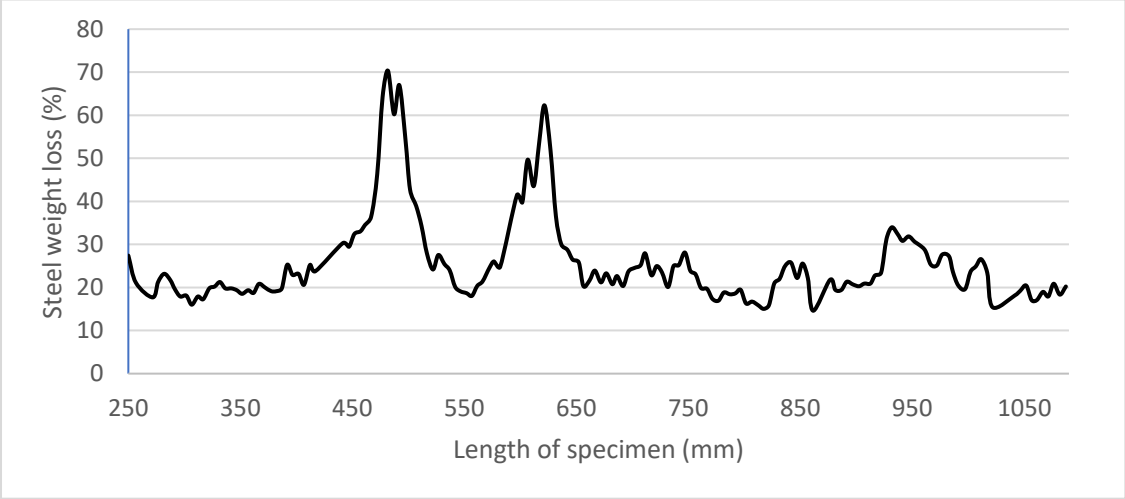

(a) Spatial variability in steel weight loss

(b) X-ray image of steel corrosion at 180 degree

Figure 1.18 Local steel weight loss along the bar length by X-ray image of beam specimen

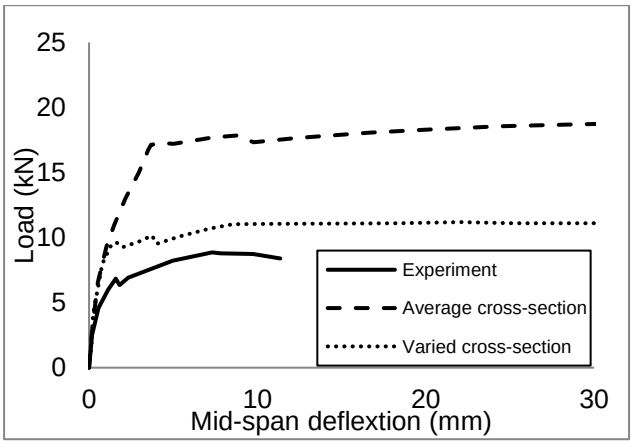

Figure 1.19 Load-displacement of simulation results and experiment of corroded beam experiment. [S. Lim et al.,2016]

From figure 1.19, the load-displacement relationship of experiment and simulation with and without considering the corrosion distribution pattern. These results show that even the same average corrosion degree were applied to both uniform and non-uniform corrosion case, but the simulation results of spatial corrosion pattern (varied cross-section) shows lower beam capacity. And it is more accurate comparing with the experimental results.

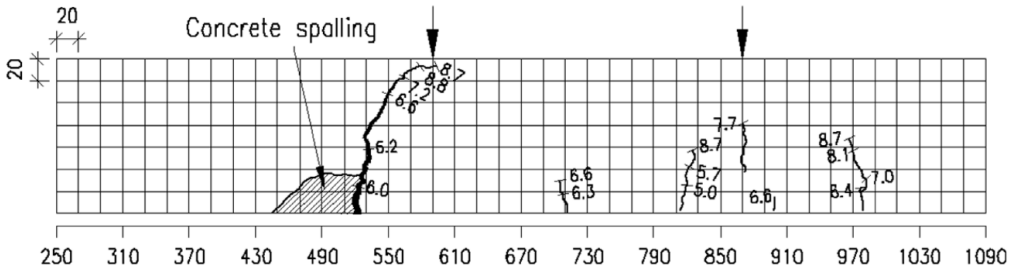

Figure 1.20 Cracking pattern of beam specimen

Figure 1.20 shows the cracking pattern of corrosion beam after the bending test. It can be seem that location of the large flexural crack and concrete spalling at the same location with the critical corrosion profiles in Figure1.18(a).

In conclusion, the simulation results from FEM method suggest that it is important to consider the influences of non-uniform corrosion of steel weight loss for the assessment of the structural performance of corroded RC structures.

The important information from this study is that even the same average corrosion degree and used in the analysis of the beam. The model with considering the spatial corrosion distribution can predicted more accurate results comparing with the model that used the mean corrosion distribution. This is because the critical corroded cross-section can lead to the failure of structural member early than the other section. Therefore, it is important to consider the non-uniform corrosion pattern of steel bar in analysis.

1.3.3 Influence of local steel corrosion on shear failure mechanism of RC members, Masahiko TSUNODA [16]

This study conducted unidirectional static loading tests of slender RC beams, of which longitudinal reinforcing steel bars were locally corroded at anchorage and support zone. The study was conducted for clarify the influence of local corrosion of longitudinal reinforcement on the shear failure mechanism of RC members. FEM of the specimens was also conducted for analyzing the failure mechanism of RC beams. In his study, the steel bar was generated the corrosion at anchorage zone in different location. After the corrosion acceleration test, the corroded beam specimen were subjected to the unidirectional static loading test. Figure 1.21 show the beam dimension in his experiment and unidirectional static loading that give to the RC beam.

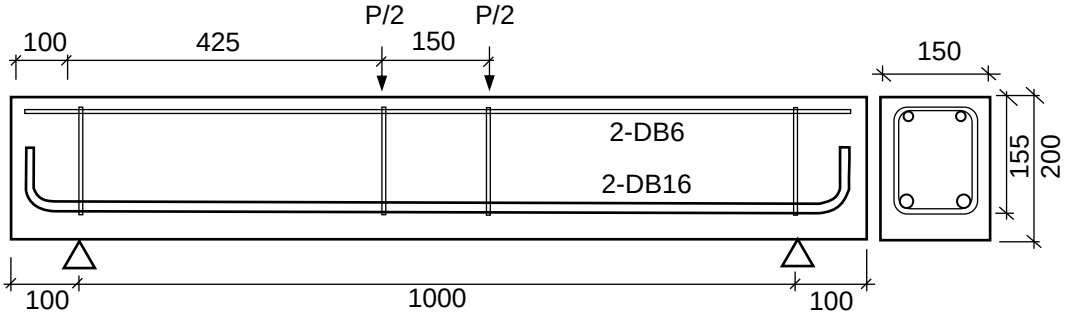

Figure 1.21 Beam experiment by M. TSUNODA

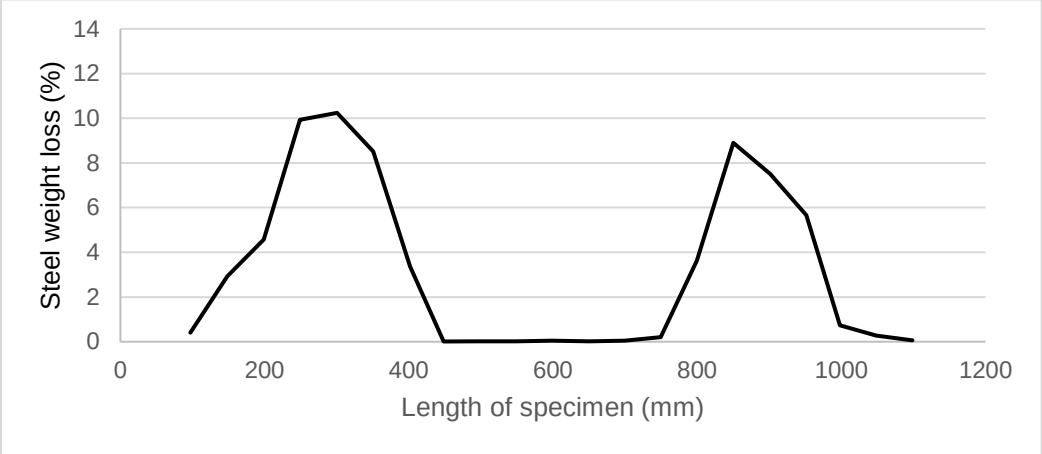

Figure 1.22 Corrosion distribution in corroded RC beam experiment [M. Tsunoda et al.]

In his experiment, one interesting results is that the beam shearing mechanism were changed depending on the corrosion profile along the longitudinal bar.

For example, the corroded beam which had the peak corrosion degree around 10% at around 287.5 mm from the left and right end of the beam (as show in figure 1.22), show a significantly increase in load capacity comparing with the beam without corrosion as show in figure 1.23.

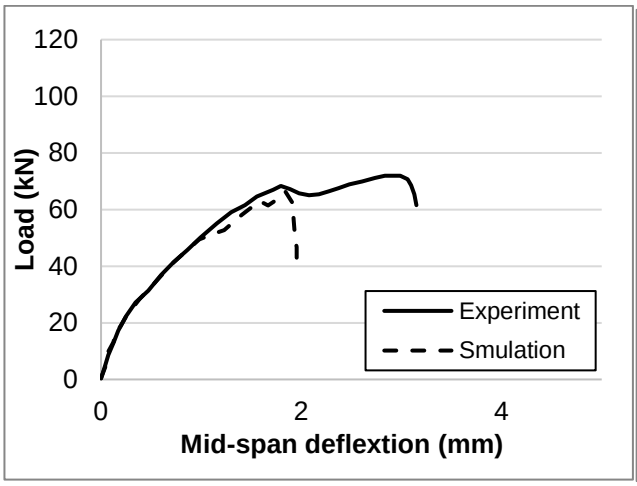

(a) No corrosion beam, BN

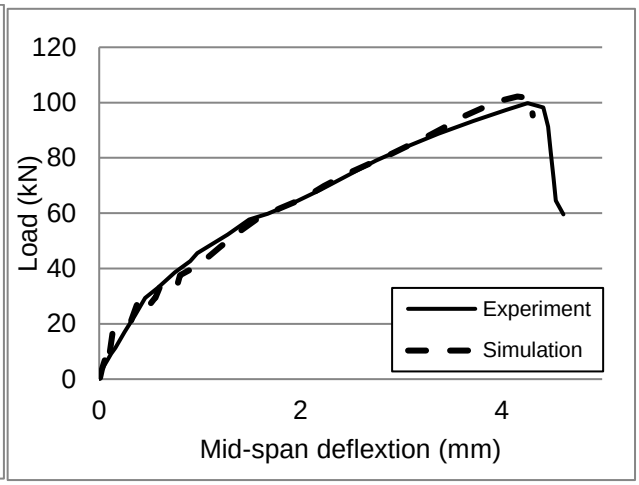

(b) Corroded beam specimen, B10-287.5

Figure 1.23 Load-displacement from experiment

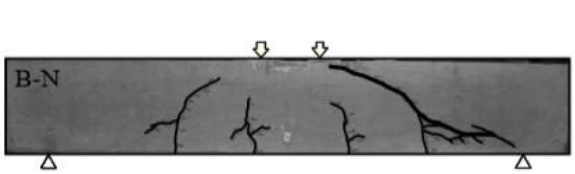

(a) Beam failure pattern after the loading

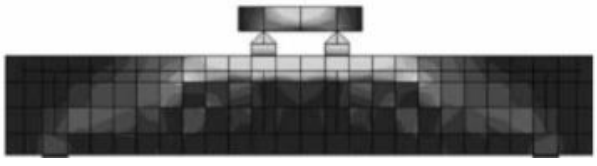

(b) Principal compressive stress distribution from FE simulations

Figure 1.24 Non-corroded beam failure pattern after the loading and principal compressive stress distribution from FEM simulation

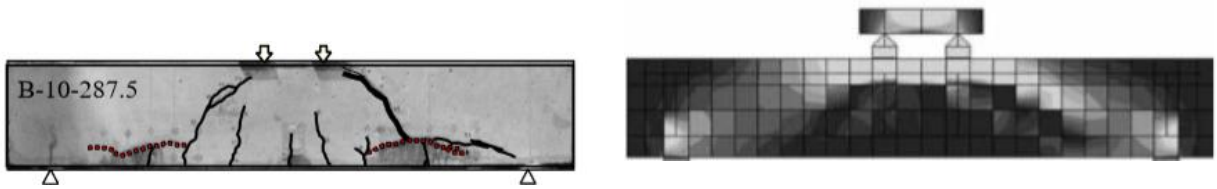

(a) Beam failure pattern after the loading (b) Principal compressive stress distribution from FE simulations

Figure 1.25 Beam failure pattern after the loading and principal compressive stress distribution from FEM simulation of beam specimen B-10-287.5.

This study indicated that the shear carrying mechanism of RC beams with the local steel corrosion changes from the truss action to the tied arch action. The main reason is that, the tension force transmitted from concrete to longitudinal reinforcement decreases due to the bond deterioration in corroded beam. As a result, the stress profile and crack distribution of RC beams with corroded steels is different from that of RC beams without corroded steels. Figure 1.24-1.25 show the stress distribution in FE analysis. It can be seen that arch rib of stress concentration formed up clearly in case of corroded beam.

In conclusion, the important information from this study is that the shear carrying mechanism of RC beams with the local steel corrosion changed from the truss action to the tied arch action. So, the local behavior strongly affects the loading mechanism of the macro structure.

1.4 Research objective

The final goal of this research is to develop the simulation system which has ability for revealing the residual capacity of corrosion induced deteriorated structure. Considering our research group's simulation systems, the ability for prediction of local failure and structural performance of concrete structure are already available in this simulation model. This means the simulation model for representing the corrosion phenomena into the RBSM simulation are necessary to develop and implement into the RBSM. Considering the previous study about the corrosion of RB structure in literature review, in order to achieve the final goal, the following objectives are set as the research's goal:

- Develop the simulation of concrete damage from the corrosion. Once the corrosion product occurred, the internal pressure will be increased. As a result, tensile stress of concrete around the corroded bar will lead to the corrosion cracking.
- Develop the simulation model for simulating the expansion of the rebar. The expansion of rebar occurred due to the change of steel phase into the voluminous rust product. This voluminous product will increase internal pressure along the corroded bar which will lead the many phenomena such as the increment of bond due to confinement, the loss of mechanical bond due to deterioration of steel-concrete interlocking and so on.
- Simulation of the deformation of rebar surface properties. When the rebar becomes corroded, the surface of rebar will change to become rough and the rust product may cause the slip between rebar and concrete. This behaviour should be considered during the development of the model.
- Develop the equivalent constitutive model for represent the loss of rebar effective cross-sectional area. In RBSM simulation, the elements are model as rigid element which cannot be deformed

in shape. Hence, some modifications of the response of spring need to be performed to represent this behaviour.

- Simulation system that consider the non-uniformity of the corrosion pattern of the rebar. As described in the literature review parts, the spatial corrosion pattern directly affects the failure criteria and capacity of the structure. So, the non-uniformity of corroded bar should be considered as an input corrosion data of corrosion model.

1.5 Outline of this Thesis

The development of chloride penetration in cracked concrete will be explained in this thesis following structure as shown below:

- Chapter 1 : Introduction
  In this chapter, detailed about research background, statement of problem and objective are explained. Some literature reviews that related to the developing of corrosion model are emphasized.
- Chapter 2 : Simulation model
  In this chapter, the method in development of each numerical simulation model, Corrosion model and Rigid Body Spring Model (RBSM) and related literature review of previous studies will be described. The development of constitutive model for the corrosion will be explained. The method for determination of the given expansive strain for simulating the same concrete damage will be explain step by step. The theoretical formulation related in numerical analysis of corrosion behaviour, namely, residual effective cross-sectional rebar area, equivalent bond deterioration constitutive model, introducing of non-uniform corrosion pattern, are also described in this section.
- Chapter 3: Model development based on pull out test experiment
  In this chapter, the method of developing the bond deterioration model is described step by step. Since the material element in RBSM are modelled as a rigid element which cannot be deformed. Some mechanism such as the loss of mechanical bond from interlocking between reduced rebar volume and concrete cannot be modelled directly. Therefore, the equivalent constitutive model for representing the loss of bond is developed. To achieve this goal, the experiment program for studying the loss of bond due to corrosion are designed. This chapter will explain the experimental plan step by step. The information that the author derived from the experiment, and how the author used that information for development of the simulation model are described.
- Chapter 4: Corroded beam simulation with effect of non-uniform corrosion pattern
  To verify the applicability of the corrosion model and study the effect of non-uniform corrosion pattern, the numerical model are used to simulate the corroded beam from previous studies. In this chapter, two corroded RC beam experiments done by S. Lim and team was used as input data for simulating the corroded beam. The effect of non-uniformity of corrosion profile on structural mechanism such as the change in local failure behaviour or the changing of failure pattern due to corrosion cracking are analysed. The simulation results were then compared with the real experimental results. The applicability and limitation of the numerical model are described in this chapter.
- Chapter 5: Corroded beam simulation with corrosion at anchorage
  In this chapter, the effect of corrosion on anchorage was investigated. The beam simulation with intentionally set the corrosion at the anchorage zone are simulated. The experiment M.

TSUNODA et al. was used for verification the simulation results. The effect of corrosion profile on structural mechanism such as the change in shear capacity, the loading mechanism or the formation of tied arch action are analysed. The simulation results were then compared with the real experimental results. The applicability and limitation of the numerical model will be described in this chapter.

- Chapter 6: Conclusions
  In this final chapter, several remarks about the capability of corrosion model are emphasized. Also, some commentaries for further project or improvement are proposed.

REFERENCES

[1] Juraj Bilcik, Ivan Holly, *Effect of reinforcement corrosion on Bond behavior,* Procedia Engineering, Volumn65, 2013, pp.248-253

[2] ACI Structural Journal 87:2, 220-231. Amleh, L., Mirza, S. (1999). *Corrosion Influence on Bond between Steel and Concrete*. ACI Structural Journal 96:3, 415-423.

[3] Al-Musallam et al., *Effect of Reinforcement Corrosion on Bond Strength*. J. Construction and Building Materials 10: 2,1996, 123-129

[4] Al-Sulaimani et al., *Influence of Corrosion and Cracking on Bond Behavior and Strength of Reinforced Concrete Member.,* ACI Structural Journal 87:2,1990, 220-231.

[5] A. Aryanto & Y. Shinohara, *Bond Behavior between Steel and Concrete in Low Level Corrosion of Reinforcing Steel*, 15 WECC, LISBO, 2012.

[6] Andrade, C., Alonso, C., and Molina, F. J., Cover Cracking as a function of bar corrosion: Part I – Experimental test, Material and Structures Vol. 26, 1993, pp.453-464.

[7] Shinohara. (2011). Effect of Confinement upon Crack Behaviors caused by Corrosion-Product Expansion around Corroding Bars. Proceeding of the 12th International Conference on Durability of Building materials and Component. Vol.3 :1577-1584

[8] David W. Law, Thomas C.K. Molyneaux, *Impact of corrosion on bond in uncracked concrete with confined and unconfined rebar,* Construction and Building Materials, Volume 155, 30 November 2017, Pages 550-559

[9] http://www.f.waseda.jp/akiyama617/research

[10] Hong Zhang, et al., *The Non-Destructive Test of Steel Corrosion in Reinforced Concrete Bridges Using a Micro-Magnetic Sensor,* Sensors 2016, 16(9), 1439; doi:10.3390/s16091439, 6 September 2016

[11] J. Jayaprakash**,** Emad Pournasiri and F. De'nan, *Effect of corrosion-damaged RC circular columns enveloped with hybrid and non-hybrid FRP under eccentric loading,* Journal of Composite Materials 49(18), August 2014

[12] A.K.H. Kwan, Z.M. Wang, H.C. Chan, *Mesoscopic study of concrete II: nonlinear fnite element analysis,* Computers and Structures 70, 1999, pp.545-556

[13] F.J.Ma, A.K.H.Kwan, *Crack width analysis of reinforced concrete members under flexure by finite element method and crack queuing algorithm,* Engineering Structures, Volume 105, 15 December 2015, Pages 209-219

[14] Kukrit Toongoenthong and Koichi Maekawa, *Interaction of pre-iunduced damages along main reinforcement and diagonalshear in RC member*, Journal of advance concrete technology, Vol. 2, October 2004, pp. 431-443
[15] Sopokhem Lim, Mitsuyoshi Akiyama and Dan M. Frangopol, *Assessment of the structural performance of corrosion-affected RC member based o experiment study and probabilistic modeling*, Engineering structures 127, 2016, pp.189-205
[16] Masahiko Tsunoda, Junichiro Niwa, *Influence of local steel corrosion on shear failure mechasiam of RC member,* Concrete research and technology, 15(2),2004, pp.69-77
[17] https://theconstructor.org/concrete/corrosion-steel-reinforcement-concrete/6179
[18] https://www.ndt.net/article/ndtce03/papers/p055/p055.htm
[19] Kukrit Toongoenthong and Koichi Maekawa, *Simulation of Coupled Corrosive Product Formation, Migration into Crack and Propagation in Reinforced Concrete Sections*, Journal of advance concrete technology, Vol. 3, June 2005, pp. 253-265
[20] Kohei Nagai, Yasuhiko Sato, Tamon Ueda, *Mesoscopic Simulation of Failure of Mortar and Concrete by 2D RBSM*, Journal of Advanced Concrete Technology, Vol.2, No.3, 2004, pp.359-374.
[21] Kohei Nagai, Yasuhiko Sato, Tamon Ueda, *Mesoscopic Simulation of Failure of Mortar and Concrete by 3D RBSM*, Journal of Advanced Concrete Technology, Vol.3, No.3, 2005, pp.385-402.
[22] Bolander, J. E., Hong, G. S., and Yoshitake, K., *Structural Concrete Analysis Using Rigid-Body-Spring Networks*, Computer-Aided Civil and Infrastructure Engineering, 15, pp.120-133, 2000.
[23] Bolander, J. E., and Hong, G. S., *Rigid-Body-Spring Network Modeling of Presetressed Concrete Members*, ACI Structural Journal, 99(5), pp.595-603, 2002.
[24] Bolander, J. E., Le, B. D., *Modeling Crack Development in Reinforced Concrete Structures Under Service Loading*, Construction and Building Materials, 13, pp.23-31, 1999.

Chapter 2
Simulation Models

2.1 General

This chapter describes about simulation systems using in this study, Rigid Body Spring Model (RBSM) and corrosion model. RBSM is a discrete analysis model developed by Kawai et al.. Analysis model is divided into polyhedral elements whose phases are interconnected by a normal spring and two shear springs. Response of the spring provides the interact between element instead of the internal behavior of each element. Then, the corrosion of reinforced concrete like reduction of rebar effective area, or corrosion expansion are developed considering the real behavior and RBSM's characteristic and applied into original RBSM. The corrosion numerical model is developed by utilizing previous experiment. In this study, numerical simulation of failure of concrete is carried out by RBSM section, while the effects of corrosion are simulated by the corrosion model.

2.2 Rigid Body Spring Model (RBSM)

2.2.1 Numerical model of concrete

In this study, the simulation is carried out by 3-dimensional RBSM, proposed by Kawai et al. (1978). In RBSM, a 3-dimensional reinforced concrete model is meshed into rigid bodies. Each rigid body consists of 6 degree of freedoms, i.e. 3 translational degrees of freedom and 3 rotational degrees of freedom at some points within its interior and connects with other rigid bodies by 3 springs, i.e. 2 shear springs and 1 normal spring [1,2]. This method simulates failure behavior by solving the equilibrium of forces of springs placed between rigid elements. Two types of elements, concrete and steel, are used to define the geometry of RC. Since crack direction may affect crack patterns, the size of each concrete element is approximately 1-2 cm^3, referred to aggregate size, while the size of the steel element is set according to the geometric complexity of the reinforcement bar arrangement (Figure 2.1). To prevent cracks propagated in a non-arbitrary direction, a random geometry, called Voronoi Diagram, is used for the element meshing.

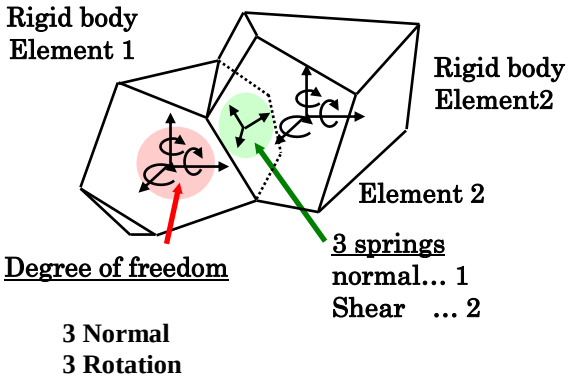

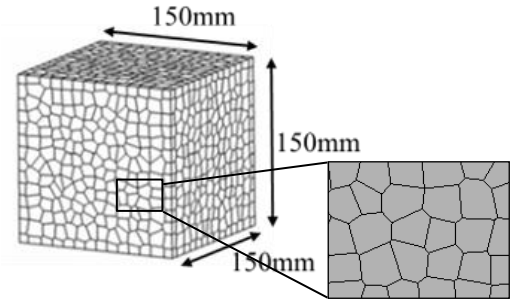

(a) Spring between element (b) Mesh of concrete element

Figure 2.1 Concrete elements in RBSM

The properties of the springs are determined so that the elements, when combined together, enable to predict the behavior of the model as accurate as that of the experimental result. In this study, the simulation system, developed by Nagai et al., is used. Figure. 2. 2 (a, b, c, d)(Nagai et al., 2005) [3,4] shows the constitutive model of the concrete element.

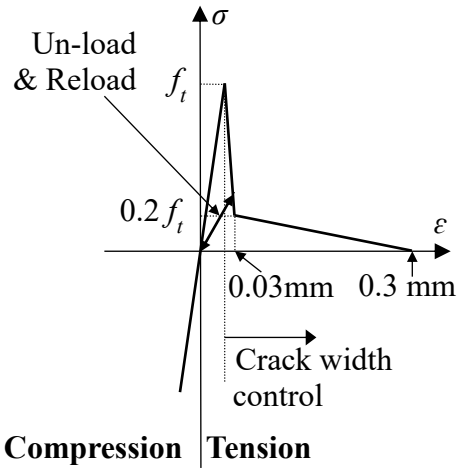

(a) Normal spring of concrete

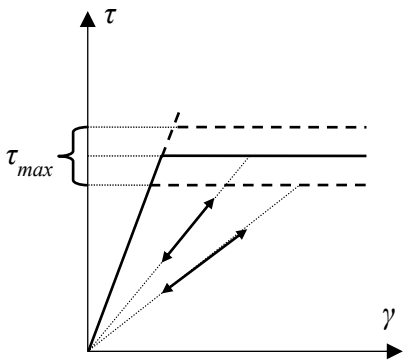

(b) Shear spring of concrete

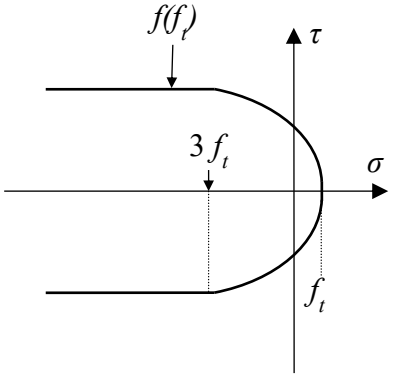

(c) τ_{max} criterion of concrete

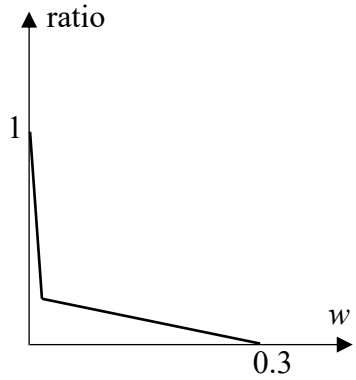

(d) Shear reduction factor

Figure 2.2 Constitutive models of concrete

2.2.2 Numerical model of steel

The geometry of steel elements is modeled in an accurate manner to properly account for the interlocking between concrete and a reinforcement bar (Figure 2.3). The normal springs of steel elements are modeled based on the stress-strain relationship of steel bars proposed by Shima et al. [5]. The stress-strain relationship used for the normal springs is represented by Eq. (2.1). Meanwhile, the shear springs used for the steel elements are assumed to be elastic.

$$\begin{aligned} \sigma &= E_s\varepsilon && if\ (\varepsilon < \varepsilon_y) \\ \sigma &= f_y && if\ (\varepsilon_y \le \varepsilon \le \varepsilon_{sh}) \\ \sigma &= f_y + (1 - e^{\frac{\varepsilon_{sh}-\varepsilon}{k}})(1.01f_u - f_y) && if\ (\varepsilon > \varepsilon_{sh}) \end{aligned} \quad (2.1)$$

Where k is $0.032(\frac{400}{f_y})^{1/3}$, σ: stress (MPa), ε: strain, f_y: yield strength (MPa), f_u: tensile strength (MPa), and ε_{sh}: initial strain hardening, assumed to be 1.5%

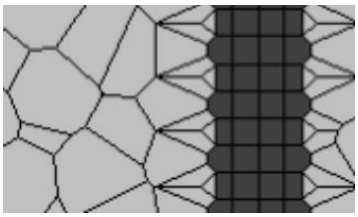

(a) Cross section of steel and concrete element

(b) 3D rebar shape

Figure 2.3 Modelling of geometric shape of rebar

2.3 Corrosion model

2.3.1 Corrosion behavior in reality and in simulation

Once the chloride penetrates reinforced concrete (RC) structures, the reinforcement becomes rust and creates corrosion product which is voluminous material. These phenomena have several effects on reinforced concrete structure, such as, the deformation of rebar due to corrosion, the increment of internal pressure due to voluminous corrosion product. However, in numerical model, the steel element is modeled as rigid element which the shape cannot be deformed. Hence, special modification need to be perform for simulating the corrosion behavior. In RBSM, the mechanical response is simulated by set of spring at the interaction between each rigid element. In order to implement the corrosion behavior, these springs was modified considering the effect of corrosion on mechanical behavior. For example, the reduction of tensile strength of rebar due to the loss of effective correctional area can be simulated by the reduction of yielding strength in rebar.

2.3.2 Expansive strain model

In 3D RBSM, the expansion of corrosion product which forms up around rebar is modeled by the increment of strain at interface between rebar and concrete. The expansion is given as initial strain to the normal spring at interface. The unbalance strain creates the internal expansion pressure to the adjacent concrete. The thickness of corrosion product is the elongation of the normal spring at interface which results from the given initial strain. The length of normal spring can be described in the following equation.

$$H = \frac{H_1 + H_2}{2} \quad (2.2)$$

where H is length of normal spring at interface, H1 and H2 are the normal distance from the phase to center of concrete element and steel element which are composing that phase respectively.

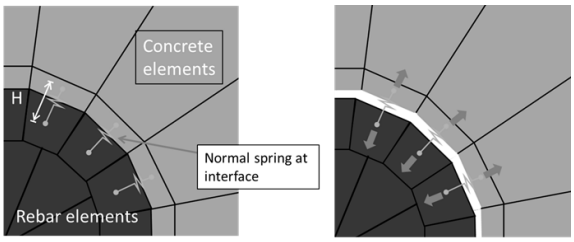

Figure 2.4 Interface between rebar and concrete and given initial strain

Simulation model of corrosion expansion is shown in Fig. 2.4. In 3D RBSM, the deformation around rebar from corrosion product is simulated by using the particularly setting of initial strain control at the interface between rebar and concrete. Eq.3 shows the given expansive strain at interface elements based on local steel weight loss data for these simulations. This value is determined by using reverse method.

In reality, the relationship between the crack width level and corrosion degree can be varied by many factors e.g. corrosion speed, rebar diameter, covering depth and so on. Hence, it is difficult to set the relationship between expansive strain and steel weight loss level for general case. In this study, the reversed method was used to find the relation between expansive strain and corrosion degree. Due to many related factors, the constitutive model for expansive strain and corrosion has been developed case by case. First, the expansive strain direct give to the interface of the simulation model that have the same dimension and same material properties as real experiment. Then, the model will gradually generate the cracking damage from expansion. By comparison the surface crack width between the experiment and the simulation, the relative ship between given expensive strain and corrosion percentage can be obtained as shown in fig 2.5

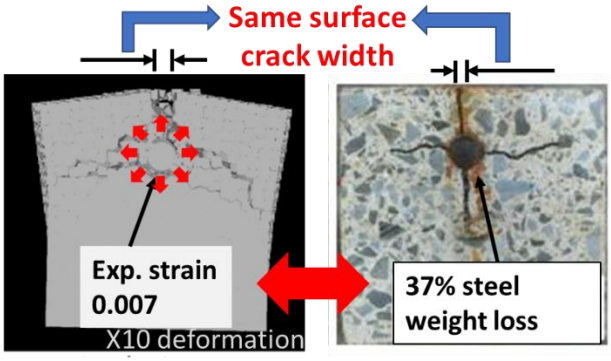

Figure 2.5 Comparison between simulation cracking and experiment for expansive strain model development

For example, to develop the expansive strain constitutive model for a corroded beam in S. Lim experiment in chapter 1 and chapter 4. First, 0.88 mm average crack width from experiment beam at 27% corrosion degree are set as target damage level. Then, the beam simulation with same covering depth and rebar diameter are given the expensive strain at interface to simulate the expansion damage. This expansive strain is gradually increased until the same average crack width was observed in the simulation. As a result, 0.86 mm bottom crack width in simulation was

observed at 0.017 given expansive strain. Hence, the specific linear relationship between expansive strain and corrosion for this simulation was made as shown in Fig. 2.6(a).
By this method, each simulation may have a different expansive strain constitutive model depending on the corrosion speed, rebar diameter, covering depth and concrete material properties. Figure 2.6 shows expansive strain constitutive model for each simulation case that used in chapter 4 and chapter5.

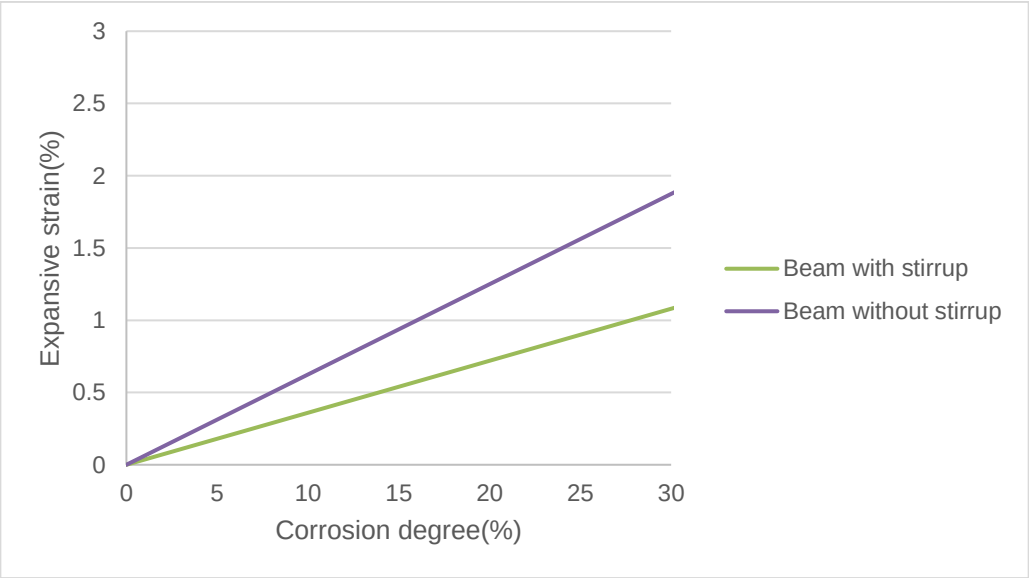

(a) Expensive strain constitutive model for S. Lim's experiment [3]

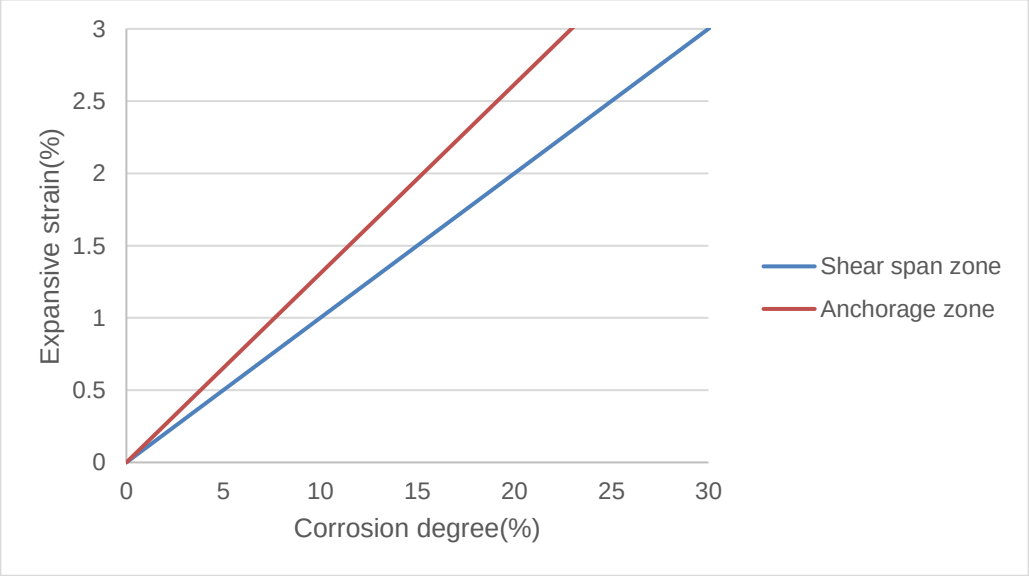

(b) Expensive strain constitutive model for M. Tsunoda's experiment [5]

Figure 2.6 Relationship between given expansive strain at interface and steel weight loss percentage for each simulation case

2.3.3 Spatial Corrosion Model

2.3.3.1 Spatial corrosion of steel bar

Normally, the corrosion is formed up non-uniformly along the rebar. To simulate this characteristic, the corrosion of rebar is model in the same manner as real specimen. The fineness of modification can model at every 5 mm along the rebar which equal to the minimum element size. In simulation, each element is connected by set of spring. For represent the reduction of cross-section area, this spring are modified the yielding strength proportional to the steel weight loss from experiment. And the expansion along the rebar also modify the expansion ratio according to these steel weight loss value.

For example, Fig. 4 illustrates the steel weight loss per 5 mm unit of length over the rebar length from the previous study by S. Lim et al. [5]. The average steel weight loss over the entry length of steel bar from experiment is 27 percent. This information was used as input of corrosion profile in the simulation at every 5 mm same as experimental data. For the steel part where the previous experiment does not provide the data (because the X-ray photogram was not taken), the average steel weight loss 27 percent is assumed to the entire locations (0-250 mm and 1090-1460 mm from the left side of the specimen). The modification of steel properties in numerical model is presented in the following chapter. For detail and simulation results will described in chapter 4.

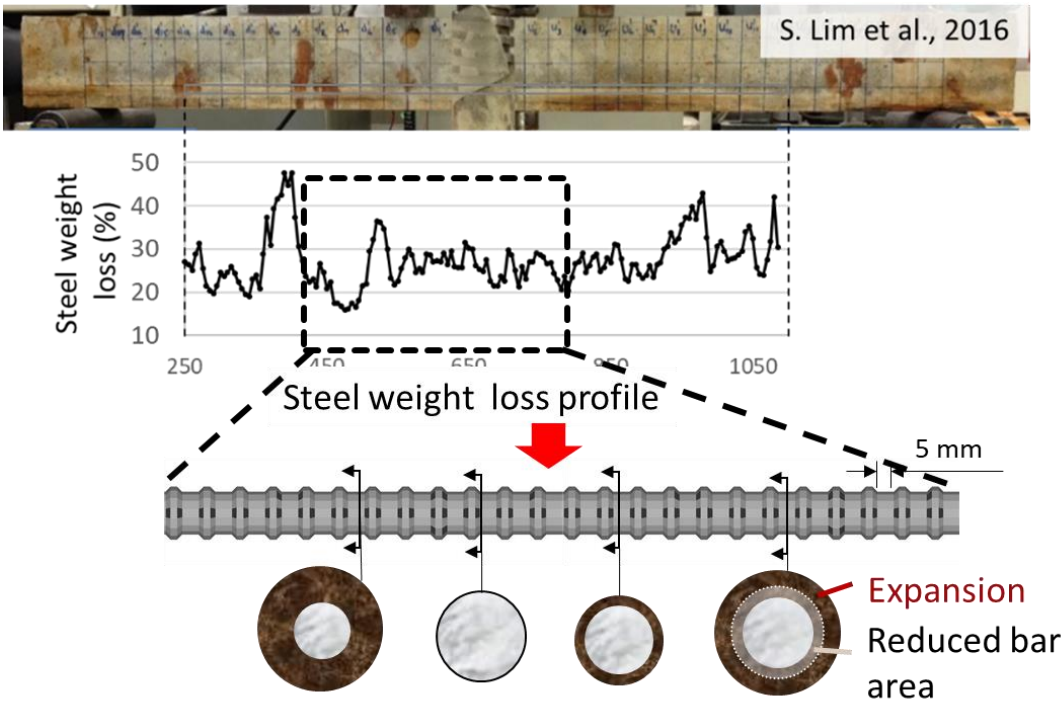

Figure 2.7 Spatial variability in the steel weight loss from expriment and simulation

2.3.3.2 Modification of constitutive model for equivalent residual cross-section of steel bar.

When reinforcement is corroded, one important mechanism is that the steel bar loses its effective cross-section area. However, in RBSM, the steel element is rigid and cannot be deformed in shape

of element. Due to this difficulty in applying the actual reduction of steel volume in the numerical model, an alternative approach was suggested by modifying the response of corroded steel rebar over the corrosion zone. Instead of reducing actual rebar area in simulation, the new stress-strain for corroded element is given by modifying constitutive model.

In reality, reinforcement's tensile strength will be decreased due to loss of effective cross-section ratio. The critical section (highest corrosion percentage) will control the maximum capacity dur to the yielding of critical section. In this numerical model, the normal spring of steel element are locally modified the yielding strength due to steel weight loss percentage information obtained from experiment.
For example, when the corrosion steel weight loss equal to 20 percent, the yielding strength of normal spring at rebar element will be multiply by 0.8 for representing the 20 percent reduction of tensile strength due to effective cross-sectional area.

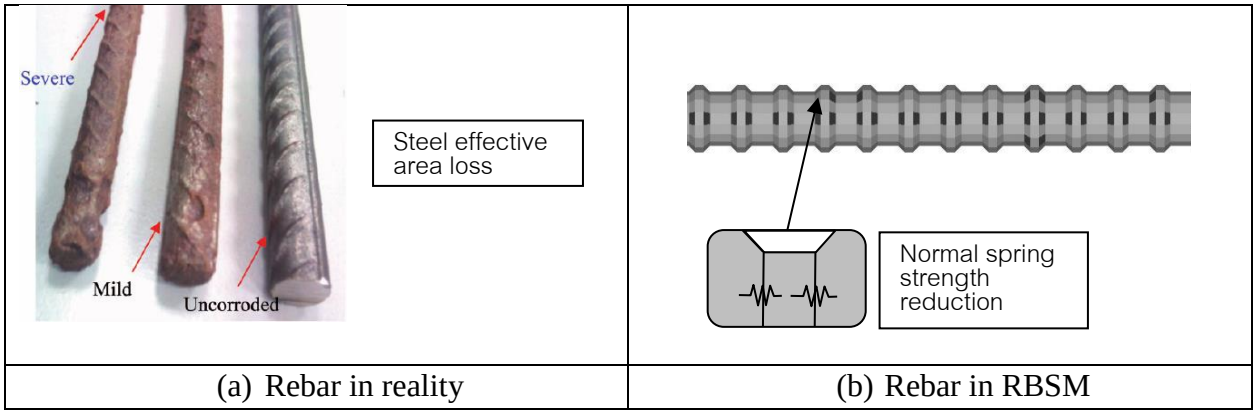

(a) Rebar in reality | (b) Rebar in RBSM

Figure 2.8 Example of normal spring modification for rebar

Corrosion process normally deteriorate the bond between rebar and concrete. Never the less, investigation of corrosion experiment indicated that the small among of corrosion can increase the bond between rebar and concrete. Based on one-week corrosion acceleration results, the pull out capacity of round bar specimens is more than two time higher than the non-corroded specimen. This complex phenomenon occurred due to the increment of internal stress by corrosion product and changing of surface properties. In this study, the equivalent modeling method was proposed to simulate these effects.
In RBSM the interaction between each rigid element are calculated by the response of normal spring and shear spring at element interface. By modeling these springs constitutive model, developer successfully introduced the effect of changing of surface roughness and increment of internal pressure.

2.3.4 Bond deterioration mode

In reality, the corrosion not only deform the rebar shapes or increase the rebar surface roughness, but also create rust product surrounded the rebar. These result in the reduction of mechanical bond due to loss of knot shape and changing in friction bond (or chemical bond) due to the changing of surface roughness. Nevertheless, in the RBSM, the material elements cannot be deformed due to the rigid body modelling. So, we cannot simulate the corrosion phenomena directly.

Therefore, the equivalent modification need to be done for representing these behaviors. In this part, the modification factor for modeling normal spring and shear spring at interface were developed based on designed experiment program. Equation 2.3 and 2.4 show the modification factor of spring properties based on corrosion degree (steel weight loss percentage).

$$M_{shear} = 200 - \frac{100}{0.5x+1} \tag{2.3}$$

$$M_{normal} = 100 - X \tag{2.4}$$

The development of this constitutive model was done by using the experiment results. Detail of experiment and the utilization of experiment results will be described in Chapter 3.

2.4 Benefit of combination of RBSM simulation and corrosion model.

By using these simulation, several benefits can be draw as following:

Initial damage

Normally, to simulate the corrosion behavior in Finite Element analysis, some failure information need to be know in advance for set the pre-crack plane. For example, a simple case like RB beam, the horizontal crack plane along the rebar need to be set in advance for release the force transfer at the crack plane. On the other hand, in RBSM analysis, the crack is automatically calculated as a result of input corrosion data. For example, by giving expansive strain, the internal crack adjacent the rebar will automatically be simulated.

Damage on mechanical bond

Damage of surrounding concrete also automatically simulated by expansion simulation. So, the reduction of mechanical bond (interlock between rebar and concrete) is automatically calculated in this simulation.

Inspect inside damage

One benefit of this numerical model is that the internal damage and internal stress are easily observed. The program can present the 3D internal crack damage or show the stress concentration at any designated cross-section, which make it convenient for classify the failure criteria or planning for retrofitting.

Revealing residual properties

We can simulate the residual capacity after the corrosion damage take place. Or even predict further corrosion damage and predict future capacity of the structure.

2.5 Conclusions

In this chapter describe about two numerical simulation system that has been used in this research, RBSM and corrosion model. In the recent study, corrosion model is then used to simulate the deterioration of reinforced concrete due to corrosion effects such as expansion crack or loss of rebar cross-section, then the mechanical properties of corroded RC member will be calculated by using RBSM.

The couple simulations are combined to create the simulation system that are able to predict the local failure of concrete considering the corrosion effect that that was directly modified from the experimental data. In RBSM, the response of normal spring and shear spring represent the mechanical response of RC member. By modifying the constitutive model of these springs, the response of spring

changed in the same manner as real corroded structure. These modifications are locally done based on corrosion information at every 5 mm. The details of simulation results from this coupling simulation will be described again in Chapter4.

REFERENCES

[1] Kohei Nagai, Yasuhiko Sato, Tamon Ueda, *Mesoscopic Simulation of Failure of Mortar and Concrete by 2D RBSM*, Journal of Advanced Concrete Technology, Vol.2, No.3, 2004, pp.359-374.

[2] Kohei Nagai, Yasuhiko Sato, Tamon Ueda, *Mesoscopic Simulation of Failure of Mortar and Concrete by 3D RBSM,* Journal of Advanced Concrete Technology, Vol.3, No.3, 2005, pp.385-402.

[3] Sopokhem Lim, Mitsuyoshi Akiyama and Dan M. Frangopol, *Assessment of the structural performance of corrosion-affected RC member-based on experiment study and probabilistic modeling*, Engineering structures 127, 2016, pp.189-205

[4] K. Watanabe, Masahiko Tsunoda and Junichiro Niwa, *Influence of Local Steel Corrosion on Shear Failure Mechanism of RC Linear Members,* Sixth International Conference on Concrete under Severe Conditions: Environment and Loading, 6 June 2010

[5] Masahiko Tsunoda, Junichiro Niwa, *Influence of local steel corrosion on shear failure mechasiam of RC member,* Concrete research and technology, 15(2),2004, pp.69-77

[6] Liyanto EDDY, Kohei NAGAI, *Effect of Stirrups Arrangement on Failure of Beam Column Joint with Mechanical Anchorages by 3D Discrete Model*, コンクリート工学年次論文集, Vol.37, No.2, pp.313-318, 2015.

Chapter 3
Bond deterioration model development based on pull out test experiment

3.1. General

In the real phenomena, when corrosion occurs, it will not only deform the rebar shapes, but also create rust product surrounded the rebar. These result in the reduction of mechanical bond due to loss of knot shape and increment in friction bond due to the changing of surface property (roughness increase).
However, in the RBSM simulation, the material elements are modelled as a rigid body which the shape cannot be deformed. So, we cannot simulate the corrosion phenomena directly. Therefore, the equivalent modification need to be done for representing these behaviors.
In the reality the bond between rebar and concrete consist the mechanical bond and local bond. While in the RBSM, the elements are interconnected to the adjacent element by shear spring and normal spring. The response of spring represents the interaction between each rigid element. Therefore, instead of modification of the element shape, we can modify the constitutive of these springs to represent the effect of corrosion in the simulation. For example, the bond deterioration or the friction loss due to the slippage of corrosion products can be represents by the reduction of shear spring strength, or the expansion of corrosion product can be simulated by the expansive strain of normal spring at steel-concrete interface.
To develop the appropriated bond deterioration model, the real experimental data are necessary. In this study, the author has conducted the corrosion acceleration test on single reinforced concrete specimen for making specimens with different corrosion degree. The pull-out test experiments were performed on concrete specimen reinforced with corroded deformed bar and corroded plain bar with different corrosion degree. By utilizing these experimental data, the author can classify the bond in RC into mechanical bond which come from interlocking between rebar knot and concrete and the chemical bond or friction at interface between concrete and rebar. The effect of corrosion on the bond deterioration at different corrosion degree can be extracted from these experiments.
This chapter describes about the development of bond deterioration model since the experiment setting step by step until the utilization of experimental data for bond model development.

3.2 Experiment program

3.2.1 Experiment concept

In this study, the author wants to classify the bond at interface between rebar and concrete and their changing when the corrosion occur. In general, the bonding mechanism between rebar and concrete involve mechanical bond and chemical bond.

By the pull-out test of concrete specimen reinforced with the round bar, the resistance force is only the friction bond which can be calculated by the rebar-concrete contact area and the maximum pull out capacity. By the pull out of deformed bar, the resistance form is the contribution between the friction and mechanical bond. Therefore, by performing the pull out test on different corrosion degree specimens, the change of these bond due to the corrosion can be extracted.

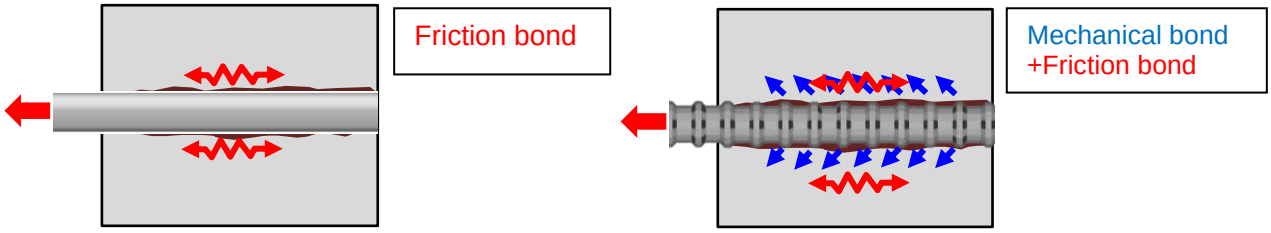

(a) Pull out test of round bar (b) pull out test of deformed bar

Figure 3.1 Resistance force in pull out of round bar and deformed bar

3.2.2 Experimental sequence

In this experiment the concrete specimens reinforced with round bar and deformed bar were prepared. After around 28 days curing in wet condition, the electrical acceleration corrosion test will be performed to accelerate the corrosion process in the specimen. After reach the target current-time, the specimens were measured the surface cracked width. Fig 3.3 shows the corrosion acceleration test and the surface crack width measurement. The specimens were then tested by the pull-out method for finding the changing of the bond at different corrosion percentage. However, in this stage, the concrete part of specimens basically had the corrosion cracking from the rust expansion. Therefore, the pull-out capacities obtained at this step would have the effect from mechanical bond deterioration from the concrete damage. Therefore, second pull out test of specimens with non-crack concrete is needed.

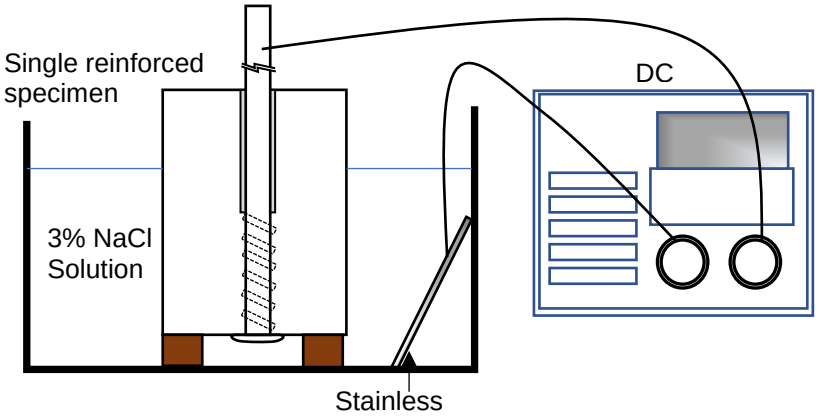

(a) Corrosion acceleration experiment (drawing)

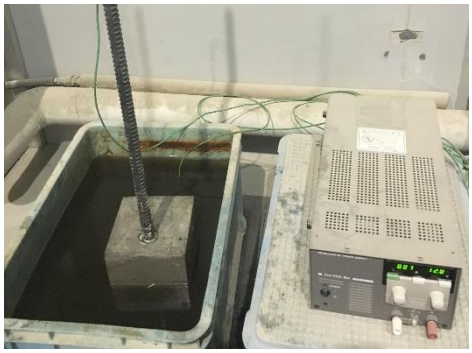

(b) Corrosion acceleration experiment (real photo)

(c) Surface crack width measurement on corroded specimen

Figure 3.2 Corrosion acceleration experiment

After the pull-out test on the cracked concrete specimen, the concrete cover was removed, and the same rebar was used again to cast the new specimen. After around 28 days of curing under wet condition, the specimen were tested by the pull-out method again for finding the changing of the bond without the effect of cracked concrete.

Fig 3.3 shows the form work of specimens that reinforced with corroded rebar. Fig 3.4 show the pull-out test experiment.

(a) Corroded bar removal

(b) Formwork of corroded reinforcement specimen

Figure 3.3 Preparation of corroded reinforcement specimen

Figure 3.4 Pull out experiment

3.2.3 Mix proportion of concrete

The mix proportion of concrete used for specimens is shown in Table 3.1.

Table3.1 Concrete mixpropertion

G_{max} (mm)	Slump (cm)	W/C [%]	S/A [%][	Unit weight kg/mm^2				AE [g/10L]
				water	cement	Fine aggregate	Coarse aggregate	
25	8±2	0.60	0.45	169	283	823	1023	13.3

3.2.4 Overview of specimens

Table 3.2 shows the list of specimens used in this study and their steel weight loss percentage after the corrosion test.

Table 3.2 List of specimen case

Name	Reinforcement	Corrosion time (weeks)	Concrete condition	Steel weight loss
RB-0W-NC	RB	0	No cracking	0
RB-1W-C	RB	18.5	Crack from corrosion	3.0
RB -2W-C	RB	37		5.3
RB -4W-C	RB	74		12.1
RB -0W-NC	RB	0	No cracking	0
RB -1W-NC	RB	18.5		3.0
RB -2W-NC	RB	37		5.3
RB -4W-NC	RB	74		12.1
DB-0W-C	DB	0	No cracking	0
DB-2W-C	DB	37	Crack from corrosion	10.5
DC-4W-C	DB	74		23.1
DB-0W-NC	DB	0	No cracking	0
DB-2W-NC	DB	37		0
DB-4W-NC	DB	74		0

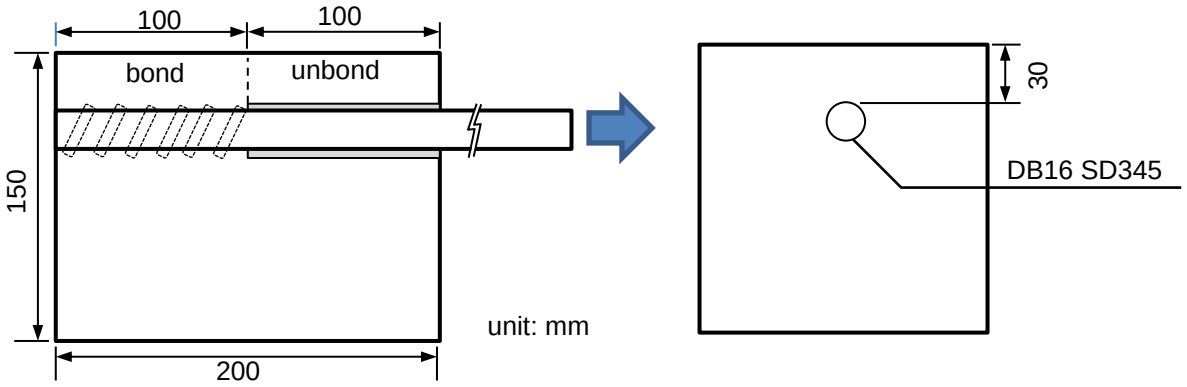

(a) Deformed bar specimen

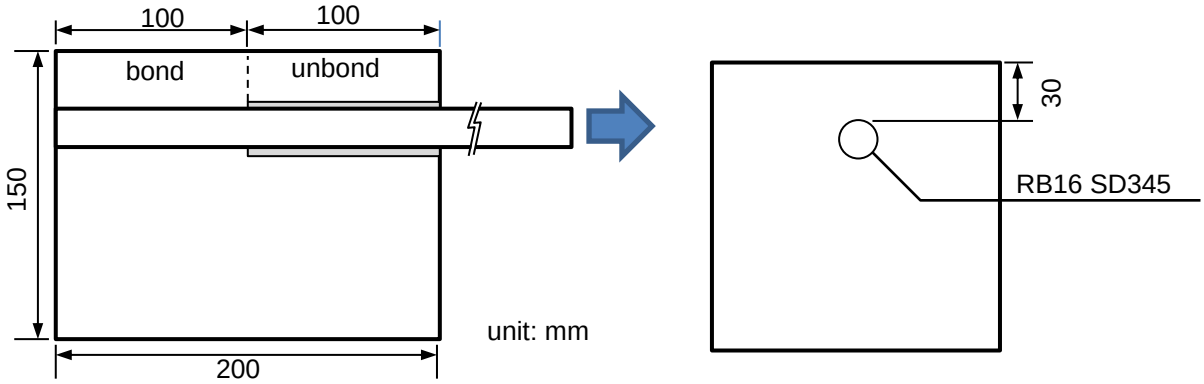

(b) Plain bar specimen

Figure 3.5 Specimen dimension

Figures 3.5 (a) and (b) show the specimen layout and pull-out test condition of RC specimens reinforced with deformed bar and plain round bar. Single reinforcement was embedded in each rectangular specimen. The test specimen was basically a concrete cube 200mmx150mmx150mm with a bar embedded coaxially. One end of the rebar was projected about 12 mm to measure the free end slip, while the loaded end was jutted out about 850mm in order to grip the rebar for applying the tensile force by loading jack. The specimens were cast using two types of 16 mm diameter rebars, plain bar and deformed with same embedment lengths. By using plasticine and plasticine the required embedment length was achieved. To achieve 100 mm embedment length at the free end of the specimen. Plasticine were used to unbond the bars from concrete over 100mm length. The plasticine neither restrains the slip of the bar nor affects the transfer of bar forces to concrete.

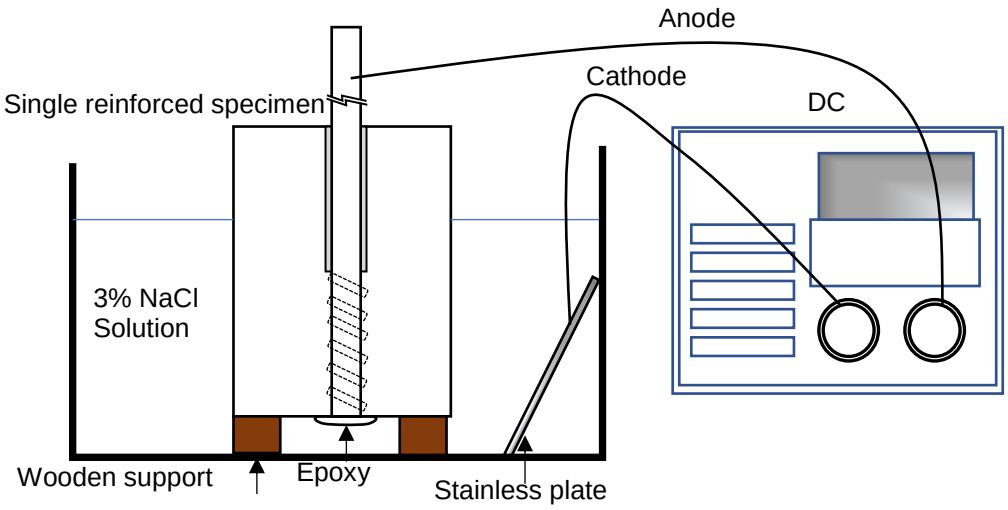

Figure 3.7 Outline of electrical corrosion acceleration test

3.2.5 Steel Corrosion acceleration experiment

Steel corrosion acceleration test was conducted at 28 days after casting in order to create longitudinal reinforcement corrosion. The method of steel acceleration test is the electric corrosion test as shown in Fig.3. All specimens had a wire connecting to the end of longitudinal reinforcement in order to apply the electric direct current by a power source. The bond length parts of specimens were soaked in 3 % NaCl solution. The free end steel bar was covered by epoxy adhesion to prevent the direct contact to the NaCl solution.
The specimens were provided electricity of 0.11A at different time to create different corrosion percentage along the rebar as show in Table3.2.

3.2.6 Evaluation of steel corrosion

To evaluate the amount of steel corrosion, the value C of Eq. XX was used as follows:

$$C = \frac{W_o - W_c}{W_c} \times 100$$

where, C is the mass reduction ratio (%), W_c is the mass per unit of length of an original steel (g/mm), W_c is the mass per unit of length of a corroded steel (g/mm). After the loading test, longitudinal reinforcements were taken out from RC members and cut in piece to measure corrosion degree. These bars were soaked in 10 % diammonium-hydrogen-citrate with 60 degree Celsius for two days and were rubbed with brushes to clean up corrosion products. Then these bars were cut into pieces with 100 mm length. Then, by comparing the loss unit weight of these corroded bar and non-corroded bar, the corrosion degree can be obtained. Fig 3.7 show the photo of steel bar in this experiment

3.2.7 Pull out experiment

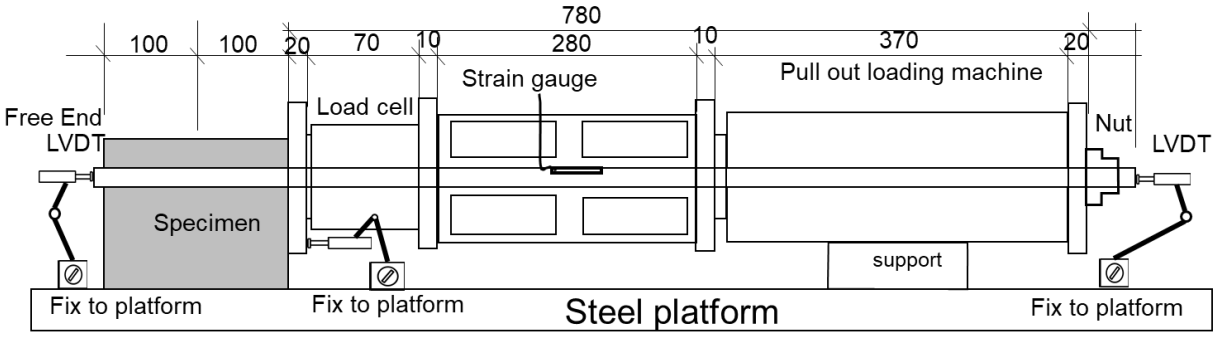

(a) Drawing of pull out test experiment

(b) Pull out test experiment

Figure 3.8 Pull out test setting and displacement measurement

Pull-out test was conduct after corrosion acceleration test reaching the target total current (time×current). The specimen was removed from the NaCl solution and cleaned the rust that leaked out from crack surface. The LVDTs were set on each end of the rebar both the free end and the loaded end. On the loaded end, the rebar was jutted out about 850mm in order to grip the rebar for applying the tensile force by loading jack. The strain gauge was placed at steel bar between concrete surface and loading jack. The pulled-out load was applied until the failure occurred (pull out capacity continuously dropped or concrete splitting crack occurred.

Fig 3.8 show the setting of pull out test experiment and the measurement of displacement and strain. The displacement of rebar at the free end pull out end and concrete surface at pull out side were recorded. The relative displacement or pulled-out length of rebar, L are calculated as follows:

$$L_p = D_e - D_s - (L \times \varepsilon) \tag{3.1}$$

where L_p is relative displacement or pulled out length, D_e displacement from LVDT at pull out end, D_s is displacement from LVDT at surface of concrete, L is rebar length at outside of concrete and ε is the strain value measure from strain gauge.

The bond capacity of specimen is calculated by Equation 3.2 as follows:

$$\tau_{max,i} = \frac{P}{A} \tag{3.2}$$

Where $\tau_{max,i}$ is the maximum bond capacity of specimen ith (N/mm^2), P is the maximum pull out capacity of specimen (N), A is the contract area between reinforced rebar and concrete (mm^2),.

3.3. Experimental results

3.3.1 Results of electric corrosion test

a) Concrete damage condition

RC specimens had some cracks (corrosion crack) along longitudinal reinforcement on their top surface (which are the thinnest covering depth) partly and some rust due to steel corrosion. Amount of rust increased with the increasement of total current (time×current). The surface crack width also increased with the total current. These cracks occurred due to the increment of internal pressure from the voluminous corrosion product. It can be seen in Fig3.9 that there was some corrosion product leaked out from the interface between rebar and concrete at pull-out end surface. Fig 3.8 shows the top surface of corroded specimen. Table XX show the average crack width of each specimen.

(a) **(b)** **(c)**

(a) , (b) Concrete surface condition of 2 weeks and 4 weeks corrosion test specimens

(b) leaking of corrosion product

Fig 3.9 Specimen after corrosion test

b) Steel damage condition

The steel weight loss of steel bar is obtained by measuring the unit weight of steel after the pull-out test. By removing the concrete for checking steel condition, the corrosion are found along the bond length location. The unbonded zone which the steel bar was wrapped by plasticine is almost no corrosion. In bond length zone, corrosion of each specimen is` higher value at the top surface side which is the thinnest covering depth.

It was confirmed that the local steel corrosion was created in all specimens by the electric corrosion test.

(a) (b)

(a) No corrosion rebar weight measuring (specimen length 99.5 mm)

(b) 2 weeks corrosion rebar weight measuring (specimen length 110 mm)

(c) (d)

(c) 3 weeks corrosion rebar weight measuring (specimen length 97 mm)

(d) 4 weeks corrosion rebar weight measuring (specimen length 116 mm)

Figure 3.10 Corroded deformed bar weight loss measurement

3.4 Development of shear spring modification based on pull out test of RB with non-crack concrete

3.4.1 Experimental results of corroded round bar with non-crack concrete

(a) Non- corroded round bar (0% corrosion)

(b) 1 week corroded round bar (3.0% corrosion)

(c) 2 weeks corroded round bar (5.3% corrosion)

(d) 4 weeks corroded round bar (12.1% corrosion)

Figure 3.11 Corroded round bar from corrosion acceleration experiment

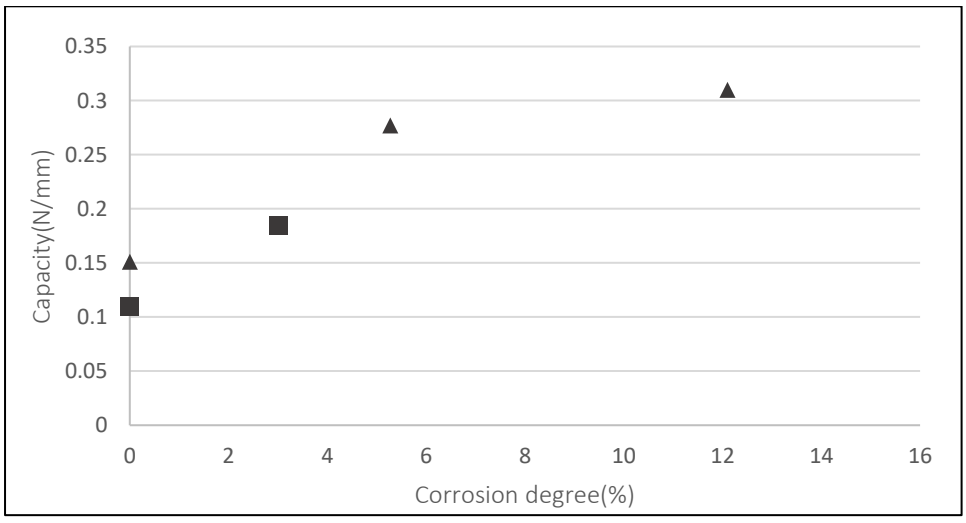

Figure 3.12 Maximum pull out capacities of corroded round bar with non-crack concrete

Fig 3.12 shows the maximum pull out capacities of corroded round bar with non-crack concrete. In case of pulling-out of corroded bar, it is obvious that once the corrosion occurred, the pull-out capacity significantly increases. This increment was occurred due to surface roughness. The maximum pull out capacity increase up to around 2 times of original capacity without corrosion.

3.4.2 Proposal for corrosion simulation/ modification of constitutive model at interface

Modification of Tua max criteria for shear spring

In RBSM simulation, the stress in normal spring affects the shear spring. As show in FixXX in chapter2 (show constitutive model of Tua max model in concrete). The increment of confinement of force in normal spring at element interphase increase the maximum shear stress in shear spring. In reality, when consider the surface condition under corrosion, the roughness of surface should provide microinterlocking between steel and concrete. Then, under the same confinement, the rough surface should provide more friction force comparing with the smooth surface. The results of pull out test of corroded plain bar at different corrosion degree also confirm this assumption.
Hence, in this part, the maximum shear stress of spring was modified with the effect of corrosion percentage.

Based on experimental results of pull out corroded round bar with good concrete, we can plot the relationship between steel weight loss percentage and increment of pull out capacity as show in Figure 3.12. Consider the real phenomena, the surfaces roughness should not be decreased. The increment of this value should not be increase more than friction between concrete. Because all experiments of pull out corroded round bar were failure by slipping pattern at interface between rebar and concrete, which means there was no cracking occurred in concrete phase. So, to model this behaviour in RBSM, the increment of Shear spring maximum shear stress at interface should not higher more than concrete. Consider these reason, the constitutive model for corrosion factor are proposed as the following equation (Equation 3.3).

$$M_{shear} = 200 - \frac{100}{0.5x+1} \tag{3.3}$$

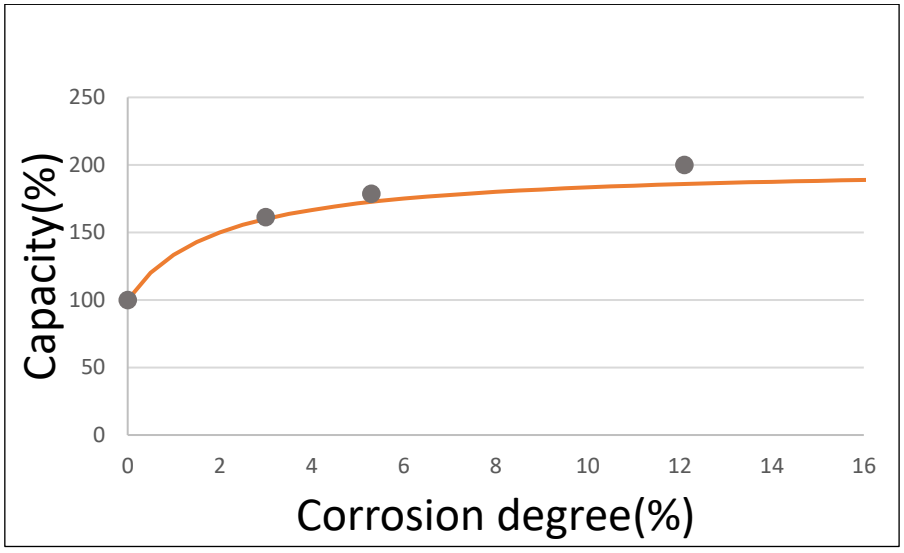

Figure 3.13 Modification of shear spring constitutive model

3.4.3 Thin model for verification

This section aims to confirm the effect of corrosion parameter on shear force or pull out capacity. So the pull out simulation with different corrosion factor were simulated for observing the effect of increment of maximum shear stress by new constitutive model.
.To cut the effect of stress transfer due to the long bond length, the short bond length specimen are simulated. The model dimension is 150x150x40 mm^3 with RB16 at 30 mm covering depth. The specimen thickness are set as 2.5 times of rebar diameter. The boundary condition was set by X-movement fix of concrete on right side. The steel was pull to the X direction at rate of 0.005 mm/step until the failure occurred.

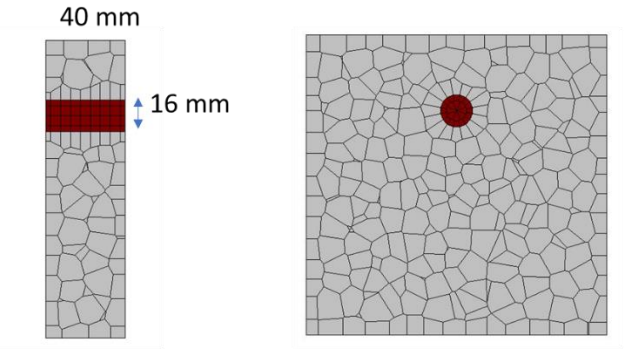

Figure 3.14 Short bond specimen for verify the equation

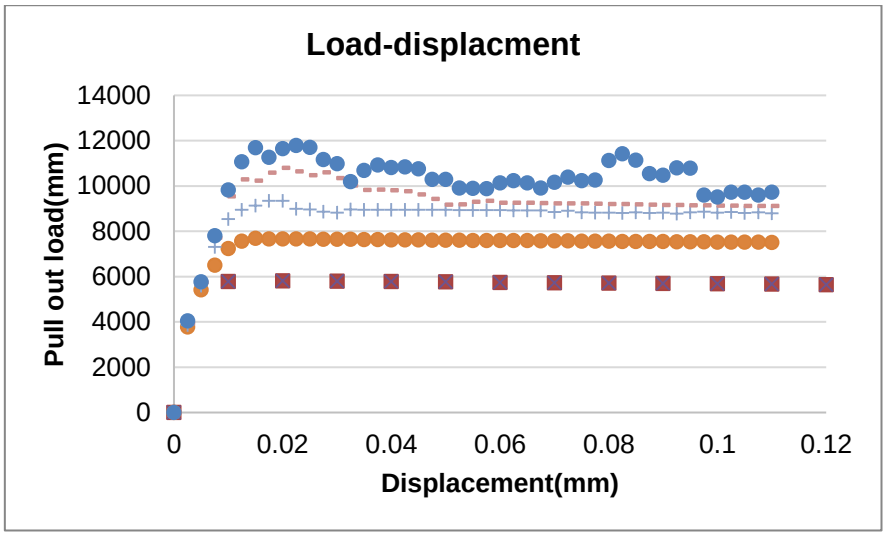

Figure 3.15 shows the load-displacement relationship of each simulation cases. The original maximum shear stress at interface are is modelled by equation 3.4

$$\boldsymbol{A} = M_{shear}[1.6TEN(IS)^2 \times [-BANE(is,2) * SN + TEN(IS))]^{\mathbf{0.4}} + \mathbf{0.15}TEN(IS)]$$

Where f_t is set as half of concrete tensile strength and BANE are stiffness of concrete. Therefore, when X_{cor} increase more than 4 times, the shear stress at interface will equal or higher than that of concrete(depend on element size), that make the failure might not occur at interface between rebar and concrete. So, the post-peak behaviour become scatter as the X_{cor} close to 4.

3.4.4. Apply to model based on pull out of round bar sound concrete experiment

The analysis models used in this study were formed up based on the previous experimental study. The concrete specimens size of 200×150×150 mm^3 reinforced with corroded plain bar diameter of 16mm. To prevent the concrete from corrosion cracking the concrete specimen reinforced with plane bar were prepared for corrosion acceleration test before removing the steel from damage concrete. The corroded steel was then used to reinforce the new casting specimen.

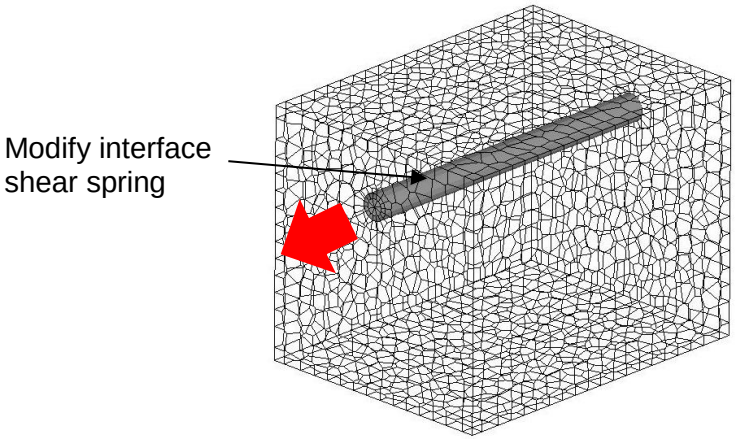

(a) Model overview

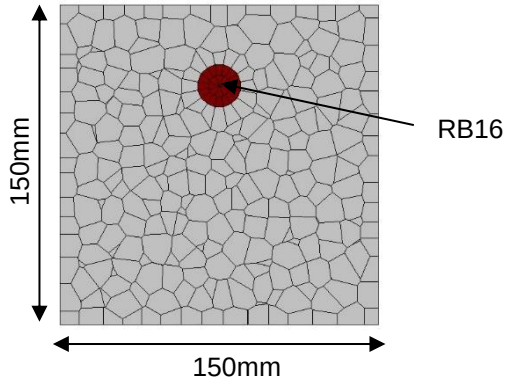

(b) Front view cross-section

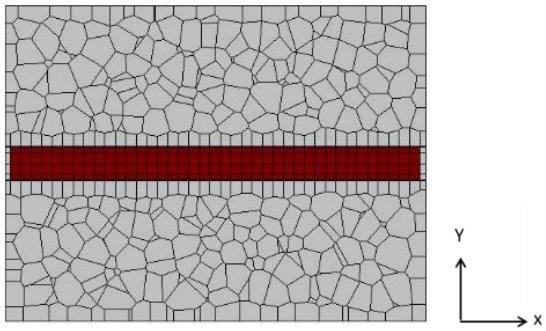

(c) Top view cross-section

Figure 3.16 Geometry of numerical model by RBSM (Unit: mm)

Table 3.3 Material properties in simulation

Term	Unit	Concrete	Reinforcement
Compressive strength	MPa	32	-
Elastic modulus		27800	184000
Yielding strength		2.74	389.0

The maximum shear stress of rebar at interface was modified based on the experimental results. Material properties obtain form cylinder compressive strength test and rebar pulling are used as input simulation material properties as showed in table 3.1.

Table 3.4 Specimen cases.

Specimen	Corrosion pattern	Average corrosion degree
N-C	None	0%
1W-RB-GC	Uniform	3.0 %
2W-RB-GC	Uniform	5.3 %
4W-RB-GC-C	Non-uniform	12 %

3.4.5 Simulation results

Figure 3.17 shows the load-displacement of pull out corroded round bar with non-crack concrete simulation at different corrosion percentage same as experiment. When consider the peak pull out capacity. The simulation can simulate the increment of maximum pull out capacity due to the changing of corrosion percentage appropriately comparing with the experimental results.

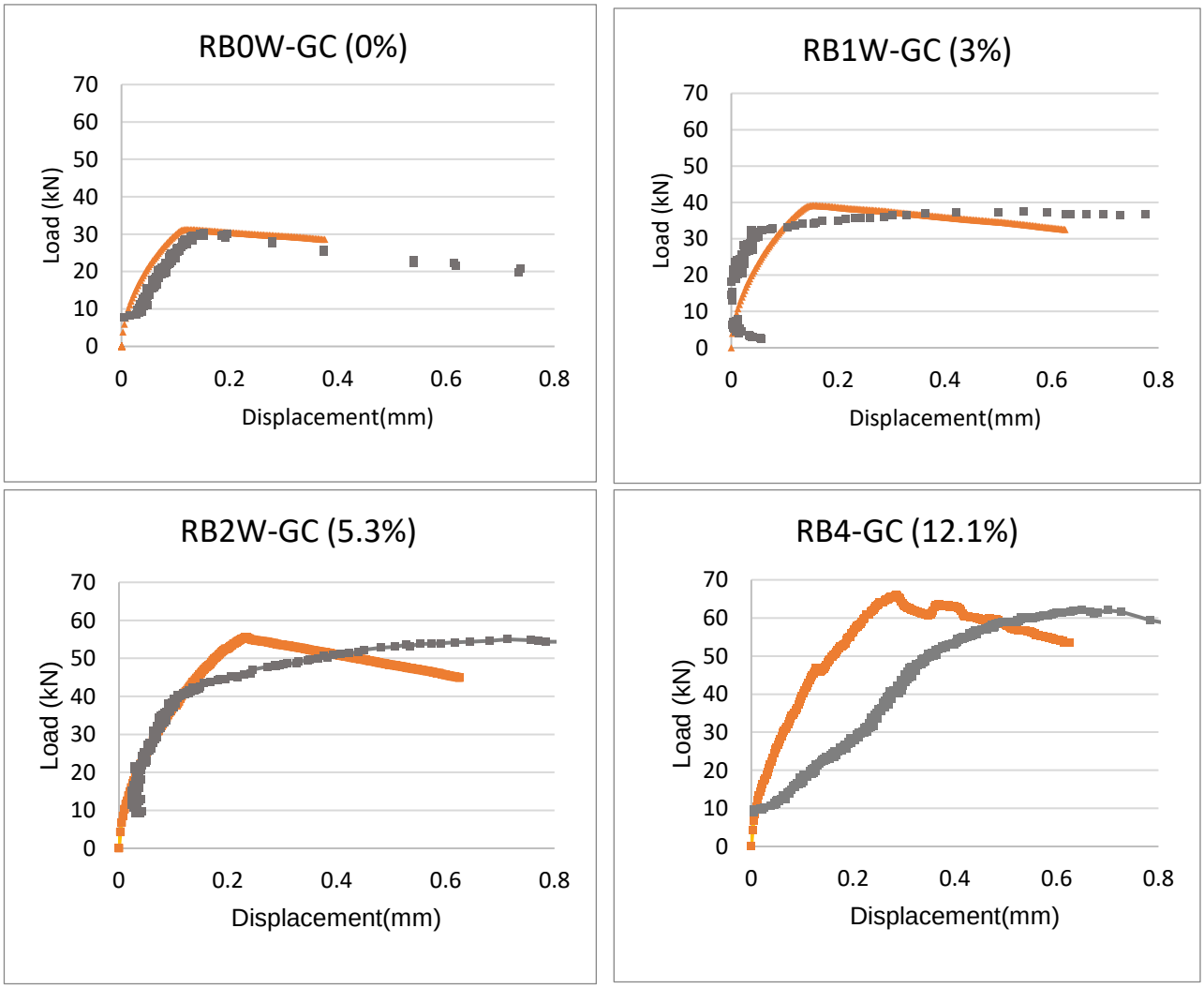

Figure 3.17 Load displacement of pull out corroded round bar with non-crack concrete simulation at corrosion percentage of 0%, 3%, 5.3% and 12.1% respectively

In case of corrosion percentage 12.1 %, simulation results show a little scatter trend comparing the other case. The reason id that when corrosion degree is 12.1%, M_{cor} value from equation 3.3 equals to 184%. Therefore, the increment of shear spring at interface will increase almost up to two time of original interface shear strength which will close to that of surrounded concrete. As a result, the local damage will not occurred at the in the face between rebar and concrete. But the failure will appear at the surrounded concrete instead.

From overview, the constitutive model for modification of shear spring was well developed and can represent the increment of surface roughness or friction bond increment appropriately.

3.4.6 Pull out test results of corroded round bar specimen with cracked concrete

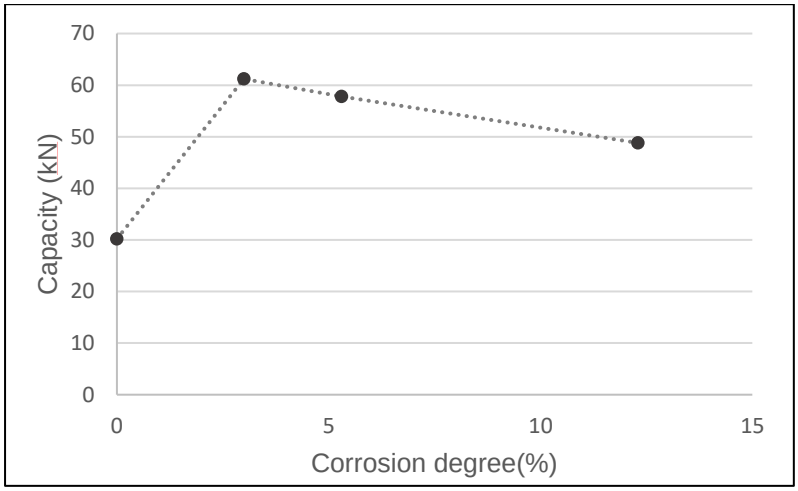

Figure 3.18 Pull out capacity of corroded round bar specimen with cracked concrete

In case of the specimen with corrosion crack, first, the pull-out capacity significantly increases even small corrosion amount taking place, then the capacity gradually drops when amount of corrosion increases due to concrete damage. This behavior is the combination between the surface roughness increment and the loss of mechanical bond between rebar and concrete that was decreased due to corrosion cracking. To simulate this behavior the simulation model of shear modification constitutive model and expansive strain model were used. The results are showed in Section 3.6.

3.5 Development of shear spring modification based on pull out test of deformed bar with non-crack concrete

3.5.1 Experimental results of corroded round bar with non-crack concrete

Fig 3.19 shows the rebar shape that was cleaned the rust after the pull out experiment finish. It can be seen that not only the surface roughness increase due to the corrosion, but the shape of the rebar knot also deformed from the original shape in no corrosion case.

(a) No corrosion deform bar

(b) 2 weeks corrosion deformed rebar

(c) 4 weeks corrosion deformed bar

Figure 3.19 Corroded deformed bar from corrosion acceleration experiment

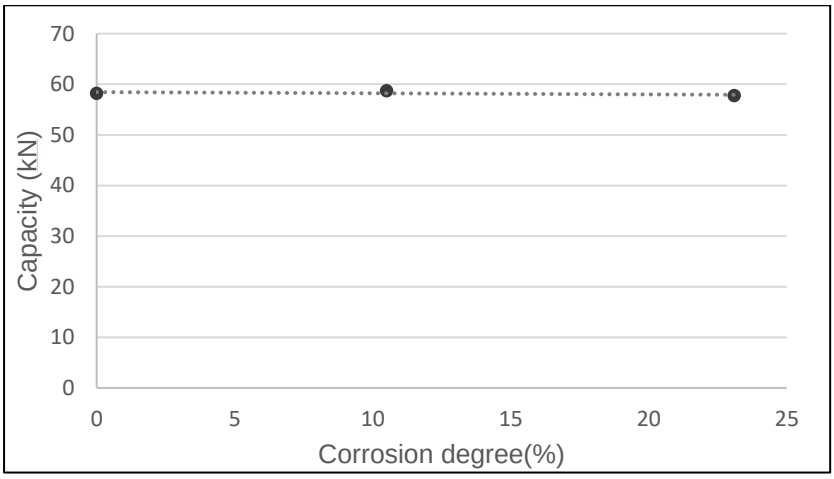

Figure 3.20 Maximum pull out capacities of corroded deformed bar with non-crack concrete

Fig 3.20 shows the maximum pull out capacities of corroded deformed bar with non-crack concrete. In case of pulling-out of corroded bar, it is obvious thateven the corrosion degree increase up to 23.1%, the pull-out capacity almost no change (less than 3% decreases comparing with the no corrosion condition). It can be assumed that the total bond of pull out the of corroded deformed bar without concrete damage is no change when the corrosion degree is lower than 23 %.

In order to extract the mechanical bond changing from the total bond, super position theory was assumed. The friction bond in equation 3.3 was subtracted from the total bond by superposition theory. The remaining mechanical bond are shown in figure 3.21.

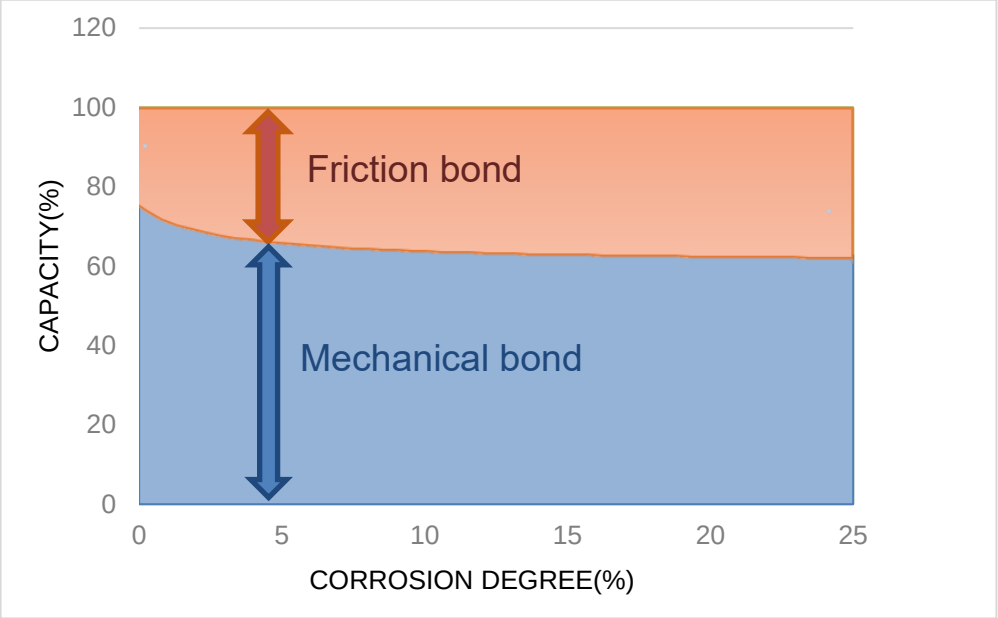

Figure 3.21 Finding mechanical bond based on superposition theory.

However, the reduction trend of mechanical bond shown in figure 3.21 containing many local behaviors such as the knot deformation, the remaining of rust at interface, the sliding-opening effect and so on. Therefore, simple linear equation was proposed to represent the reduction from these behaviors.

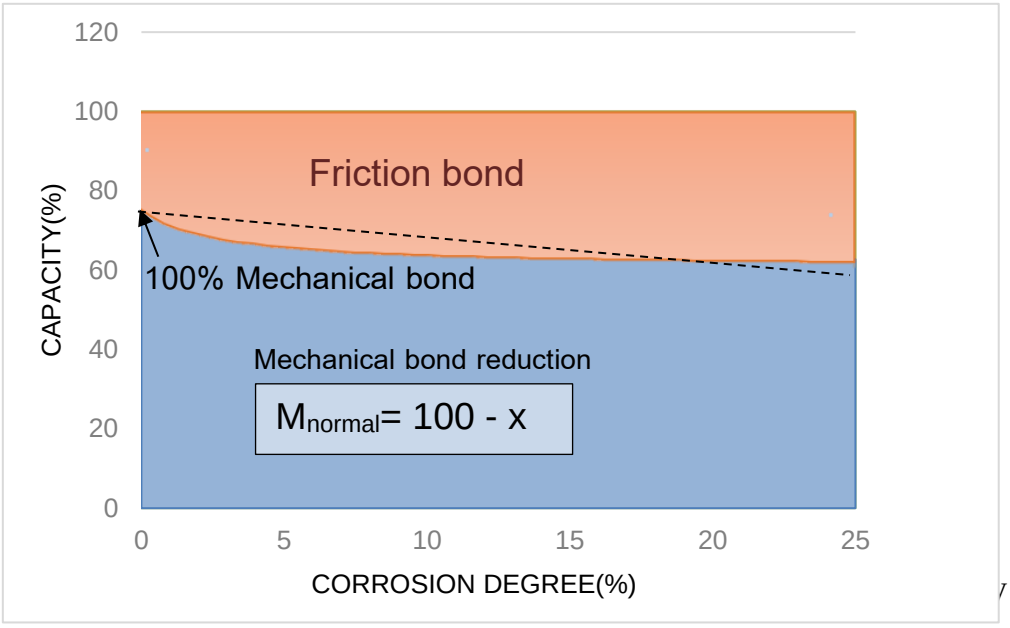

The modification factor of normal spring constitutive model based on corrosion percentage are proposed as the following equation (Equation 3.4).

$$M_{normal} = 100 - X \tag{3.4}$$

Where M_{normal} is the modification factor for normal spring stiffness and capacity, X in the corrosion percentage ($0 < X < 23$)

3.5.2. Apply to model based on pull out of deformed bar sound concrete experiment

The analysis models used in this study were formed up based on the previous experimental study. The concrete specimens size of 200×150×150 mm^3 reinforced with corroded deformed bar of 16 mm diameter. The bond length is 100 mm from the free end. The interface modification due to the deterioration model of normal spring and shear spring which states developed in section 3.5.1 and 3.4.1 were applied at the interface between rebar and concrete at the bond length. Figure 3.23 shows the dimension of simulation. The list of simulation cases is shown in table 3.5.

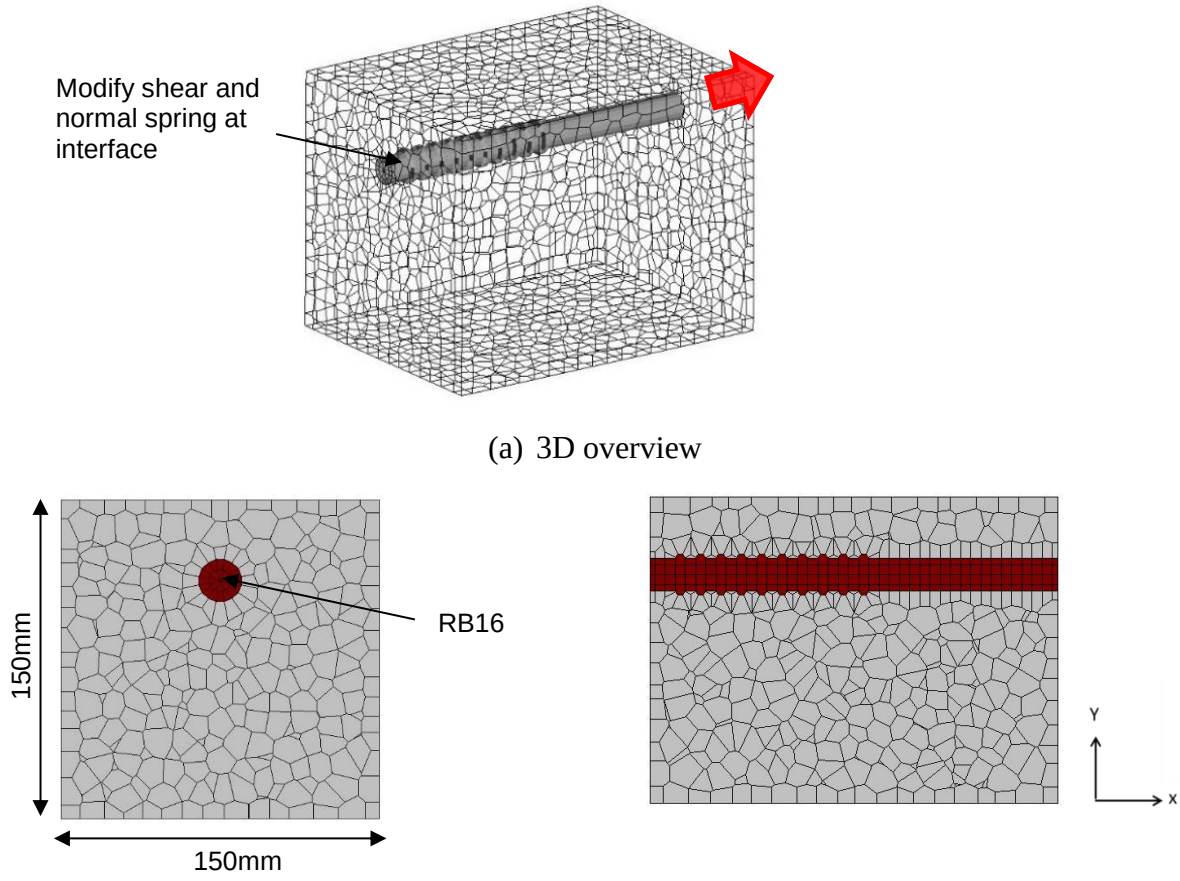

(a) 3D overview

(b) Side view crossection

(c) Top view crossection

Figure 3.23 Geometry of numerical model by RBSM (Unit: mm)

Table 3.4 Material properties in simulation

Term	Unit	Concrete	Reinforcement
Compressive strength	MPa	32	-
Elastic modulus		27800	184000
Yielding strength		2.74	389.0

The maximum shear stress of rebar at interface was modified based on the experimental results. Material properties obtain form cylinder compressive strength test and rebar pulling are used as input simulation material properties as showed in table 3.4.

Table 3.5 Specimen cases.

Specimen	Corrosion pattern	Average corrosion degree
N-C	None	0%
2W-DB-GC	Uniform	10.5 %
4W-DB-GC-C	Uniform	23.1 %

3.5.3 Simulation results

Figure 3.24 shows the load-displacement of pull out corroded round bar with non-crack concrete simulation at different corrosion percentage same as experiment. When consider the peak pull out capacity. The simulation can simulate the increment of maximum pull out capacity due to the changing of corrosion percentage appropriately comparing with the experimental results.

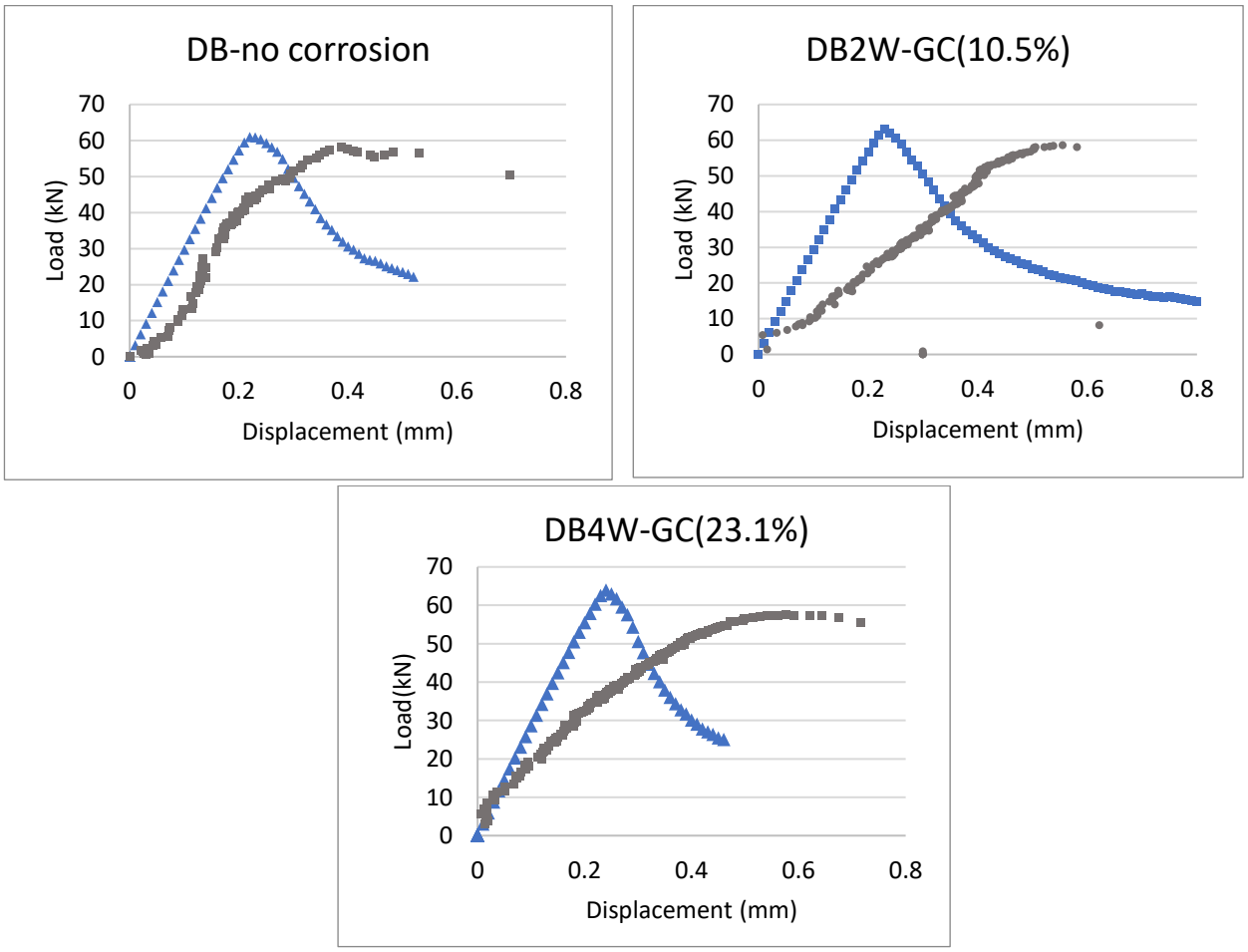

Figure 3.24 Load displacement of pull out corroded deformed bar with non-crack concrete simulation at corrosion percentage of 0%, 10.5% and 23.1% respectively

From the simulation results, the simulation can simulate the peak pull out capacity of the experimental results appropriately based on input corrosion percentage. In case of no corrosion, simulation results show a similar trend comparing with the experimental results. While in case of 10.5% and 23.1% corrosion degree, the experimental result shows the less stiffness than simulation results. From overview, the constitutive model for modification of normal spring was well developed and worked will with the shear spring and can represent the similar bond changing at the interface appropriately.

3.5.6 Pull out test results of corroded deformed bar specimen with cracked concrete

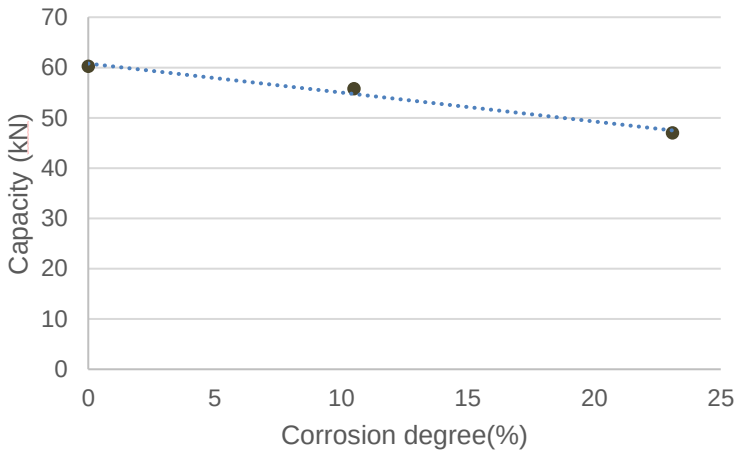

Figure 3.18 Pull out capacity of corroded deformed bar specimen with cracked concrete

In case of the specimen of corroded deformed bar with corrosion crack, the capacity gradually drops when amount of corrosion increases due to concrete damage. Even the increment of interface roughness should increase the pull-out capacity. But the pull-out capacity also was affected by the mechanical bond loss from the cracking of concrete and loss of rebar knot shape. To simulate this behavior the simulation model of shear and normal spring constitutive model modification and expansive strain model were used. The results are showed in Section 3.6.

3.6. Apply to model based on pull out of round bar and deformed bar with crack concrete

3.6.1 Model geometry

In order to verify the applicability of the bond deterioration model with the expansion model, the simulation results of pull out test of specimens reinforced with corroded round bar and deformed bar had been used. The concrete specimens size of 200×150×150 mm^3 reinforced with corroded deformed bar and rounded of 16 mm diameter were modelled. The bond length was set as 100 mm from the free end for the specimens reinforced with deformed bar. The specimen reinforced with round bar was set the bond length as 200 mm for the entire bar length. The interface modification due to the deterioration model of normal spring and shear spring which states developed in section 3.5.1 and 3.4.1 were applied at the interface between rebar and concrete at the bond length. The expansion simulation was also set to the bond length interface. Figure 3.24 shows the dimension of simulation. The list of simulation cases is shown in table 3.6.

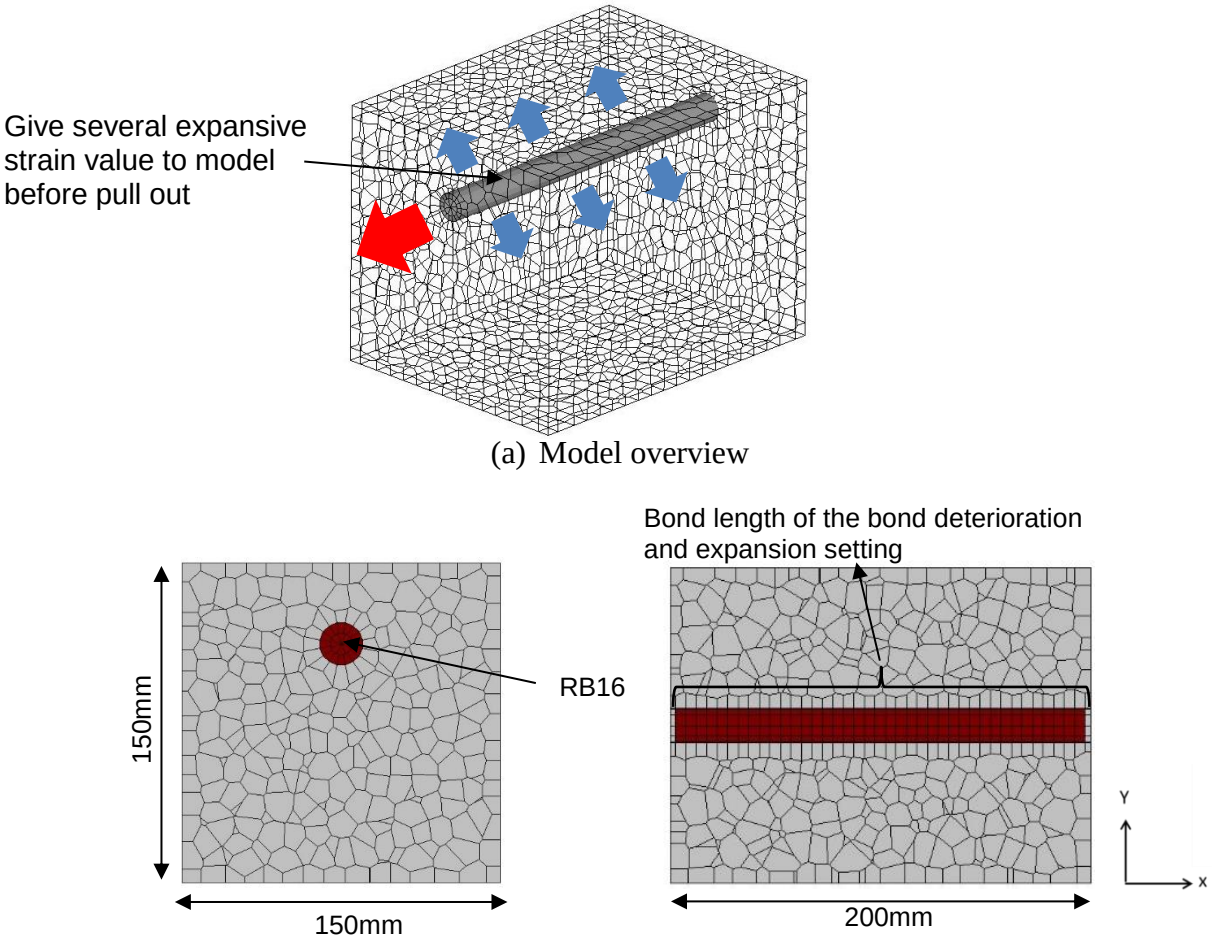

Figure. 3.24 Model overview for round bar with expansion simulation

Table 3.6 Specimen cases.

Specimen	Reinforcement	Corrosion pattern	Average corrosion degree
2W-RB	RB16	Uniform	5.3 %
4W-RB	RB16	Uniform	12 %
2W-DB	DB16	Uniform	10.5 %
4W-DB	DB16	Uniform	23.1 %

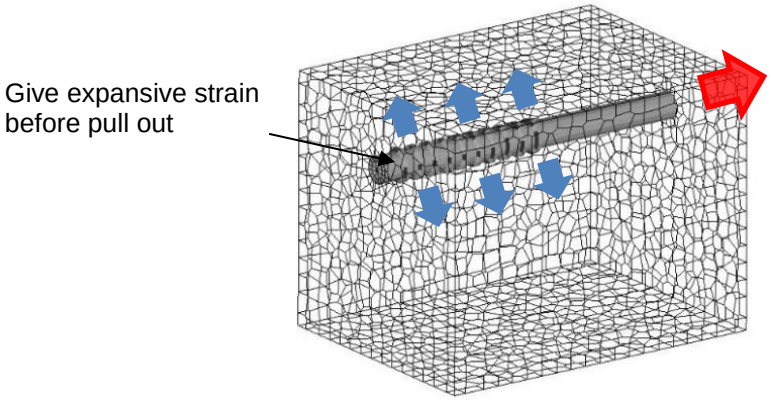

(a) 3D overview

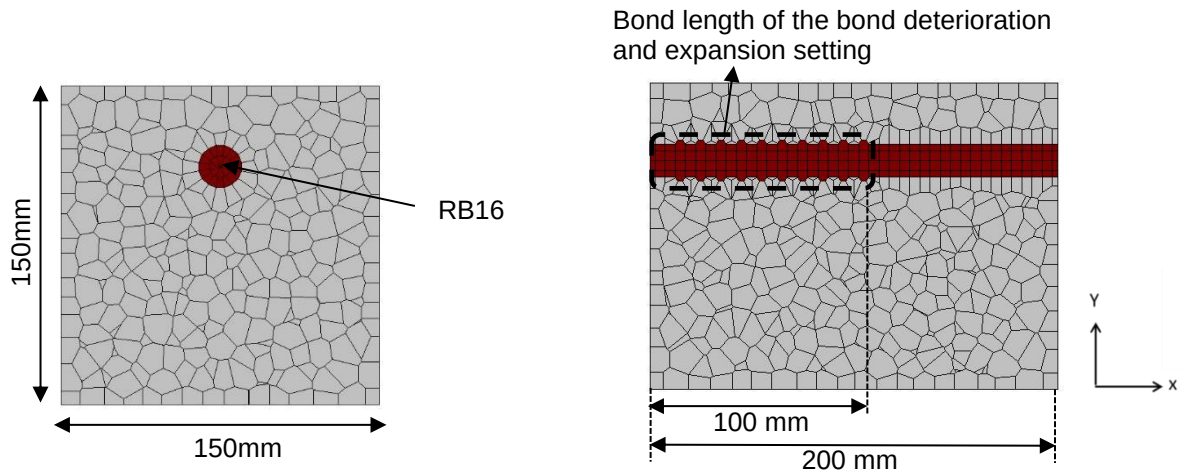

(b) Side view crossection (c) Top view crossection

Figure 3.25 Geometry of numerical model by RBSM (Unit: mm)

3.6.2 Simulation results

Figure 3.17 shows the load-displacement of pull out corroded round bar with non-crack concrete simulation at different corrosion percentage same as experiment. When consider the peak pull out capacity. The simulation can simulate the increment of maximum pull out capacity due to the changing of corrosion percentage appropriately comparing with the experimental results.

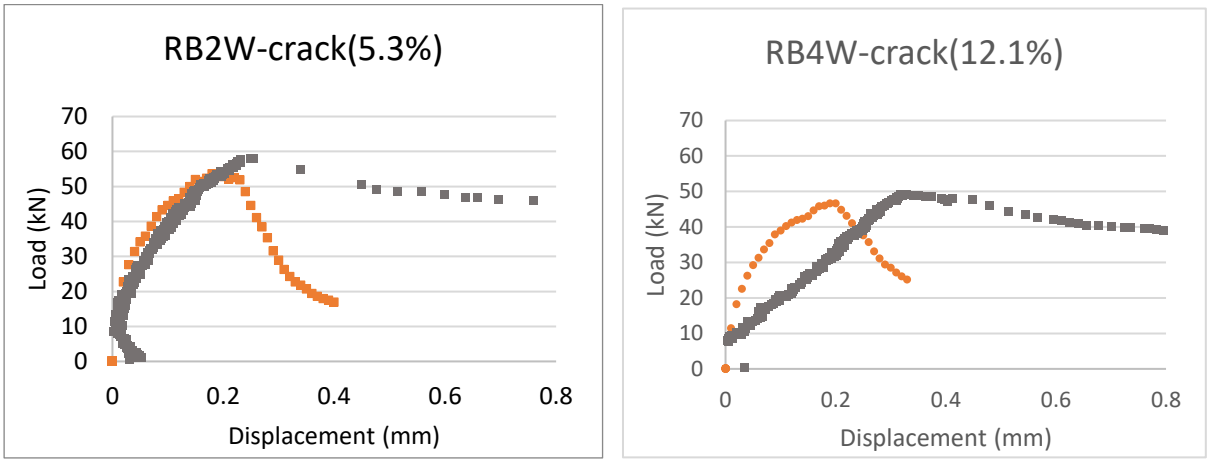

(a) Simulation of pulled-out RB with cracked concrete

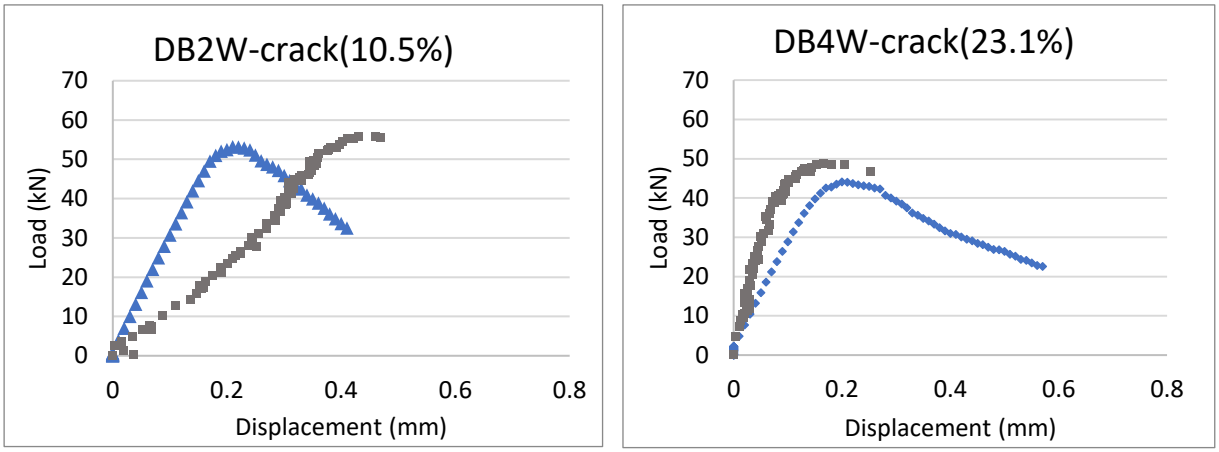

(b) Simulation of pulled-out DB with cracked concrete

Figure 3.26 Load-displacement of pull out specimen with cracked concrete

3.6 Conclusion

In this chapter, the constitutive models of bond deterioration were well developed based on the designed experiment program. The changing of the chemical bond and mechanical bond was extracted from the experiment results and was used for developed the modification factors in shear spring and normal spring. The concrete specimens reinforced with round bar and deformed bar were subjected to the corrosion acceleration test to generate the different corrosion percentage on the reinforcement. The corrosion acceleration electrical current-time were varied in each specimen for obtaining different corrosion percentage. (0, 3, 5,3 and 12.3% in round bar reinforcement and 0, 10.5 and 23.1% in deformed bar specimen). To eliminate the effect of corrosion cracking concrete, the specimen with non-crack concrete were prepared. After the pull-out test on cracked concrete specimen, the cover concrete was removed. The same corroded rebars were used as reinforcement in casting of new specimen. The pull-out tests were performed on non-crack concrete specimen. The pull-out capacity of different corrosion percentage and different type of reinforcement (round bar and deformed bar) were analyzed. The new constitutive model of shear spring and normal spring were proposed based on the changing of maximum pull-out capacities at different corrosion degree.

In order to verify the applicability of constitutive model and the compatibility with expansion model, the simulation model of pull out experiment with and without cracking concrete were simulated using the bond constitutive model and expansive strain model. The simulative model well predicted the peak pull out capacities of the experiment specimens correctly based on input corrosion percentage and expansion model. It can be concluded that the bond deterioration model was well developed and working well with the expansion model.

Chapter 4
Corroded beam model simulation with effect of non-uniform corrosion pattern

4.1 Introduction

This chapter aim to verify applicability of the numerical model that had been developed in Chapter 2 and Chapter3. By the combination of the spatial corrosion model, expansive strain model and bond deterioration model into RBSM simulation, the numerical system can considers the change of steel properties and expansion damage on adjacent concrete based on steel weight loss, the bond deterioration and non-uniformity of corrosion pattern. In this study the corroded beam models are simulated and analysed for verification the applicability of simulation model. The corrosion information is obtained from previous experimental study of corroded beam test [5]. Reinforcements in the simulation are modified at every 5 mm based on corrosion profile obtained from experiment. Two corroded beams with different corrosion pattern, but have same average corrosion degree, are simulated for verifying the influence of local corrosion on the beam behaviour. The beam failure pattern and mechanical performance were obtained as simulation results and were then analysed and compared with the experimental results.

4.2 Corrosion beam experiment by S. Lim et al. [6]

Simulation beam used in this study were modeled based on the previous experiment of Sopokhem Lim and team, in 2016. He had conducted the experiment about corrosion acceleration on RC beam for studying the effect of spatial corrosion on structural behavior. Several corroded RC beam experiments were conducted to study different amount and different pattern of corrosion. After the corrosion acceleration test, the digital camera and X-ray technique were used to measure the corrosion profile along the rebar. Then, the corroded beams were subjected to the mechanical loading test the find the residual capacity. The FEM simulation were conducted and compared with the experimental results to confirm the necessity of non-uniform corrosion in prediction of corroded beam simulation.

In S. Lim's experiment, a deformed bar grade SD 345 with diameter of 13 mm diameter was used as longitudinal reinforcement. The beam dimension is 1460x140x80. Concrete covering depth is 20 mm from the bottom surface of the beam. Figure 4.1 show the beams dimension with and without stirrup and loading test location used in his study.

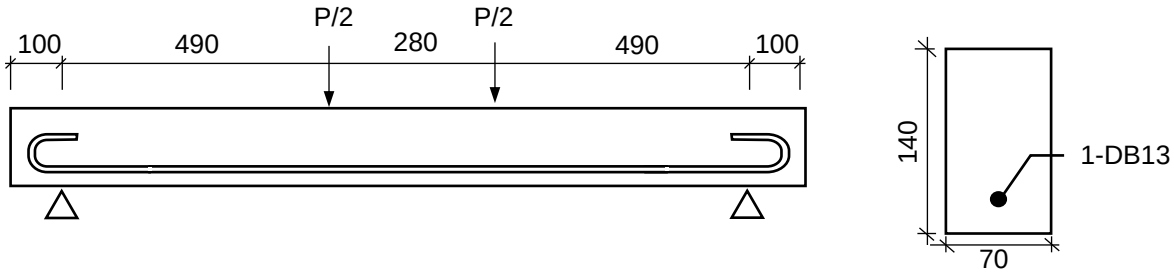

(a) Beam without stirrup

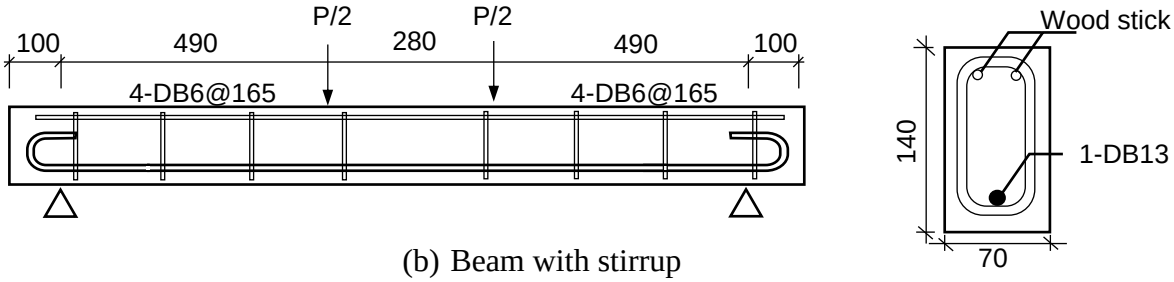

(b) Beam with stirrup

Figure 4.1 Dimension of beam in corrosion acceleration experiment

In his study, Gumbel distribution function was used to estimate the corrosion profile along the rebar. He conducted two set of simulation for each beam. First simulation is the simulation with uniform corrosion pattern that have the same average corrosion degree as the experiment, second simulation is the non-uniform corrosion pattern that the corrosion pattern was calculated by using Gumbel distribution function based on scale factor and location factor from the experimental results.

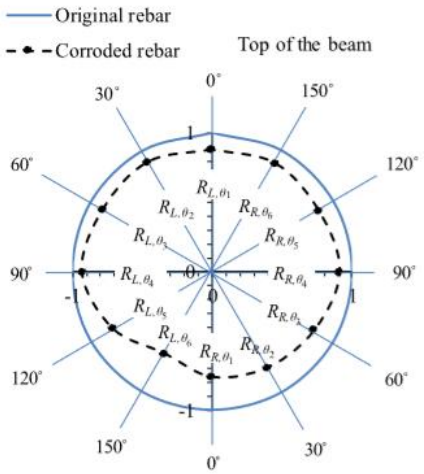

Construction of residual steel cross-section area via 12 residual radii of the steel rebar

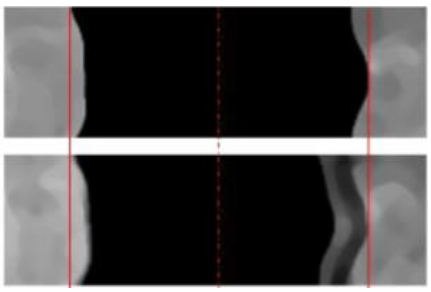

Alignment of non-corroded and corroded rebar

Figure 4.2 (a) construction of the residual steel cross section area vis 12 residual radii pf steel rebar (b) alignment of the non-corroded and corroded rebars at a corresponding location

The X-ray apparatus was used to visualize the steel corrosion in RC beam from different 12 viewing angles. The steel weight loss of rebar along the longitudinal bar was calculated by taking photo by X-ray digital camera technique from different viewing angles. The local steel weight loss of rebar per length of 5 mm, denote *Rw*, can be estimated by averaging the steel weight loss from six viewing angles using the following formula:

$$Rw = \frac{1}{k}\sum \frac{W_{\theta n} - W'_{\theta n}}{W_{\theta n}} \quad (1)$$

When $W_{\theta n}$ and $W'_{\theta n}$ are the weights of non-corroded and corroded rebars at a viewing angle based on the volume estimated by X-ray photogram, respectively, θn denotes the viewing angle in which n ={1,2,3,4,5,6} and *k* is the number of viewing angles which equal to 6 in this study. Figure 4.2(a) show the conceptual photo for this calculation by giving an example of X-ray photogram data at 1 section. The 12 residual radii were estimated using the projected longitudinal areas of corroded bar as shown in figure 4.2 (b). By measuring the alignment from central line of rebar before and after corrosion at different angles, the residual cross-section of rebar can be calculated.

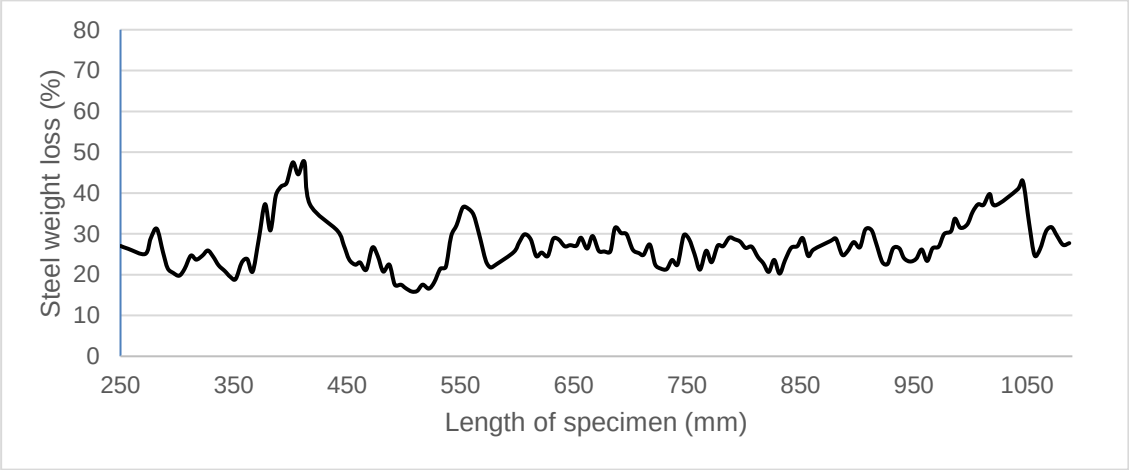

(a) Spatial variability in steel weight loss

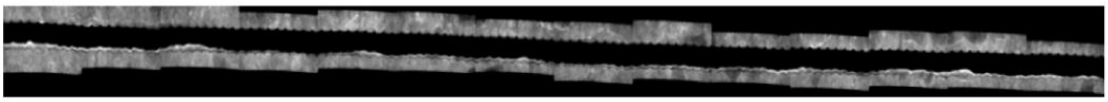

(b) X-ray image of steel corrosion at 180 degree

Figure 4.3 Local steel weight loss along the bar length by X-ray image of Beam without stirrup

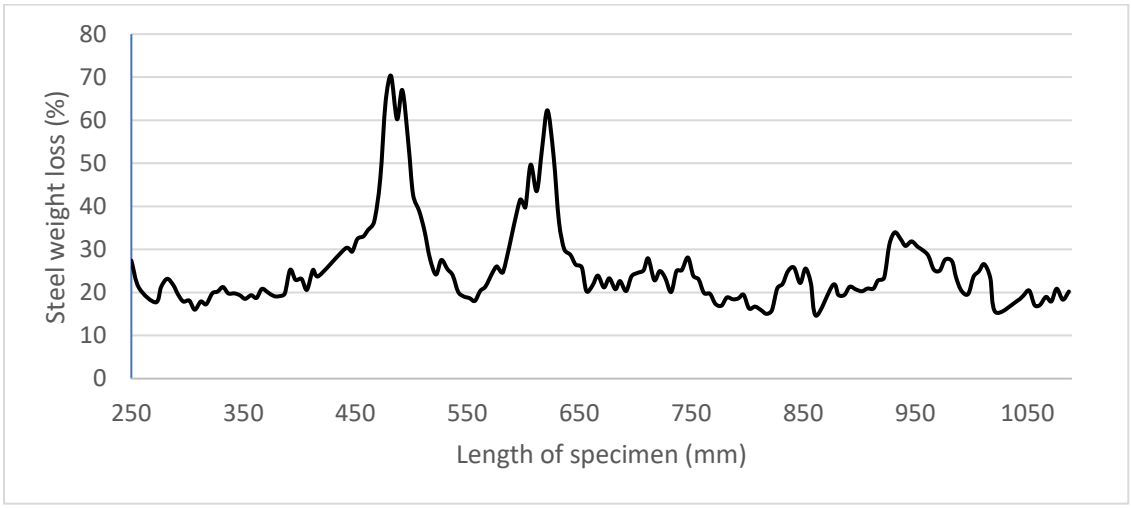

(c) Spatial variability in steel weight loss

(d) X-ray image of steel corrosion at 180 degree

Figure 4.4 Local steel weight loss along the bar length by X-ray image of beam with stirrup

Figure 4.3 and figure. 4.4 show the steel weight loss profile along the rebar of beam specimen with stirrup and without stirrup by X-ray technique. The average corrosion degree for beam without stirrup and with stirrup is 27.23 and 25.54% respectively. By using this data, the location and scale factor of corrosion can be calculated by mathematic method. Then, the Gumbel distribution function was used to estimate the corrosion along the rebar for simulation. Finite element simulations were simulated using the corrosion profile from Gumbel distribution estimator and uniform corrosion pattern with the same average corrosion value for each beam. The simulation load-displacement relationship was show in figure 4.5.

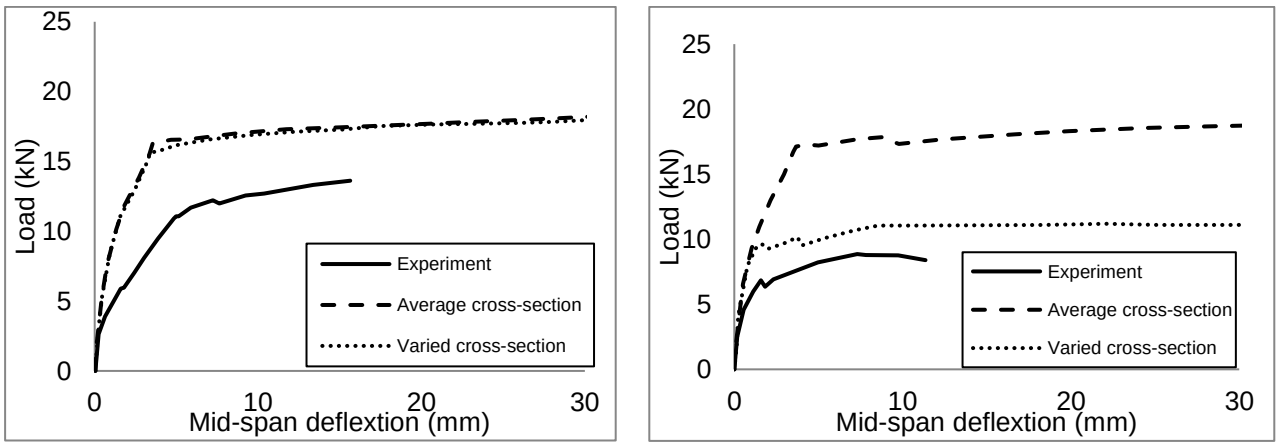

(a) Beam without stirrup (b) Beam with stirrup

Figure 4.5 Load-displacement of simulation results and experiment of corroded beam experiment with and without stirrup case. [S. Lim et al.,2016]

From figure 4.5(b), the simulation results shows that even the same average corrosion degree were applied to both uniform and non-uniform corrosion case, but the simulation results of spatial corrosion pattern(varied cross-section) shows more accurate results comparing with the experimental results.

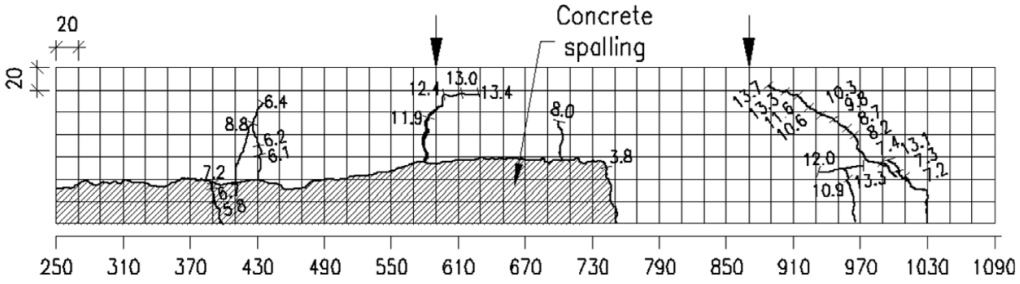

(a) Cracking pattern of beam specimen without stirrup

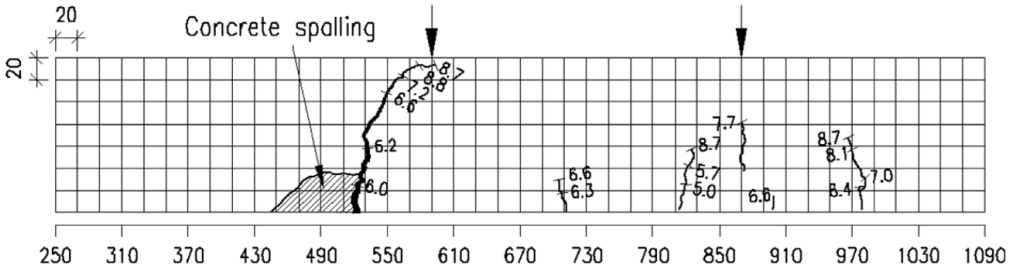

(b) Cracking pattern of beam specimen with stirrup

Figure 4.6 (a) Cracking pattern after unidirectional loading (b) the corrosion patterns along the beam of beam by X-ray image

Figure 4.6 shows the cracking pattern of corrosion beam after the bending test. By comparing this information with its steel weight loss along the beam length in figure 1.7(a) and 1.8(a), it reveals that the primary localized crack that leads to the beam collapse occurs at the local maxima of the steel weight loss. It can be inferred that the local damage of the corroded RC beams can be physically capture when the non-uniform steel weight loss along the reinforcements is adequately assessed.

In conclusion, the simulation results from FEM method suggest that it is important to consider the influences of non-uniform corrosion of steel weight loss for the assessment of the structural performance of corroded RC structures.

4.3 Simulation model of corroded beam with stirrup

4.3.1 Geometry of simulation model

The analysis models used in this study were formed up based on the previous experimental study by Sopokhem et al. (2016). They performed electrical corrosion acceleration on single RC beam specimens for observation of the crack pattern due to loading on corroded beam at different corrosion degree (Sopokhem et al. (2016)). The concrete specimens size of 1460×140×80 mm^3 reinforced with D13 rebar (nominal diameter = 12.7 mm) were subjected to external direct electric current of 0.11 A/cm^2 to accelerate the corrosion process. In this study, cuboid model with single

reinforcement at 20 mm covering depth from bottom of beam which same as in the experiment of Sopokhem et al. are modelled for analysis. The simulation models are separated into two groups, corroded beam with stirrup and without stirrup, with different corrosion patterns. Analysis model is meshed into meso-scale element having average sizes approximately 10.0×10.0×10.0 mm^3. Two pin support and two loading point are set at same location as in the experiment. The load is given at the two pin point above the beam, and there is no friction between the loading concrete element and the beam. Also, the interface between concrete support and beam is set as friction free condition. This 3D-RBSM model contains 26843 elements and 62458 elements for beam simulation without and with stirrup, respectively. The input tensile strength of steel bar and concrete are 388 MPa and 3.24 MPa, respectively. Expansive strain was applied to the interface between rebar and concrete for generating the corrosion expansion. Subsequently, the mechanical loading was given in the same manner as experiment. Figure. 4.7 shows the reinforced concrete beam simulation by RBSM in this study.

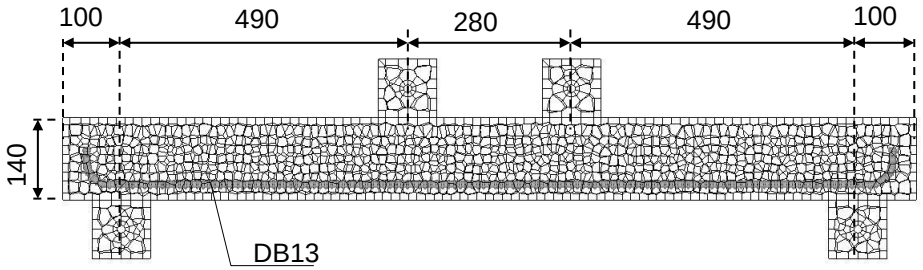

(a) Simulation beam without stirrup

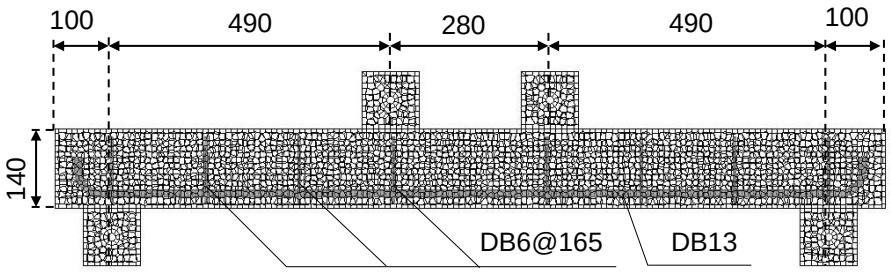

(b) Simulation beam with stirrup

Figure 4.7 Geometry of numerical model by RBSM (Unit: mm)

Table 4.1 Beam material properties.

Term	Unit	Concrete	Reinforcement
Compressive strength	MPa	53	-
Elastic modulas		33600	200000
Yielding strength		3.24	388.0

4.3.2 Corrosion patterns

In this study, a non-corroded beam simulation and corroded beam with different corrosion pattern are simulated for investigate the effect of spatial corrosion on the RC beam. Two different steel weight loss profile are set for the simulations. The first corrosion case is the uniform corrosion pattern at 27 percent along the bar. Second case is non-uniform corrosion obtained from 3D x-ray technique of Sopokhem et al. (2016) as shown in Figure 4.3(a) and Figure 4.4(a). The spatial variable steel weight loss is start from 250 mm to 1090 mm in rebar length direction. The other zone, 0 to 250 and 1090 to 1490 mm, does not have information from the experiment, so the corrosion level is set as uniform 27 %. The average steel weight loss is 27 percent. Table 2 shows each corrosion pattern in the simulations.

Table 2 Simulation cases.

Specimen	Corrosion pattern	Average corrosion degree	Comment
w/o stirrup	None	0%	No corrosion is given.
	Uniform	27.2 %	Uniform 27% corrosion is given.
	Non-uniform	27.2 %	Corrosion profile from experiment.
With stirrup	None	0%	No corrosion is given.
	Uniform	25.5 %	Uniform 27% corrosion is given.
	Non-uniform	25.5%	Corrosion profile from experiment.

4.3.3 Expansion simulation

The constitutive model of corrosion degree and expansive strain model was developed based on inverse method as explain in chapter 2. The expansion constitutive model is shown in Fig. 4.8

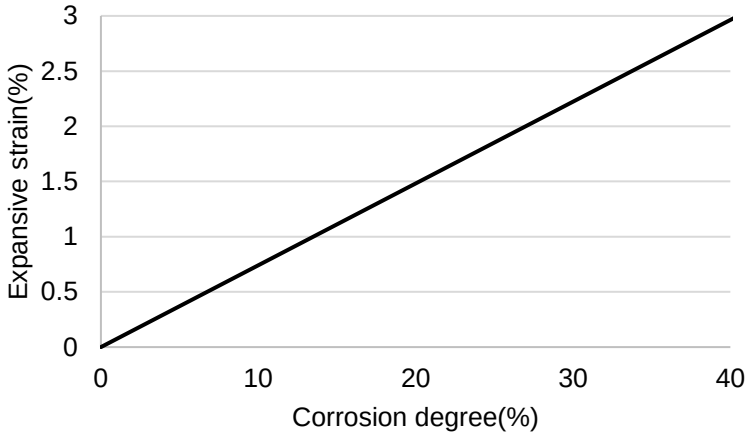

Figure. 4.8 Corrosion degree-expansive strain constitutive model

4.3.4 Loading condition

After the corrosion crack damage was introduced to the specimen, load was then applied to the beam to find the residual capacity. Fig. 8 shows the boundary condition for the loading process.

Two pin supports below RC beam are set in fixed movement condition (fixed in X, Y, Z direction for right support and fixed in Y, Z direction for left support), while loading is given at two pins above the specimen at rate of 0.0005 mm/step in the downward Y direction as shown in Fig. 4.4.

4.4 Analysis results

4.4.1 Corrosion cracking

By using the constitutive model in Figure. 4.8, the expansion of corroded beam simulation of uniform corrosion pattern and non-uniform corrosion pattern were simulated. In case of uniform corrosion beam by uniform expansion at 25.5% and 27.2% corrosion degree was applied for the whole longitudinal bar of beam with and without stirrup, respectively. In case of non-uniform corrosion beam, the expansion was simulated by using the steel weight loss profile in figure 4.3 (a) and figure 4.4(a). The location where the X-ray photogram did not collect the data was assumed to be uniform corrosion rate at 25.5% and 27.2% corrosion for beam with and without stirrup, respectively.

Figure 4.9(a)-(b) and figure 4.10(a)-(b) show the 3D surface overview of corroded beams after corrosion expansion simulation. Expansive strain was given to the interface between rebar and concrete at rate of 0.05 μstrain/step. Cumulative given expansive strain were 9 μ strain and 17 μ strain for stirrup and non-stirrup beam. As a result, the crack propagates to the bottom surface of beam which is the thinnest covering depth as shown in figure 4.9 (b) and figure 4.10(b). Some crack can be observed at the side of the beam at the hooked-up part of anchorage. Figure. 4.9(c) and Figure 4.10(c) shows the bottom beam crack from the experiment at span length of 250 to 1090 mm. For the beam without stirrup case, the average bottom beam crack width from simulation result in case of non-uniform corrosion is 0.86 mm while the experiment bottom crack width is 0.88 mm (Fig. 4.9(c)). For the beam with stirrup, the average bottom beam crack width from simulation result in case of non-uniform corrosion is 0.250 mm while the experiment bottom crack width is 0.252 mm (Fig. 4.10(c)). However, the direction of crack in simulation is straighter near to the central line of bottom beam more than the experimental result which crack direction is scatter to side of the beam as shown in Fig. 4.6(c). This result occurred due to the restrain of the element size. Due to the concrete element size which is around 10mm, the expansion crack at the bottom surface may not perfectly simulated.

(a) Front view of expansion simulation

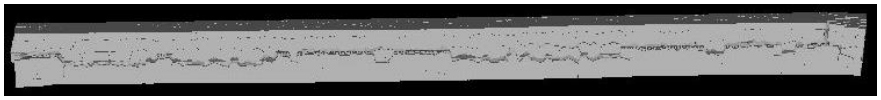

(b) Bottom view of expansion simulation

(c) Bottom beam crack width from experiment at length of 250-1090 mm [5]

Figure 4.9 Corrosion cracking of non-stirrup beam simulation before loading

(a) Front view of expansion simulation

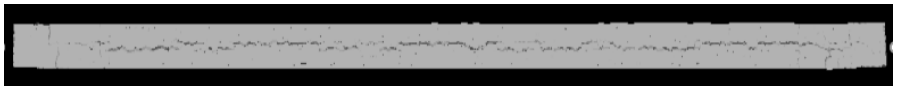

(b) Bottom view of expansion simulation

(c) Bottom beam crack width from experiment at length of 250-1090 mm [5]

Figure 4.10 Corrosion cracking of stirrup beam simulation before loading

4.4.2 Load-displacement relationship

Beam's load-displacement relationships for each simulation case and real experimental data are shown in figure 4.11 and figure 4.12. The load is defined as the total force acting at two pin point above the beam, while displacement is the vertical displacement of loading point in downward direction. For non-stirrup beam, the maximum capacity of each simulation case is 15.9 kN, 13.0 kN and 11.9 kN for no corrosion, uniform corrosion and spatial corrosion cases respectively. For stirrup beam, the maximum capacity of each simulation case is 24.0 kN, 18.3 kN and 12.6 kN for no corrosion, uniform corrosion and spatial corrosion cases respectively. In the experimental specimens (Sopokhem et al., 2016), it was reported that the steel bar was yielded, and the specimen showed flexural behaviour before failed by reach the shear capacity as shown by the dot line in Fig. 4.11 and 4.12. In case of simulation, beam with corrosions shows lower stiffness and capacity than no corrosion case due to initial damage from corrosion which are bond deterioration and steel cross section reduction. For the non-stirrup beam, even the corroded beams have the same stiffness, the beam with spatial corrosion shows lower capacity due to different local behaviour which will be discussed in the next section. For the stirrup beam, since the critical corrosion cross-section is locate at the middle of loading span, so the stiffness of each beam are clearly different between no corrosion, uniform corrosion and non-uniform corrosion case. And due to stirrup, the shear capacity of simulation beam increase, and simulation beams showed flexural behaviour before shear failure pattern occurred. Comparing with no corrosion case, the corroded beam's stiffness becomes close to the experimental result.

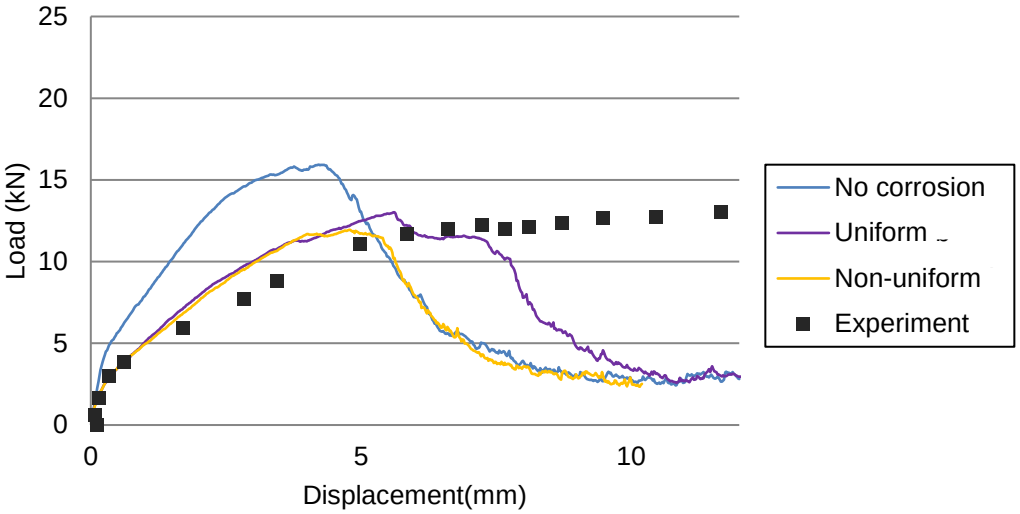

Figure 4.11 Load-displacement relationship in each simulation case for non-stirrup beam

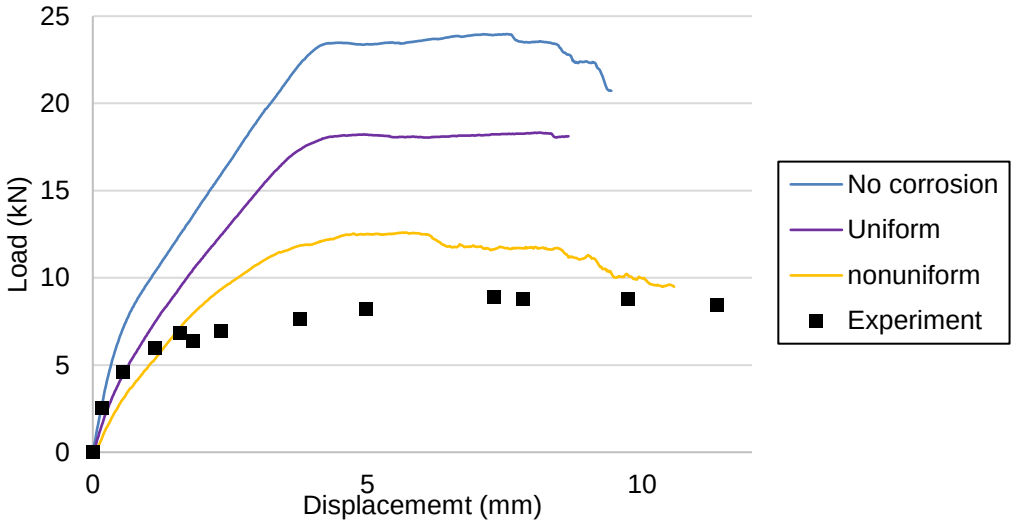

Figure 4.12 Load-displacement relationship in each simulation case for non-stirrup beam

4.4.3 Strain distribution along the rebar

For the non-stirrup beam, figure 4.13 shows the local strain distribution along the rebar for corroded beams simulation 10 percent capacity before and after the peak load. The strain distribution was check when then displacement were around 4.0 mm and 5.6 mm displacement for non-uniform corrosion beam and 4.2 mm and 6.2 mm for uniform corrosion beam, respectively. The strain distribution of uniform corrosion and non-uniform corrosion are represented by purple line and yellow line, respectively. Before the peak load, there are no significant difference between strain distribution between uniform corrosion case and non-uniform corrosion case as shown in Fig. 4.13 (a). Fig. 4.8 (b) shows the strain distribution at around 10 percent capacity dropped after the peak load. In case of non-uniform corrosion case, the local strain along the rebar at 400, 600 and 1000 mm location show higher strain than the other locations. This yielding location is corresponding to the given corrosion profile in Fig. 4.3(a). While in case of uniform corrosion, there are not significant difference in strain in each location, even after the beam starts to failure.

Even the corroded beams show similar stiffness, the local behaviour were different due to the corrosion pattern.

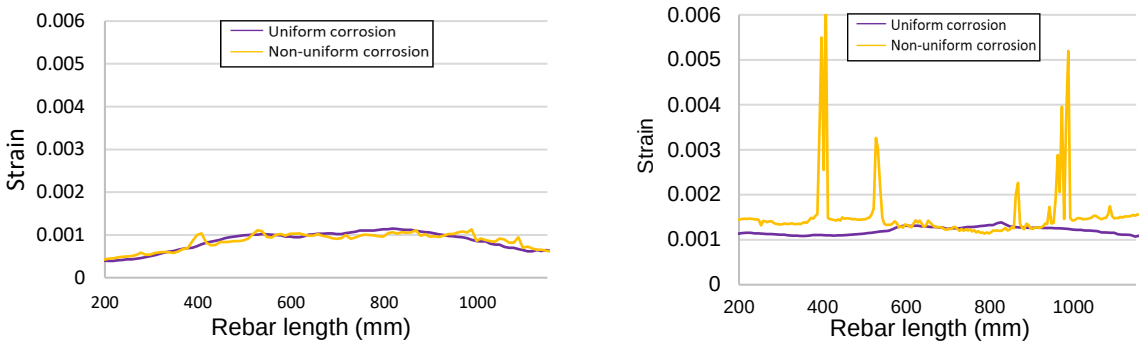

(a) Strain before peak load (b) Strain after peak load

Figure 4.13 Strain distribution along the reinforcement for non-stirrup beam

In case of stirrup beam, figure 4.14 shows the local strain distribution along the rebar for corroded beams simulation before and after the peak load. The strain distribution was check when then displacement were around 3.5 mm and 7.5 mm displacement for both uniform corrosion beam and non-uniform corrosion beam. The strain distribution of uniform corrosion and non-uniform corrosion are represented by purple line and yellow line, respectively. Before the peak load, the strain distribution of non-uniform corrosion shows high rebar elongation at 480 mm and 630mm as shown in Fig. 4.14(a). And these two sections were elongated more after the peak loading as shown in figure 4.14(b). These yielding locations show a good agreement with the corrosion profile from experiment which the critical corrosion section 70%, 67% and 63% are located at 470mm, 480mm and 620mm respectively. While the beam with uniform corrosion, the peak elongation is not appear before the peak load, and random occur between two loading pins location. These results show that the numerical model can correctly simulate different local behaviour based on different input corrosion profile.

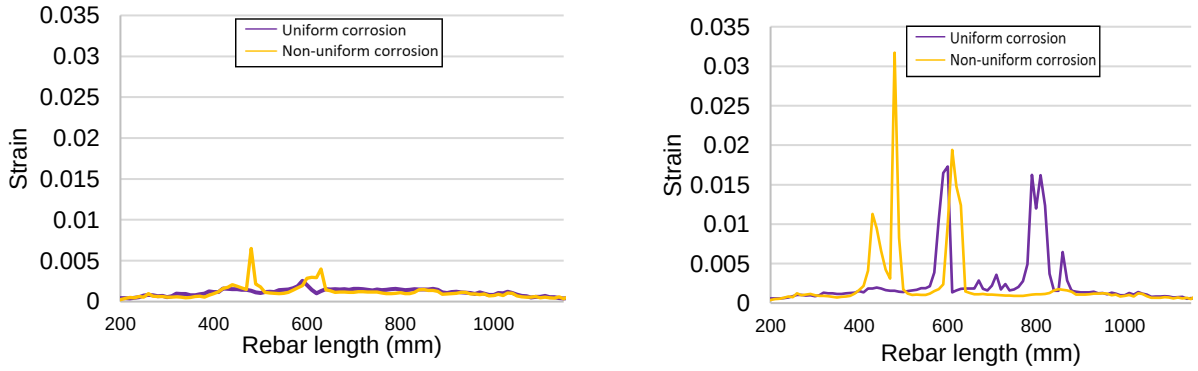

(a) Strain before peak load (b) Strain after peak load

Figure 4.14 Strain distribution along the reinforcement for stirrup beam

4.4.4 Crack failure patterns

- **Non-stirrup beam**

Figure 4.15 shows the internal crack pattern and the 3D surface overview crack of each case. In case of no corrosion case, Fig. 4.15 (a), the beam failure pattern indicates a shear failure. A diagonal crack plane can be observed between the loading point and support at the left and right side of the beam. This is typical failure pattern that can found in beam loading tests that the shear capacity is lower than flexural capacity.

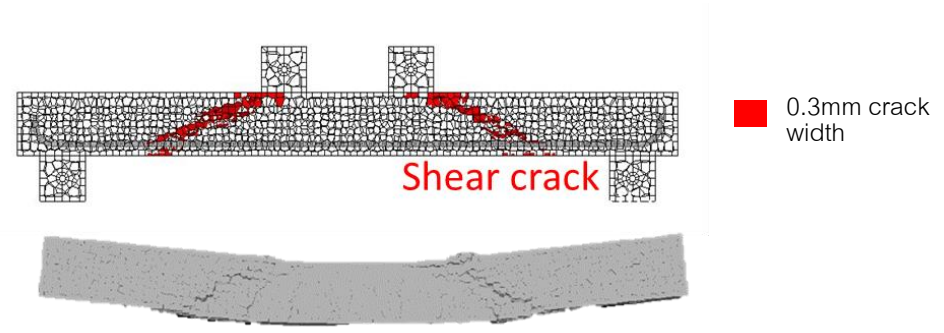

(a) No corrosion beam

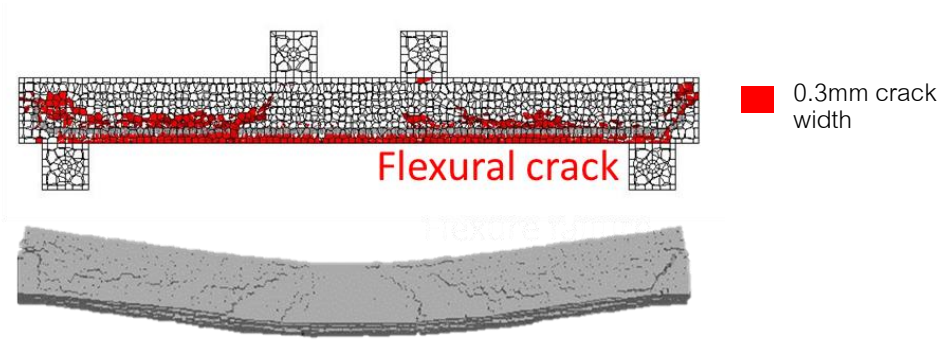

(b) Uniform corrosion beam

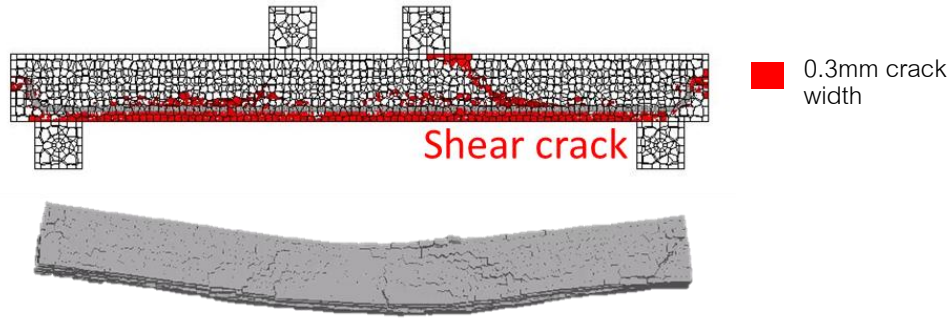

(c) Non-uniform corrosion beam

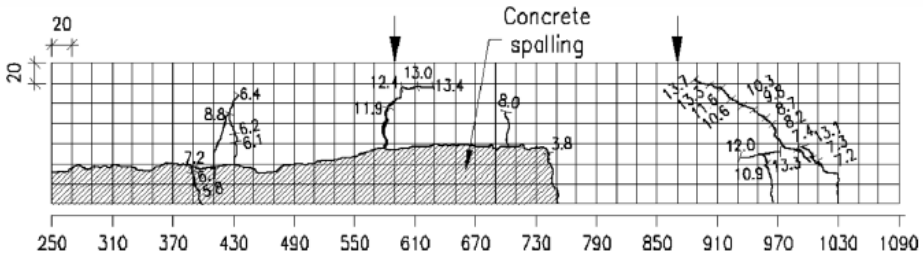

(d) Experimental result by S.Lim, 2016 [6]

Figure 4.15 Internal crack pattern and surface overview at failure of non-stirrup beam (a) simulation of beam with no corrosion damage (b) simulation of beam with uniform 27 % steel weight loss along the bar (c) spatial variable corrosion from X-ray data and (d) crack pattern from experiment by Sopokhem et al. (2016)

For the beams with initial corrosion damage, the crack near the bottom part of beam can be observed in both cases. In case of the uniform corrosion case, Fig. 4.15 (b), a crack from corrosion expansion was appeared along the longitudinal rebar length at the bottom of the beam. After applying the load, the beam behaviour change from shear failure in corrosion case became the flexural failure which can be observed at bottom part of the beam. This occurred because of the initial damage from corrosion reduce the flexural capacity the beam. In case of using real spatial corrosion from the experiment, Fig. 4.15 (c), the crack pattern is a combination of flexural cracks and shear cracks. Yielding of rebar is observed by strain distribution in Fig. 4.13 (b). Distribution of cracks at bottom of beam can be observed, while the shear-compression failure appears on the right side of specimen which is similar to the experimental result crack pattern in Fig. 4.15 (d). Due to the corrosion, the rebar effectiveness was decreased, and the surrounded concrete around the rebar was damaged by the expansion. This reduces the mechanical bond between the rebar and concrete and lets the flexural capacity decrease. Also, the initial crack damage from expansion can lead to the propagation of shear crack in the right span of the beam. Considering these effect, the beam simulation with non-uniform corrosion damage can simulated the failure pattern of the experiment beam reasonably.

- **Stirrup beam**

Figure 4.16 shows the internal crack pattern and the 3D surface overview crack of each case. For the corroded beam, corrosion crack along the longitudinal rebar length can be observed at the bottom of the beam. This corrosion crack has smaller size comparing with the beam without stirrup due to the stirrup confinement. After the loading, in case of no corrosion and uniform corrosion case, figure. 4.16 (a) and figure 4.16 (b), the beam failure pattern indicates a flexural failure. Flexural cracks can be observed between the loading point pin location which is the maximum moment span. For the corroded beam with non-uniform corrosion pattern, a shear failure pattern can be observed as shown in figure 4.16(c). Shear crack occurred at the left shear span of the beam. This cracking is corresponding with the critical corroded cross-section and the yielding of longitudinal bar which is described in section 4.4.3. This result indicated that the initial crack damage from corrosion can lead to the propagation of shear crack in the left span of the beam. Considering these effect, the beam simulation with non-uniform corrosion damage can simulated similar failure pattern as the experiment beam correctly.

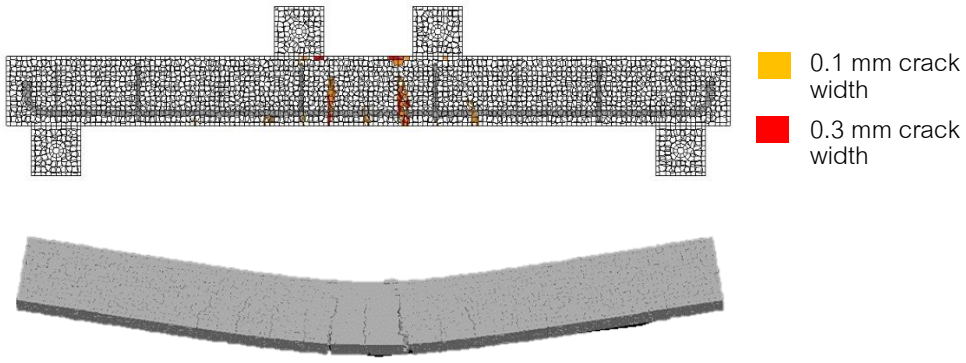

(a) No corrosion beam

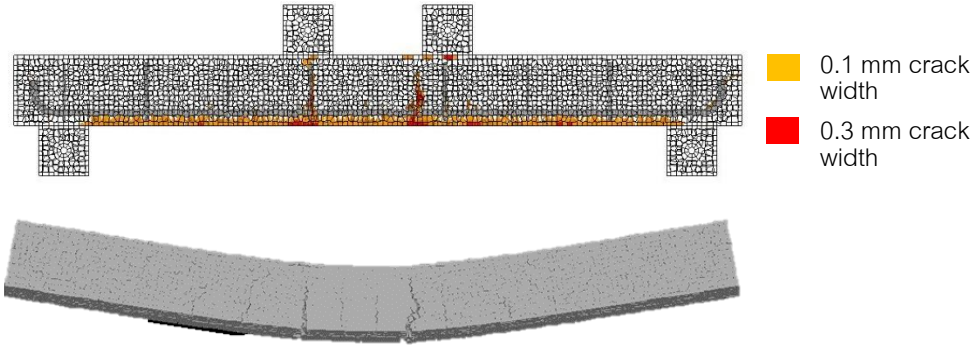

(b) Uniform corrosion beam

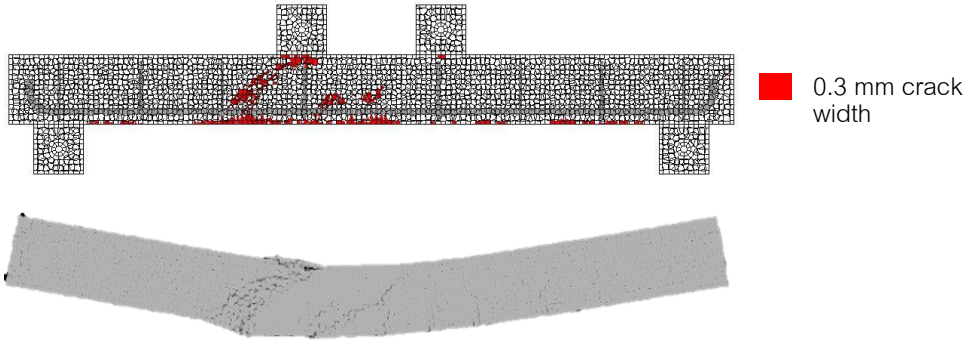

(c) Non-uniform corrosion beam

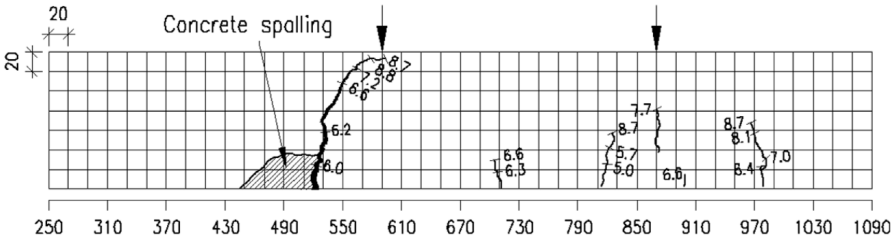

(d) Experimental result by S.Lim, 2016 [6]

Figure. 4.16 Internal crack pattern and surface overview at failure of stirrup beam (a) simulation of beam with no corrosion damage (b) simulation of beam with uniform 25.5 % steel weight loss along the bar (c) spatial variable corrosion from X-ray data and (d) crack pattern from experiment by Sopokhem et al. (2016)

4.5 Effect of initial damage from corrosion on beam stiffness and crack opening

In this section, the crack opening behavior of corroded beam and non-corroded beam simulation during loading were investigate. It can be observed from Load-displacement relationship in figure 4.11 and 4.12 that the beam with corrosion shows a lower stiffness comparing with non-corroded beam. The main different between corroded beam and non-corroded beam is the initial damage from the corrosion. Figure 4.17show the calculation of crack width of single crack at the bottom of simulation beam.

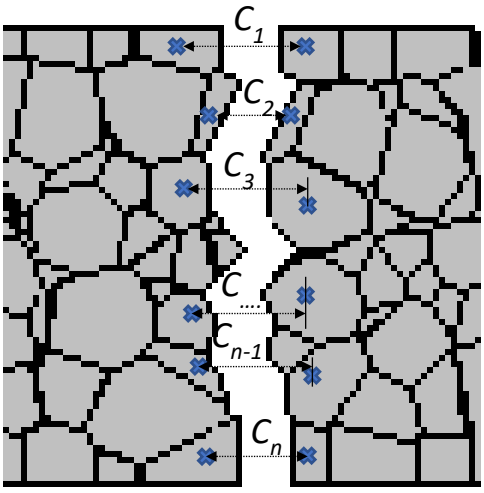

Figure. 4.17 Calculation of crack width in RBSM

The calculation of crack width in RBSM is done by Equation 4.XX

$$C_{avg,i} = \frac{C_1+C_2+\cdots.+C_n}{n} \quad (4.1)$$

Where $C_{avg,i}$ is the crack width of crack ith, C_n is the displacement between element 2 element over the crack, n is number of element in crack direction.

Figure 4.18 and figure 4.19 show the bottom cracking damage at length of 595 to 865 mm of stirrup beam with and without corrosion after loading, respectively. In case of non-corroded beam, there are two major cracks and three small cracks at the bottom beam between two loading in location. In case of corroded beam, the initial damage from corrosion appeared as the longitudinal crack at the center of bottom surface of corroded beam. After the loading, two large flexural crack and four small cracks appeared between two loading pin location as show in figure 4.19.

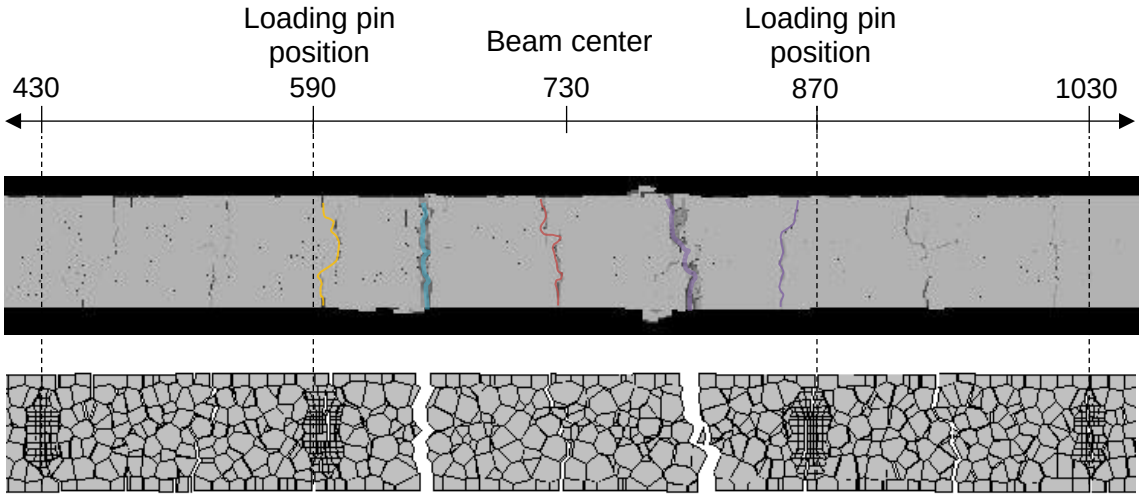

Figure 4.18 Bottom beam crack width after loading of no corrosion beam simulation

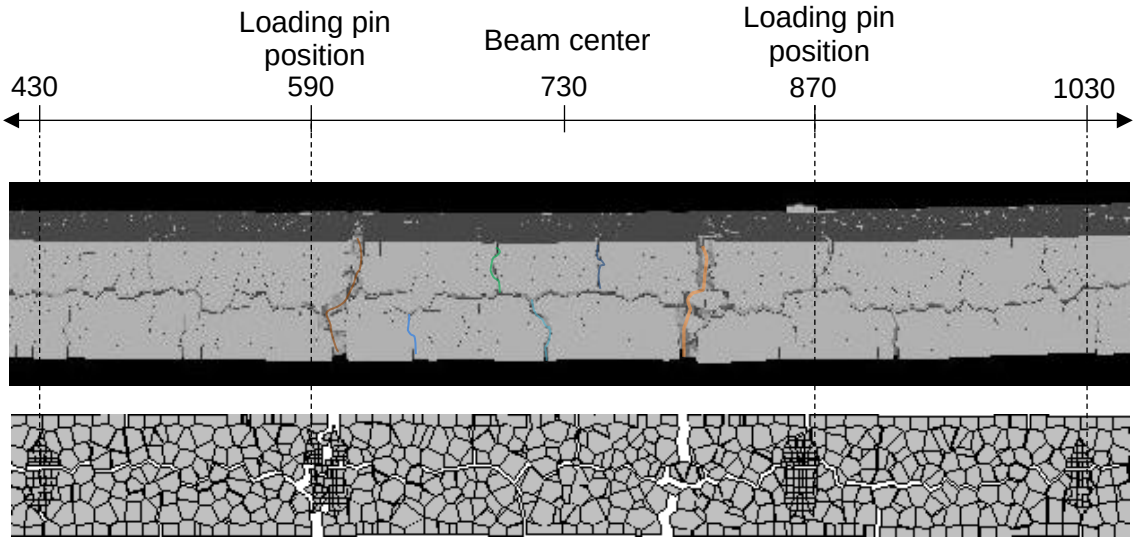

Figure 4.19 Bottom beam crack width after loading of uniform corroded beam simulation

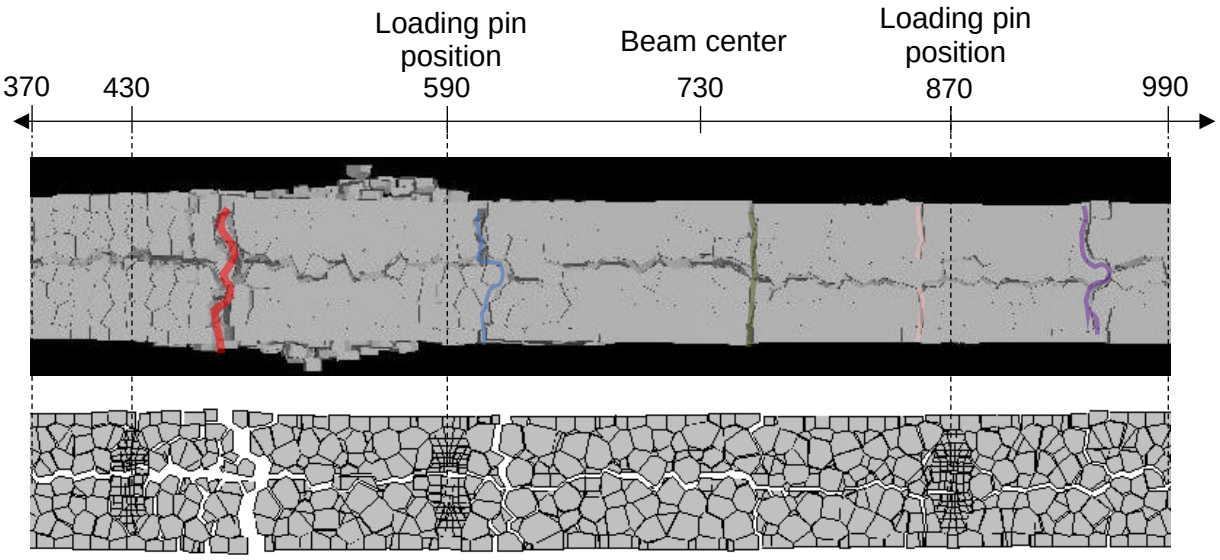

Figure 4.20 Bottom beam crack width after loading of non-uniform corroded beam simulation

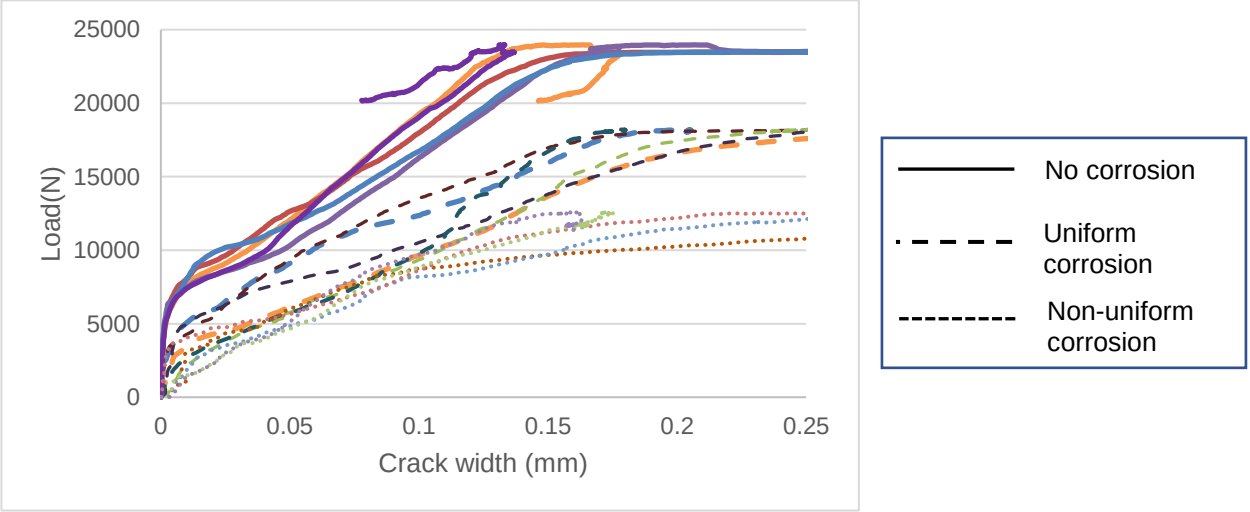

Figure 4.21 Bottom beam crack width opening and loading relationship

Figure 4.21 shows the crack width opening and load relationship. The dense line, dash line and dot line show the crack width opening along the bottom beam between two loading location of non-corroded beam, uniform corrosion beam and non-uniform corrosion beam respectively. Due to the expansion, the vertical crack line can be observed at central of the bottom surface of corroded beams. This concrete cracking damage degraded the mechanical bond between rebar and concrete and reduce the ability of cover concrete to restrain the elongation of rebar. As a result, the corroded beam have different stiffness and crack opening speed due to initial corrosion damage.

From the crack opening-load relationship, it can be observed that these trends have two stiffness, before and after flexural crack opening. In case of non-corroded bar, the second stiffness that the crack start to open rapidly is from load of around 6000kN, while that of the uniform corrosion simulation is around 2000 kN. In case of non-uniform corrosion case, the crack opening speed is further increased than the uniform corrosion case. It is clearly seen that the crack opening of the corroded beam is open earlier and larger than the crack width of non-corroded beam at the same loading, and this effect further increase by considering the non-uniform corrosion case. These

crack opening results in the stiffness reduction of corroded beam in load-displacement relationship comparing with non-corroded beam as shown in figure 4.12.

The result from this section indicate that the initial damage from corrosion affected on the stiffness reduction of the corroded beam. Due to the vertical cracking from expansion, the cover concrete lost ability to confine and restrain the elongation of reinforcement steel. Therefore, the flexural loading crack will propagate earlier in the beam with corrosion damage.

4.6 Conclusions

In this chapter, the corrosion model of spatial corrosion, expansive strain model, and bond deterioration model were combined into RBSM simulation for simulating the corroded beam experiment. The beam with no corrosion, uniform corrosion and non-uniform corrosion were simulated to see the effect of non-uniformity of corrosion pattern. Based on the simulation results, the following conclusion is drawn.

1. The simulation is this chapter combine all corrosion model that had been developed in chapter 2 and chapter 3 for simulating the behaviour of corroded beam model. The simulation results confirmed that all constitutive model for corrosion model are working well with each other in prediction of the corroded beam behaviour.
2. The spatial corrosion from experiment was concerned as an input in modelling the rebar model. By input the data of corrosion degree and location of those corrosion level, the simulation results the non-uniform corrosion pattern in RC structure.
3. In case of corroded beam, beam's stiffness and peak capacity were decreased due to initial damage from corrosion.
4. Even the stiffness of uniform corrosion and non-uniform corrosion simulations are not significantly different, considering the strain distribution along the rebar, the local behaviour are different. The non-uniform corrosion case shows different local yielding which corresponding to the peak corrosion degree or critical section given corrosion pattern.
5. And according to the corrosion pattern and local damage, the failure patterns beam simulation can be changed.
6. The crack opening -loading relationship indicate that the flexural loading crack will occur faster in the beam that have initial damage from corrosion. As a result, the corroded beam will have lower stiffness than non-corroded beam.

REFERENCES

[1] Mitsuyoshi Akiyama and Dan M. Frangopol. 2014. *A Long-term seismic performance of RC structures in an aggressive environment:emphasis on bridge piers*. Structure and Infrastructure Engineering, Vol. 10, No. 7, pp. 865–879.

[2] D. Qiao, H. Nakamura, Y. Yamanoto, et al.. 2016. *Crack patterns of concrete with a single rebar subjected to non-uniform and localized corrosion Constr*. Build. Mater., 116, pp. 366-377.

[3] K.Nagai, Y. Sato and T.Ueda. 2004. *Mesoscopic simulation of failure of mortar and concrete by 2D RBSM*. Journal of Advanced Concrete Technology. Vol. 11; 2, pp. 359-374.

[4] K.Nagai, Y. Sato and T.Ueda. 2005. *Mesoscopic simulation of failure of mortar and concrete by 3D RBSM*. Journal of Advanced Concrete Technology. Vol. 11; 3, pp. 385-402.

[5] Sopokhem Lim a, Mitsuyoshi Akiyama and Dan M. Frangopol. *2016. Assessment of the structural performance of corrosion-affected RC members based on experimental study and probabilistic modeling*. Engineering Structures 127. pp. 189–205.

[6] Lim. S, Akiyama M, Frangopol DM. *Assessment of the structural behavior of corrosion-affected RC beam: eperimental study and modeling*. InProceedings of the fifth international symposium on life-cycle civil engineering, IALCCE2016, October 16-20, 2016 Deflft, The Netherlamd. London: CRC Press/Balkema, Taylor & Francis Group plc; 2017

Chapter 5
Corroded beam model simulation with effect of corroded anchorage

5.1 Introduction

Corrosion frequently occurs at some part of structure that undesired contact with moisture, like support or connection between desk. In reality, collapse at the connection is one of the most common failure modes of reinforced concrete bridges and buildings. In this sense, studying the effect of corrosion induced damage on connection part or anchorage is important to predict the performance of corroded structure.

This chapter aim to verify the effect of corrosion at anchorage on the loading mechanism of RC beam by using the numerical model that had been developed in Chapter 2 and Chapter3. The simulation of RC beam model with intentionally set different corrosion pattern at the anchorage will be simulated for studying the behavior of corroded RC structure with anchorage damage.

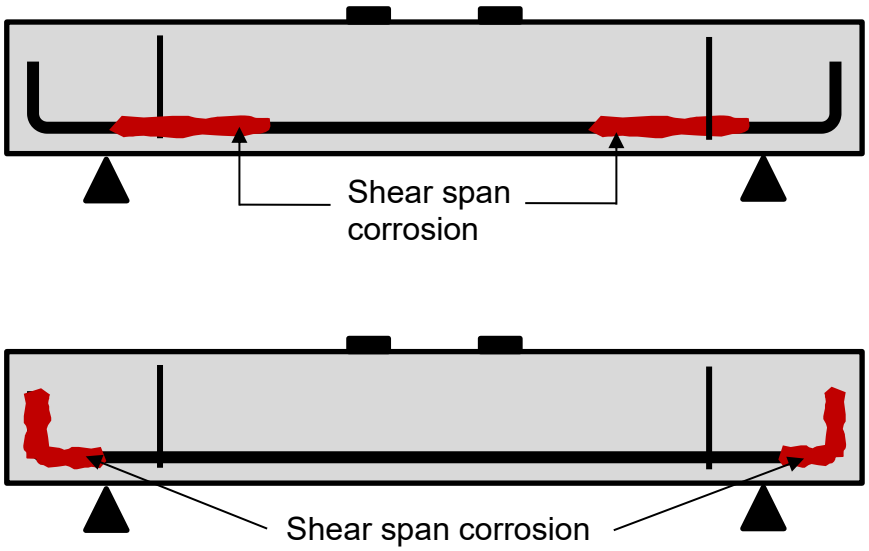

Figure 5.1 conceptual figure for corroded beam with anchorage damage.

The corrosion information is obtained from previous experimental study of corroded beam test [1]. Reinforcements in the simulation are modified at every 5 mm based on corrosion profile obtained from experiment. Two corroded beams with corroded reinforcement at anchorage end and corrosion at shear span are simulated for study the effect of different corrosion pattern on the beam behavior. The beam failure pattern and mechanical performance were obtained as simulation results and were then analyzed and compared with the experimental results conducted by M. TSUNODA et.al., 2016. Effect of different corrosion pattern at anchorage zone with sufficient and not sufficient anchorage (no hook part) length will be investigated.

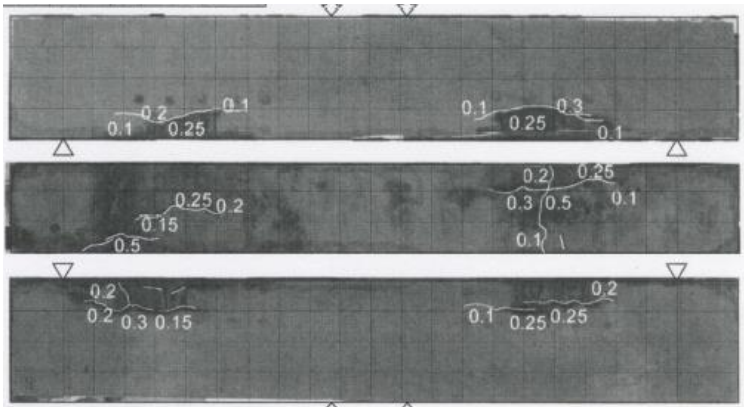

Figure 5.2 Corroded beam experiment by M. TSUNODA, 2016

5.2 Corrosion beam experiment by M. TSUNODA et al. [6]
(Influence of local steel corrosion on shear failure mechanism of RC members, Masahiko TSUNODA)

Simulation beam used in this study were modeled based on the previous experiment of Masahiro TSUNODA and team, in 2016. He had conducted the experiment about corrosion acceleration on RC beam for studying the effect of spatial corrosion on structural behavior. By using a wet sponge place at designate location, beams with corrosion at with different location can be obtain.

This study conducted unidirectional static loading tests of slender RC beams, of which longitudinal reinforcing steel bars were locally corroded at anchorage and support zone. The study was conducted for clarify the influence of local corrosion of longitudinal reinforcement on the shear failure mechanism of RC members. FEM of the specimens was also conducted for analyzing the failure mechanism of RC beams.

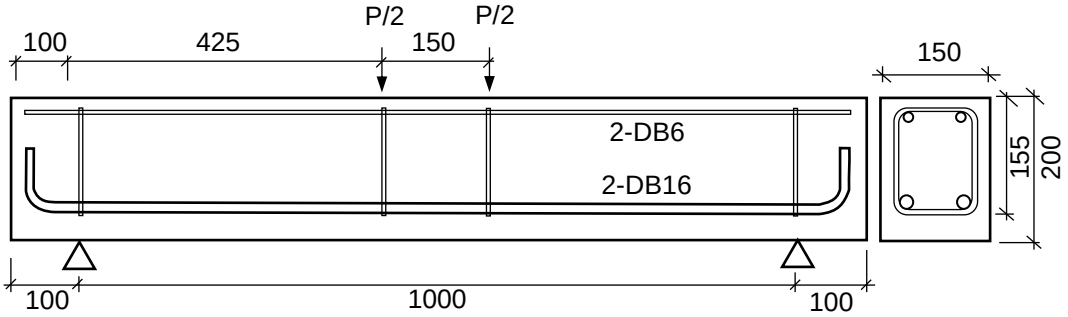

Figure 5.3 Beam experiment by M. TSUNODA

Figure 1.11 show the beam dimension in his experiment and unidirectional static loading that give to the RC beam. Teflon sheets were inserted between the specimen and the supports to prevent the horizontal friction. Load, mid-span vertical displacement, and vertical displacement at supports were measured.

Steel corrosion acceleration test was conducted in order to create corrosion along the longitudinal reinforcement. Specimens had some wires connecting to the end of longitudinal reinforcement in order to apply the electric direct current by a power source. Sponges soaked in 3 % NaCl solution were partly attached on the bottom surface of a specimen at different location to permeate Cl- into concrete. In order to prevent the corrosion of assembly steel bars and shear reinforcements, these steel bars were covered by epoxy adhesion at the contact portion with longitudinal reinforcement. By this method he can control the corrosion location of the beam specimen. Figure 5.4 shows the steel weight loss percentage along the rebar. In beam specimen B-10-287.5 the peak corrosion degree around 9% and 10% was located at around 287.5 mm from the left and right end of the beam as show in figure 5.4 (a). For beam B-10-400, the peak corrosion degree around 9.5% and 13% was located at around 400mm mm from the left and right end of the beam respectively.

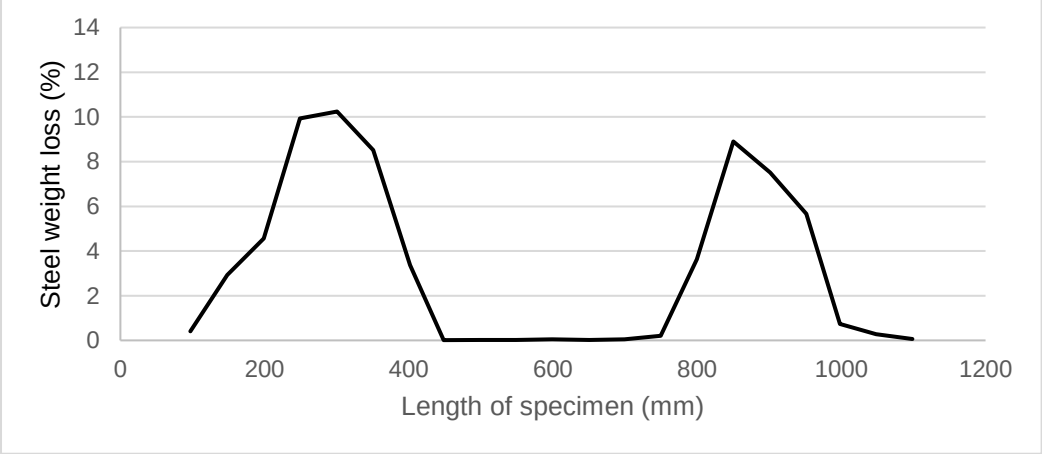

(a) Beam specimen, B-10-287.5

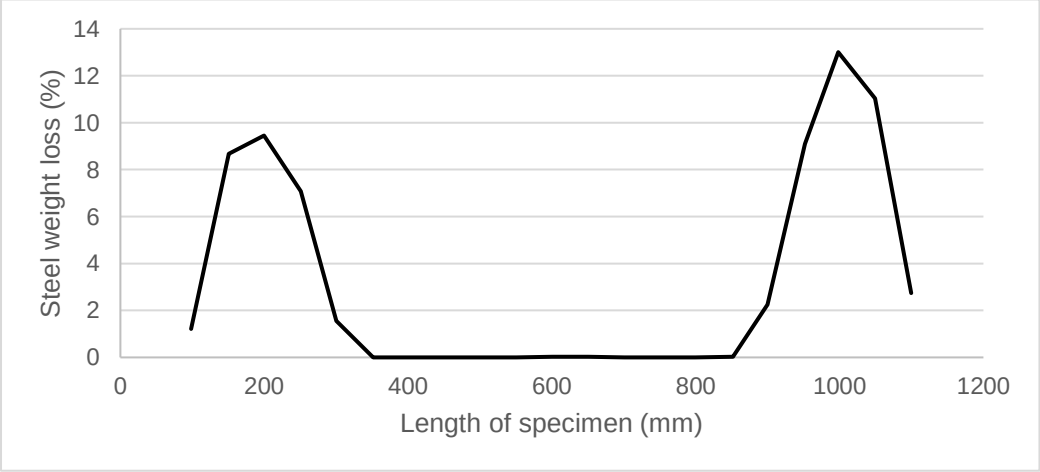

(b) Beam specimen B-10-400

Figure 5.4 Corrosion distribution in corroded RC beam experiment [M. Tsunoda et al.]

As a result of corrosion test, concrete damage condition RC members had some corrosion cracks along longitudinal reinforcement on their side surface partly. And the steel were damaged locally due to different corrosion profiles. After the corrosion acceleration test, the corroded beam specimen were subjected to the unidirectional static loading test.

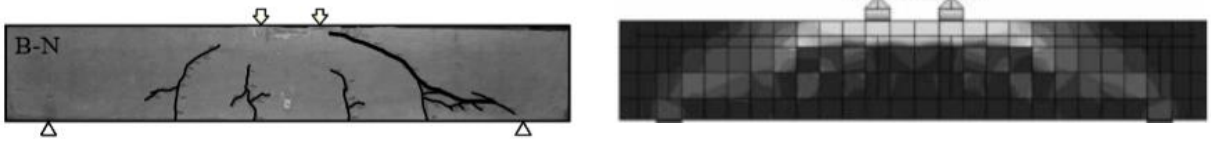

(c) Beam failure pattern after the loading (d) Principal compressive stress distribution from FE simulations

Figure 5.5 Non-corroded beam failure pattern after the loading and principal compressive stress distribution from FEM simulation

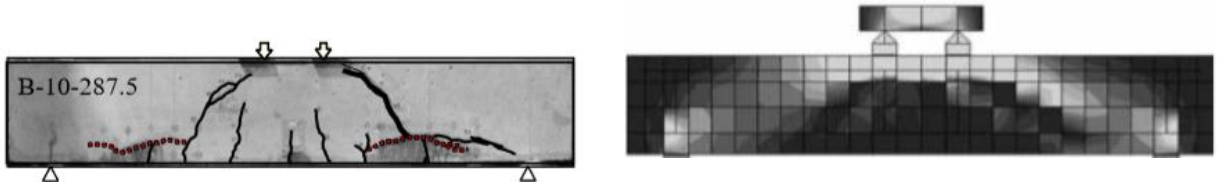

(c) Beam failure pattern after the loading (d) Principal compressive stress distribution from FE simulations

Figure 5.6 Beam failure pattern after the loading and principal compressive stress distribution from FEM simulation of beam specimen B-10-287.5.

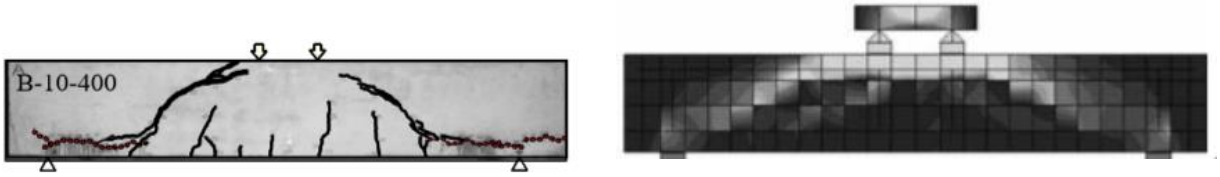

(e) Beam failure pattern after the loading (f) Principal compressive stress distribution from FE simulations

Figure 5.7 Beam failure pattern after the loading and principal compressive stress distribution from FEM simulation of beam specimen B-10-400

Figure 5.5-5.7 shows the crack distribution of specimen after the loading and principal compressive stress distribution from FEM simulation. In case of corroded beams, this study indicated that the diagonal and flexural cracks was initiated and propagated by the corrosion crack near the support(figure 1.14(a)) or the shear span along the longitudinal bar (figure 1.14(a)).
In case of corroded beams, the tension force transmitted from concrete to longitudinal reinforcement decreases due to the bond deterioration. As a result, the stress profile and crack distribution of RC beams with corroded steels is different from that of RC beams without corroded steels.

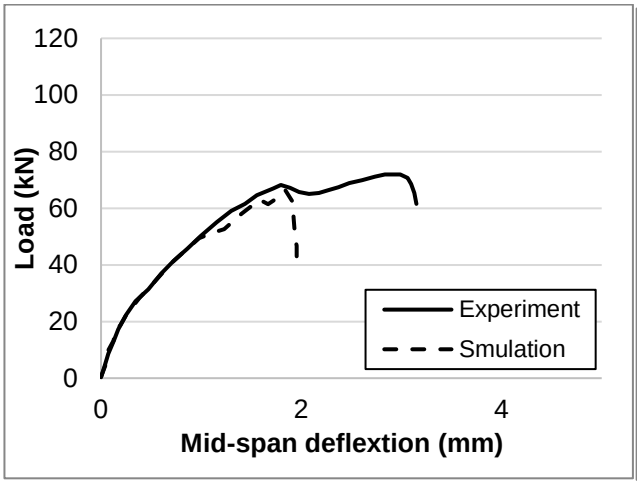

(b) No corrosion beam, BN

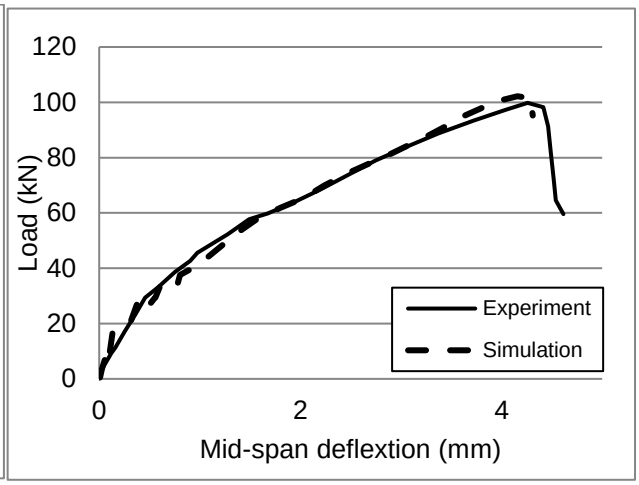

(b) Corroded beam specimen, B10-287.5

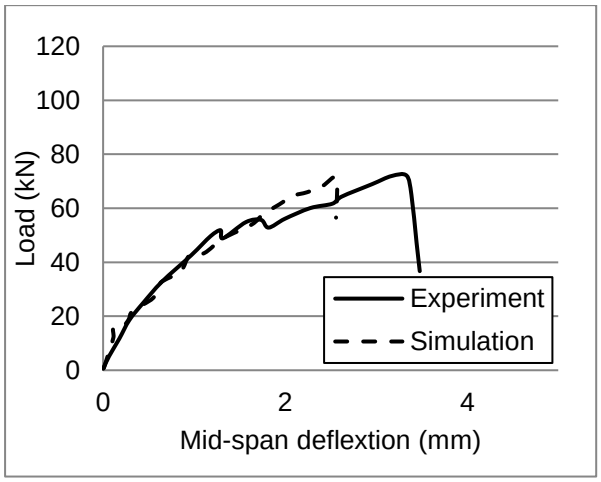

(c) Corroded beam specimen, B10-400

Figure 5.8 Load-displacement from experiment

Figure 5.8 shows the load-displacement curves obtained by experiments and the FE analyses from different corroded beam. Comparing between no corrosion beam, BN and corroded beam, B-10-278.5, the beam capacity of corroded beam was higher than the no corrosion beam. The reason is that the shear carrying mechanism of RC beam with steel corrosion are changed due to the corrosion of steel bar. When consider the stress distribution in Figure 5.5 -5.7, it found that the tied arch action are formed-up in corroded beam B-10-278.5. Figure 5.6 (b) shows that the angle of the arch rib of RC beams with corroded steels is lower than that of RC beams without corroded steels, figure 5.5 (b). The area of high degree of principal compressive stress of RC beams with corroded steel is also larger than that of the RC beam without corroded steels. It means that the shear carrying mechanism of a RC beam with steel corrosion changes from the truss action to the tied arch action due to bond deterioration between concrete and longitudinal reinforcements. This change can make the load after the diagonal crack propagation increase.

The important information from this simulation are that the shear carrying mechanism of RC beams with the local steel corrosion changes from the truss action to the tied arch action. In addition, the arch rib formed by the principal compressive stress distribution depended on the steel corrosion position and affected the shear carrying capacity.

In conclusion, the shear carrying mechanism of RC beams with steel corrosion changes from the truss action to the tied arch action. The contribution of tied arch action depends on the position of the steel corrosion and affects the shear carrying capacity. For example, the shear capacity of RC beams with steel corrosion at both sides of shear span increases strongly due to high contribution of the tied arch action. And the damage of concrete should be considered because it will lead to the failure pattern of the beam. In this study, diagonal cracks were initiated by corrosion cracks near the support at lower load compared with RC beams without steel corrosion.

5.3 Simulation model of corroded beam with stirrup

5.3.1 Geometry of simulation model

The analysis models used in this study were formed up based on the previous experimental study by M. TSUNODA et al. (2016). They performed electrical corrosion acceleration on reinforced concrete beam specimens with specific corrosion location at anchorage zone and shear span zone. The concrete specimens size of 1200×200×150 mm^3 reinforced with 2-D16 rebar with 37 mm covering depth and stirrup DB 6 (as shown in figure 5.3) were subjected to external direct electric current of 0.11 A/cm^2 to accelerate the corrosion process. In this study, cuboid model with single reinforcement at 20 mm covering depth from bottom of beam which same as in the experiment of et al. are modelled for analysis. The simulation models are separated into two groups, corroded beam with stirrup and without stirrup, with different corrosion patterns. Analysis model is meshed into meso-scale element having average sizes approximately 15.0×15.0×15.0 mm^3. Two pin support and two loading point are set at same location as in the experiment. The load is given at the two rigid pins above the beam, and there is no friction between the loading support element and the beam. Also, the interface between concrete support and beam is set as friction free condition. This 3D-RBSM model contains 78896 elements. The input tensile strength of concrete are 2.76 MPa, 3.21 MPa and 2.53 MPa for beam with no corrosion, corrosion at shear span and corrosion at anchorage, respectively. The input tensile strength of steel bar is 384 MPa for all cases. Material properties are show in table 5.1. Expansive strain was applied to the interface between rebar and concrete for generating the corrosion expansion. Subsequently, the mechanical loading was given in the same manner as experiment. Figure. 5.9 shows the reinforced concrete beam simulation by RBSM in this study and loading condition.

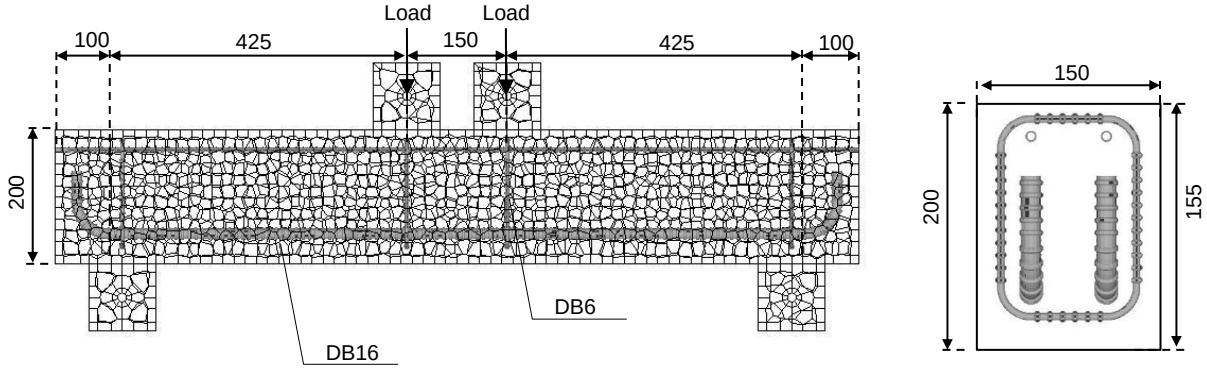

Figure. 5.9 Geometry of numerical model by RBSM (Unit: mm)

Table 4.1 Beam material properties.

Case	Term	Unit	Concrete	Reinforcement
BN (no corrosion)	Compressive strength	MPa	32.2	-
	Elastic modulus		27800	184000
	Yielding strength		2.76	384.0
B10-287 (corrosion at shear span)	Compressive strength		36.8	-
	Elastic modulus		26100	184000
	Yielding strength		3.21	384.0
B10-400 (corrosion at anchorage)	Compressive strength		32.0	-
	Elastic modulus		25300	184000
	Yielding strength		2.55	384.0

4.3.2 Corrosion patterns

In this study, a non-corroded beam simulation and corroded beam with different corrosion pattern are simulated for investigate the effect of spatial corrosion on the RC beam. Two different steel weight loss profile are set for the simulations. The first corrosion case is the uniform corrosion pattern at 27 percent along the bar. Second case is non-uniform corrosion obtained from 3D x-ray technique of Sopokhem et al. (2016) as shown in Figure 4.3(a) and Figure 4.4(a). The spatial variable steel weight loss is start from 250 mm to 1090 mm in rebar length direction. The other zone, 0 to 250 and 1090 to 1490 mm, does not have information from the experiment, so the corrosion level is set as uniform 27 %. The average steel weight loss is 27 percent. Table 2 shows each corrosion pattern in the simulations.

Table 2 Simulation cases.

Specimen	Corrosion pattern	maximum corrosion degree	Comment
w/o stirrup	None	0%	No corrosion is given.
	Shear span	10.0 %	Uniform 27% corrosion is given.
	Anchorage	13.0 %	Corrosion profile from experiment.

4.3.3 Expansion simulation

The constitutive model of corrosion degree and expansive strain model was developed based on inverse method as explain in chapter 2. The expansion constitutive model is shown in Figure 5.8

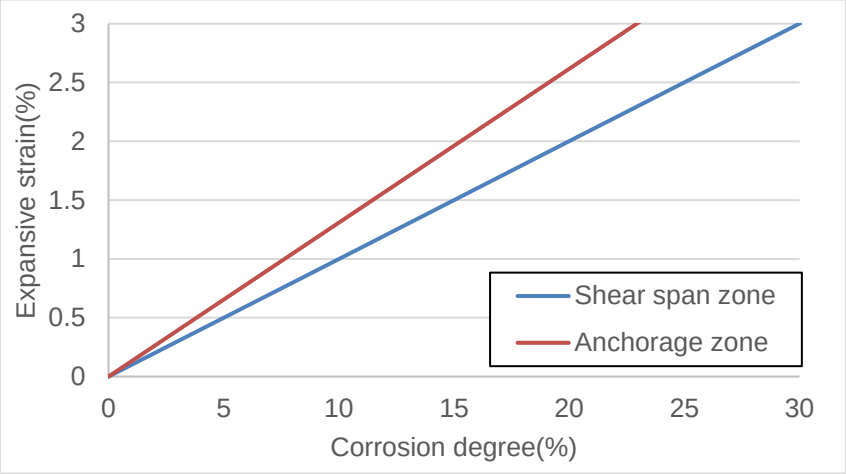

Figure. 5.10 Expansive strain constitutive model for corrosion at shear span and anchorage zone

The red line and blue line represent expansive strain constitutive model for the corrosion at anchorage zone and shear span zone, respectively. In case of the expansive strain at the anchorage zone, the constitutive model stiffness is higher than the shear span zone due to the confinement. Because of stirrup, the model required higher expansive strain to achieve the same surface crack width as real beam experiment comparing with non-stirrup zone.

5.3.4 Loading condition

After the corrosion crack damage was introduced to the specimen, load was then applied to the beam to find the residual capacity. Figure 5.9 shows the boundary condition for the loading process. Two pin supports below RC beam are set in fixed movement condition (fixed in X, Y, Z direction for right support and fixed in Y, Z direction for left support), while loading is given at two pins above the specimen at rate of 0.0005 mm/step in the downward Y direction as shown in Fig. 5.9.

5.4 Analysis results

5.4.1 Corrosion cracking

By using the constitutive model in figure 5.10, the expansion of corroded beam simulation of uniform corrosion pattern and non-uniform corrosion pattern were simulated. In case of B10-287.5 or shear span corrosion beam, corrosion profile with maximum value of 10.2 % and 9.0 % as show in figure 5.4(a) was applied for the whole longitudinal bar. In case of B10-400 or anchorage corrosion beam, corrosion profile with maximum value of 9.5 % and 13.0 % as show in figure 5.4 (b) was applied for the whole longitudinal bar.

Figure 5.11 (a)-(b) and figure 5.12 (a)-(b) show the 3D surface overview of corroded beams after corrosion expansion simulation in side view and bottom view. Expansive strain was given to the interface between rebar and concrete at rate of 0.05 μstrain/step. Cumulative given expansive strain were 9 μ strain and 17 μ strain for stirrup and non-stirrup beam. As a result, the crack propagates to the bottom surface of beam which is the thinnest covering depth as shown in figure 4.9 (b) and figure 4.10(b). Some crack can be observed at the side of the beam at the hooked-up part of anchorage. Figure. 5.11 (c) and Figure5.12 (c) shows the bottom beam crack from the experiment.

For the beam with corrosion at shear span, corrosion crack appeared along the longitudinal bar location at side and bottom beam at around 200-400 mm from end of the beam This cracking pattern is correspond to the corrosion pattern. The average bottom beam crack width from simulation result is 0.24 mm while the experiment bottom crack width is around 0.25 mm (Figure 5.11 (c)). For the beam with corrosion at anchorage, the average bottom beam crack width from simulation result is 0.3 mm while the experiment bottom crack width is 0.28 mm (Fig. 5.12(c)). The crack propagated from 300 from the beam end to the end of the beam. In both case, the crack appears at side and bottom of the beam. From the overview, the simulation can simulate similar corrosion crack location and size same as in the experimental results.

(d) Front view of expansion simulation

(e) Bottom view of expansion simulation

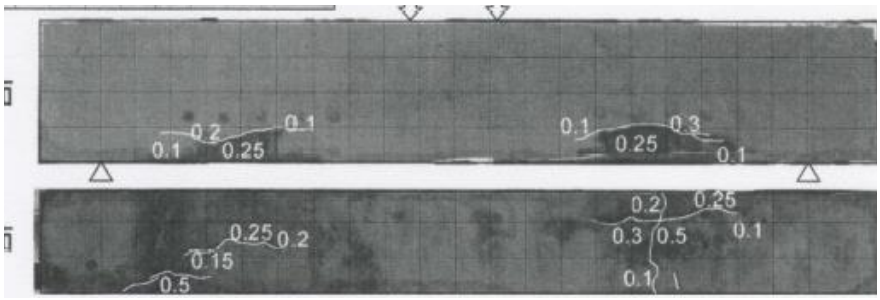

(f) Bottom beam crack width from experiment B10-287.5 [5]

Figure. 5.11 Corrosion cracking of shear span corroded beam

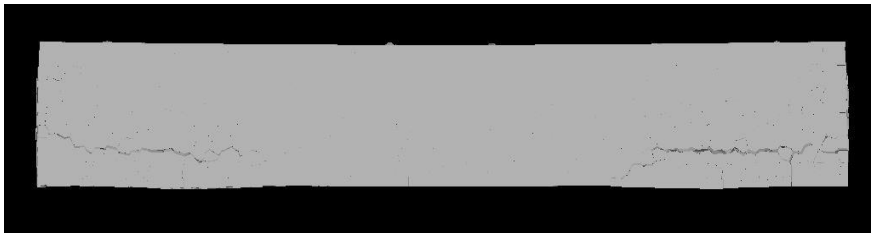

(d) Front view of expansion simulation

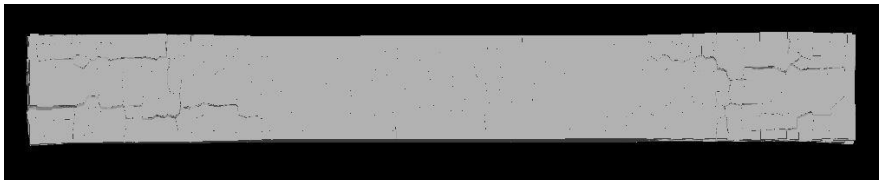

(e) Bottom view of expansion simulation

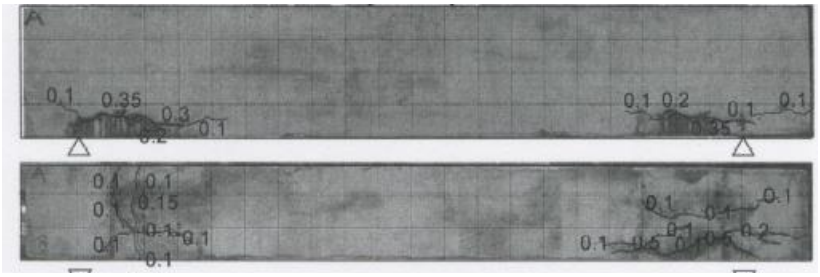

(f) Bottom beam crack width from experiment B10-400 [5]

Figure. 5.12 Corrosion cracking of corroded anchorage beam

5.4.2 Load-displacement relationship

Beam's load-displacement relationships from simulation and real experimental data are shown in figure 5.13 and figure 5.14, respectively. The load is defined as the total force acting at two pin point above the beam, while displacement is the vertical displacement of loading point in downward direction. For the simulation results, the maximum capacity of each simulation case is 105 kN, 104 kN and 86 kN for no corrosion, shear span corrosion and anchorage corrosion cases respectively. For Tsunoda's experiment, the maximum capacity of each simulation case is 72.0 kN, 99.8 kN and 72.1 kN for no corrosion, shear span corrosion and anchorage corrosion cases respectively.

In the experimental beam (M. Tsunoda et al., 2010), it was reported that the beam shear carrying mechanism was changed from truss action to tied-arch action due to the bond deterioration between longitudinal reinforcement and concrete. When the corrosion occurred at the shear span, the tension force transmitted from concrete to the longitudinal reinforcement decrease due to the bond deterioration. This tied-arch action mechanism increases the beam capacity.

In case of simulation, the beam with corrosion at shear span zone did not show reduction in capacity even the initial damage from corrosion take place. This enhancement may be the results from tied-arch action. In case of beam with corrosion at anchorage, the simulation beam shows lower capacity comparing with the other two case. The simulations exhibited the flexural behavior after the shear failure pattern occur. While in the experiment results, the beam suddenly collapsed

after the shear failure occurred. It can be observed that the shear carrying capacity is higher than the experimental results. This may be the results of interlocking between rigid element of concrete at meso scale. When consider the residual capacity of corroded beam, the simulation can predicted the residual capacity of corroded beam similar the experimental results.

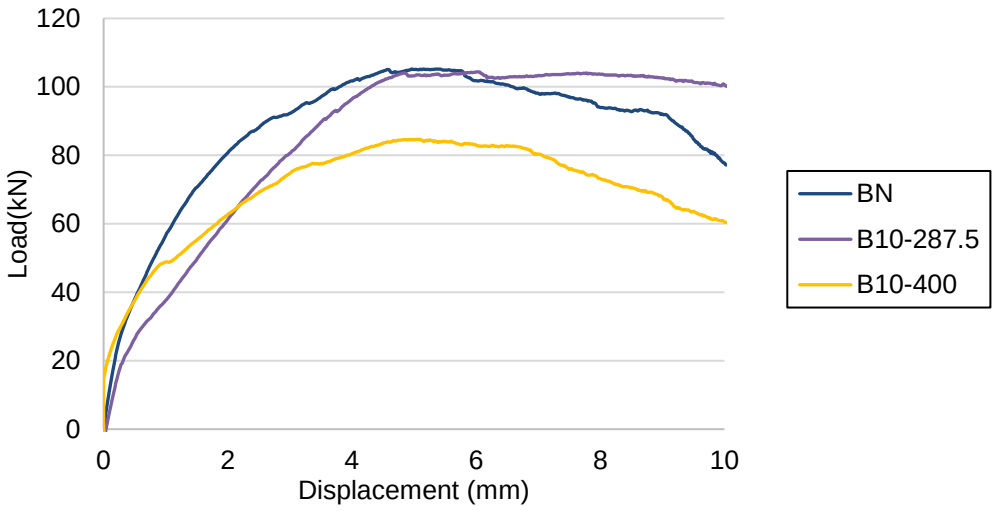

Figure 5.13 Load-displacement relationship in each simulation case

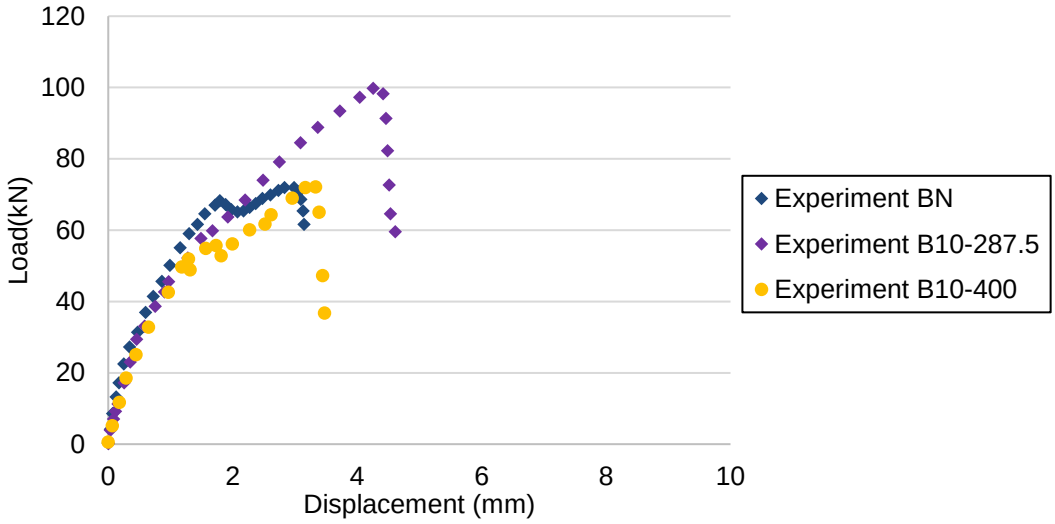

Figure 5.14 Load-displacement relationship from experiment [ref]

5.4.3 Crack failure patterns

Figure 5.15-5.17 shows the internal crack pattern and the 3D surface overview and experiment loading's crack of each beam case.

The shear failure pattern can be observed in all simulation cases. In case of shear span corroded beam, the corrosion crack along the longitudinal bottom bar appeared at between 150 mm to 440 mm from left and right end of the beam which is corresponded to the input corrosion pattern.

In case of anchorage corroded beam, the corrosion crack along the longitudinal bottom bar appeared at around 340 mm from the beam's and propagated along the rebar till the left and right end of the beam which is also corresponded to the input corrosion pattern.

When considering the crack plane direction, even all simulation cases appeared the shear failure pattern, but the crack plan has different angle in each case. In case of no corrosion beam and anchorage corroded beam, the shear crack plane propagation starts from 343 mm from the beam end at bottom reinforcement level and end at the top loading pin location. While in case of beam with longitudinal bar corroded at shear span, the crack plane is start from around 440 mm from the left end of beam and propagated to the top surface at the loading pin location. So, the incline angle of these crack planes is about 40 degree for non-corroded beam and anchorage corroded beam, and 60 degree for the beam with longitudinal bar corroded at shear span, respectively. (as shown in figure 5.18)

Therefore, it can be observed from both simulation and experimental results that the diagonal crack plane of shear span corroded beam is steeper than the other case. (figure 5.15 to figure 5.17) The different in cracking angle is a result from the initial corrosion damage. As see from figure 5.11 and figure 5.12, the corrosion created crack along the longitudinal bar at side of beams. These initial cracks have different pattern due to the input corrosion profile. During the mechanical loading, the shear cracks were propagated from this initial crack and results in a different failure pattern.

It can be concluded that the different corrosion pattern can lead to a different failure pattern, and these results give a good agreement with the experiment crack pattern. By considering the different corrosion degree and location, the numerical model can simulate similar failure pattern as the experiment beam correctly.

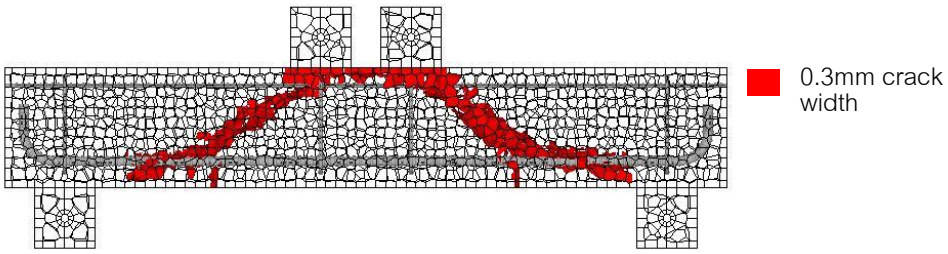

(a) Internal crack

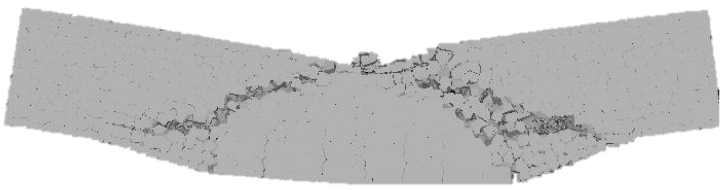

(c) 3D surface overview

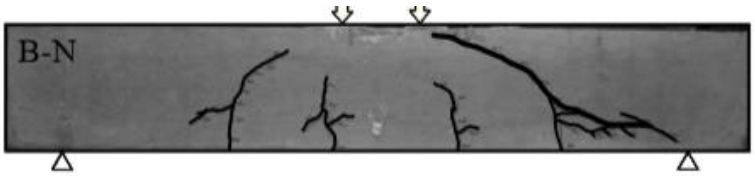

(d) Experiment

Figure 5.15 No corrosion beam failure pattern by simulation model and experiment

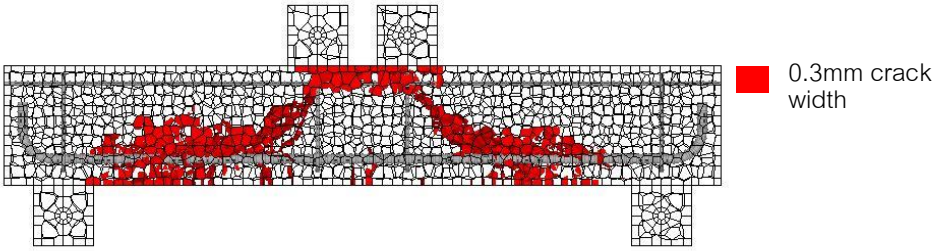

(a) Internal crack

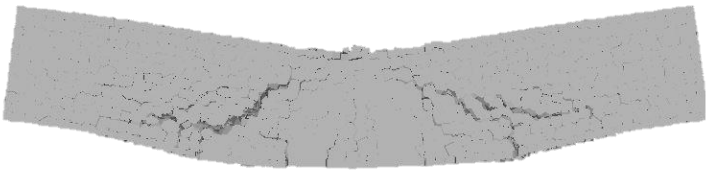

(b) Beam with corrosion at shear span

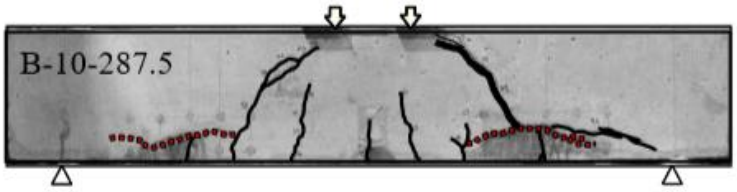

(c) Experiment

Figure 5.16 Shear span corrosion beam failure pattern by simulation model and experiment

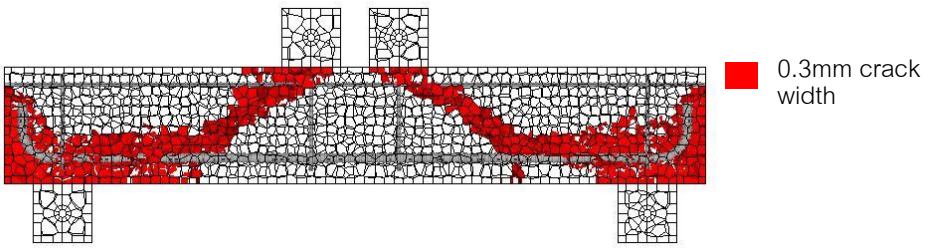

(a) Internal crack

(b) Beam with corrosion at shear span

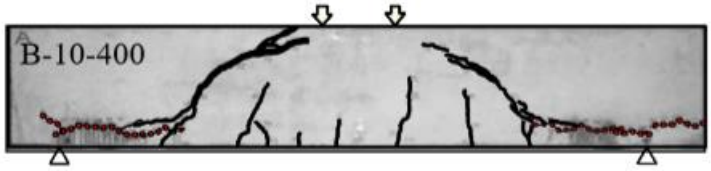

(c) Experiment

Figure 5.17 Anchorage corrosion beam failure pattern by simulation model and experiment

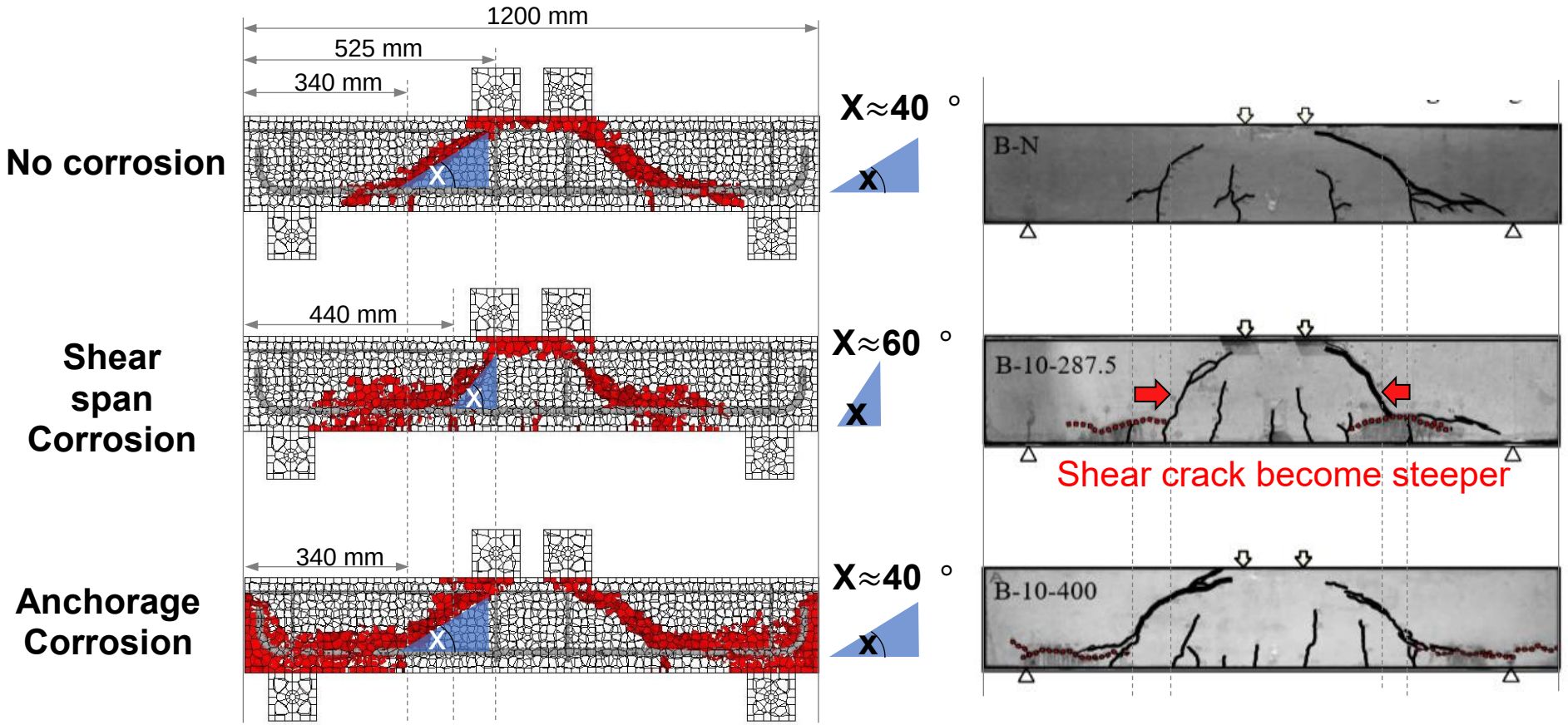

Figure 5.18 Angle of shear cracking plane

5.4.4 Internal stress

Figure 5.18 shows the internal stress distribution at peak load of each simulation cases. The red element shows the compressive stress concentration. These figures show that the angle of the arch rib of RC beam with corrosion is higher than the non-corroded beam. Also, the angle of arch rib in shear span corrosion beam is steeper than the other case. This means the shear carrying mechanism of RC beam with steel corrosion at shear span changed from the truss action to tied arch action due to the bond deterioration between concrete and longitudinal bar. This change can make the load after the diagonal crack propagation increase. Especially, in case of the beam with corrosion at shear span (figure 5.19 (b)), it can be observed that the compressive stress concentration at the shear span corrosion beam is higher than the other case. Due to the initial damage from corrosion, the shear crack plane of B10-287.5 is shifted into the center of the beam and steeper than the other case. This allows this beam to have larger arch rib area. As a result, even the initial damage from corrosion occurred, but the shear capacity of corroded shear span beam does not drop comparing with the non-corroded beam as shown in load-displacement relationship in previous section. In case of beam with anchorage corrosion (figure 5.19(c)), the corrosion occurred at the anchorage does not affect the stress transfer between the rebar and concrete at shear span. Also the diagonal crack size and location is quite similar to non-corroded beam case. As a result, the arch action was not form up clearly as beam with shear span corrosion. Therefore, the shear capacity does not increase, but decrease due to the initial damage from corrosion and loss of steel bar section.

In conclusion, the shear carrying mechanism of beam with steel corrosion changed from truss action to tied arch action due to the loss of stress transfer between rebar and concrete at corrosion zone. Moreover, the arch rib formed by the principle compressive stress distribution depended on the reinforcement corrosion location. This behavior affects the shear carrying capacity.

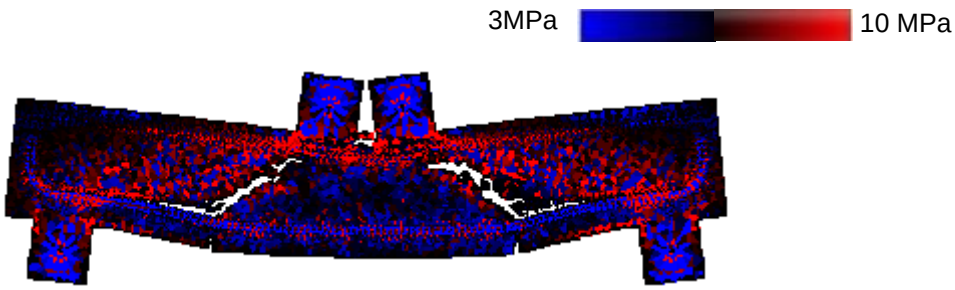

(a) Non-corroded beam

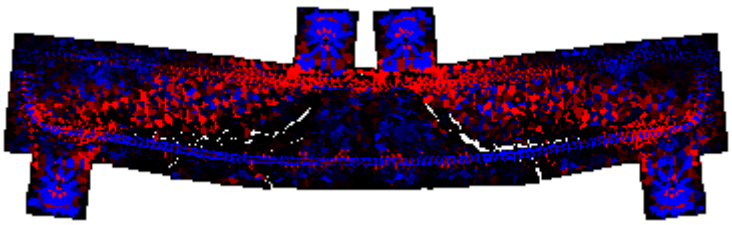

(b) Beam with corrosion at shear span

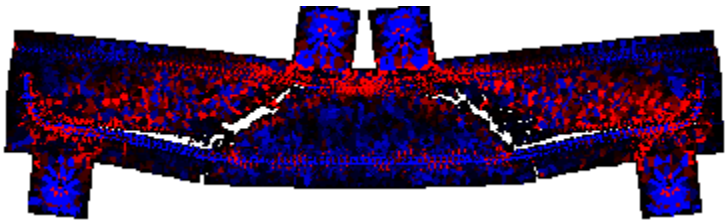

(c) Beam with corrosion at anchorage

Figure 5.19 Internal stress from each simulation beam

5.5 Conclusions

In this chapter, the corrosion model developed in chapter 2 and 3 were combined into RBSM simulation for simulating the corroded beam that intentionally set the corrosion location at around the anchorage zone. The beam with corrosion at anchorage and corrosion at shear span are simulate and observe the shear carrying mechanism comparing with the experimental results. Based on the simulation results, the following conclusion is drawn.

1. The simulation is this chapter combine all corrosion model that had been developed in chapter 2 and chapter 3 for simulating the behavior of corroded beam model. The simulation results confirmed that all constitutive model for corrosion model worked reasonably based on input corrosion profile.
2. Based on different input corrosion profile, different corrosion cracking pattern can be observed as shown in figure 5.18. This cracking pattern and crack width are similar to the previous experiment results of the same corrosion profiles.
3. In case of non-corroded beam, the beam's shear capacity is higher than the experiment results. This may be the effect of interlocking of rigid element at meso-scale. Therefore, the shear capacity is higher than reality.
4. The shear carrying mechanism of RC beam can be changed from truss action to tied arch action due to the loss of bond between longitudinal bar and concrete depending on the corrosion location. And this phenomenon increases the shear capacity of corroded member.
5. According to the corrosion pattern and local damage, the failure patterns beam simulation can be changed.

REFERENCES

[1] Masahiko Tsunoda, Junichiro Niwa, *Influence of local steel corrosion on shear failure mechasiam of RC member*, Concrete research and technology, 15(2),2004, pp.69-77

Chapter 6
Conclusion

6.1. General conclusions

The model for simulating the corrosion induce damage at the local behavior were developed in this study. New design experiment and literature studies were used to develop the new model for prediction of corrosion local behavior. The model was then applied into the original RBSM simulation. The numerical model for prediction the residual capacity and damage behavior of RC structure considering the local damage from corrosion can be achieved.

- **Simulation scheme is well developed**

From the overview, the simulation scheme was developed well. By considering and inducing the corrosion damage such as rust expansion, bond deterioration, rebar reduction and non-uniformity of corrosion pattern before applying the mechanical loading to the model, the simulation model can simulate the failure pattern in the same manner as the real structure based on the induced local damage. The residual capacity of corroded RC member can be simulated.

- **Constitutive models of corrosion are well developed**

The constitutive models of bond deterioration are well developed based on the designed experiment. In order to extract the changing of the chemical bond and mechanical bond, experiment program is well designed. The concrete specimens reinforced with round bar and deformed bar were subjected to the corrosion acceleration test to generate the different corrosion percentage on the reinforcement. The corrosion acceleration electrical current-time were varied in each specimen (0, 1, 2 and 4 weeks at rate of 0.11A electric current). As a result, the different corrosion percentage along the rebar can be obtained (0, 3, 5,3 and 12.3% in round bar reinforcement and 0, 10.5 and 23.1% in deformed bar specimen). To eliminate the effect of cracking of surround concrete from corrosion expansion, the specimen with non-crack concrete were prepared. After the pull-out test on cracked concrete specimen, the cover concrete was removed. The same corroded rebars were used as reinforcement in casting of new specimen. By the method, the new specimens reinforced with corroded rebar without concrete damage can be obtained. The pull-out test were performed on non-crack concrete specimen. The pull-out capacity of different corrosion percentage and different type of reinforcement (round bar and deformed bar) were analyzed. The new constitutive model of shear spring and normal spring were proposed based on the changing of maximum pull-out capacities at different corrosion degree. Subsequently, in order to verify the applicability of constitutive model, the simulation model of pull out experiment were simulated using the new constitutive model. The simulative model well predicted the peak pull out capacities of the experiment specimens. The compatibility of bond deterioration model and expansion model were verified by simulation of pull out specimen with cracked concrete. The simulation results show a good tendency of pull out capacity comparing with

the experimental results. So the bond deterioration model was well developed and working well with the expansion model.

- **Application on corroded RB member results**

By combination of all corrosion constitutive model (expansive strain model, shear spring and normal spring deterioration model, rebar reduction and non-uniformity of corrosion pattern) into RBSM, the simulation can predict the internal behavior and residual capacity of corroded RC structure reasonably. Based on the simulation results of corroded RB beam in chapter 4, the stiffness reduction and residual capacity of corroded beam due to the initial damage from corrosion were simulated well. The local behavior like the cracking along the longitudinal bar from rust expansion and the strain distribution showed different patterns due to different corrosion pattern. After the peak load, simulation model with non-uniform corrosion pattern shows a local yielding at the same location with peak corrosion degree in experiment data. The beam with the real input non-uniform corrosion pattern from experiment shows a similar failure pattern as experiment beam. The simulation with using uniform corrosion pattern shows a different failure pattern from experimental results. From the overview, simulation can simulate different failure behaviors considering the local corrosion pattern appropriately.

6.2 Conclusion for each chapter

- Chapter 1: Introduction
  In this chapter, detailed about research background, statement of problem and objective are explained. The corrosion behaviours that deteriorate the structure performance such as the expansion of corrosion product, the reduction of reinforcement bar and the non-uniformity pattern of corrosion are discussed. Moreover, the previous studies about corrosion damage simulation by FEM analysis such as fine meshing model, artificial crack plane simulation by multi-mechanical element plane are also emphasized.
- Chapter 2: Simulation model
  In this chapter describe about the numerical simulation systems that were used in this research, RBSM and corrosion model. The constitutive models for corrosion simulation including the reduction of steel area, the non-uniformity of corrosion, the expansion of corrosion product and the bond deterioration model are described. In RBSM, the response of normal spring and shear spring represent the mechanical response of RC member. By modifying the constitutive model of these springs, the response of spring changed in the same manner as real corroded structure. These modifications are locally done based on corrosion information at every 5 mm. This chapter also explains about how to create the expansive strain-corrosion percentage constitutive model by using inverse method the find the relationship between numerical model and real specimen/structure. The constitutive model of normal spring and shear spring modification based on corrosion percentage are shown.
- Chapter 3: Model development based on pull out test experiment
  In this chapter, the method of developing the bond deterioration model is described step by step. In the reality, once the corrosion occurs, not only the formation for corrosion product, but the reinforcement bar also loss it original shape. However, the material element in RBSM are modelled as a rigid element which cannot be deformed. On the other hand, the bond between material in RBSM are represented by the interaction of normal spring and shear spring at

interface. Therefore, the equivalent constitutive model for representing the loss of bond is developed. The pull-out experiment program for studying the loss of bond due to corrosion are designed. By pulling out the corroded bar under different condition like, rebar shape (round bar, deformed bar), damage of concrete from corrosion cracking and different corrosion percentage. The changing of mechanical bond and friction bond including the effect of concrete cracking can be obtained. By analysing this experiment data, the modification of normal spring and shear spring for representing the loss of mechanical bond and chemical bond at different corrosion degree can be achieved.

- Chapter 4: Corroded beam simulation with effect of non-uniform corrosion pattern
  To verify the applicability of the corrosion model on member scale simulation and study the effect of non-uniform corrosion pattern, the numerical model of corroded beam with different corrosion pattern are simulated. In this chapter, the previous corroded beam experiments done by S. Lim and team was used as input data for simulation. The steel corrosion profiles at every 5 mm obtained by digital camera technique was used to modify the steel property and corrosion damage simulation. The corrosion patterns were set as no corrosion, uniform corrosion and non-uniform corrosion. The effect of non-uniformity of corrosion profile on structural mechanism such as the change in strain distribution along the longitudinal bar or the changing of failure pattern due to initial damage from different corrosion profiles can be simulate reasonably. The beam's stiffness and beam's flexural capacity reduction are well simulated. The simulation results were then compared with the real experimental results, and it showed a good agreement with experimental results in term of residual capacity and failure pattern.
- Chapter 5: Corroded beam simulation with corrosion at anchorage
  Because the collapse at the connection is one of the most common failure modes of reinforced concrete structure, in this chapter, the effect of corrosion at anchorage zone was investigated. The beam simulation with intentionally set the corrosion at the anchorage zone are simulated.
  The corrosion profiles are separated into two cases, including the corrosion of rebar at shear span and the corrosion of rebar at anchorage zone. The experiment M. TSUNODA et al. was used for verification the simulation results. The effect of corrosion profile on structural mechanism such as the change in shear capacity, the loading mechanism or the formation of tied arch action are analysed. The residual capacity of corroded beam are well predicted and similar to that of experiment. The changing of shear cracking plane location and direction can be simulated well comparing with the experiment. The simulation can show a different detail in local damage based on different input corrosion profiles.
- Chapter 6: Conclusions
  In this final chapter, several remarks about the capability of corrosion model are emphasized. Also, some commentaries for further project or improvement are proposed.

6.3. Recommendations for future study and application for real structure

In the current state, the quality and accuracy of the simulation results depending on the available data. In chapter 4 the simulation system can predict the residual capacity of the corroded structures and their failure pattern appropriately based on the sufficient input information. With detailed corrosion data at every 5 mm by X-ray photogram technique, this simulation is very powerful tool to predict the behavior of corroded structure. However, in the real field application, the available of corrosion

information is limited based on the investigation method. In this sense, the quality of simulation on real field application is depended on the input information.

Level of available data.

Normally, the overall information of structure such as rebar size, rebar location, covering depth and material properties can be known by the blueprint or drawing from structure design. However, when considering the capacity of corroded structure, the corrosion percentage is one of the important data that affect the residual capacity. Then, the simulation accuracy will depend on the level of data available which can be classified into three cases as following.

a. All data available.

If the destructive method is allowable, for example, the removing of cover concrete to see the corroded reinforcement condition as show in Fig. 6.1, the accurate information of corrosion along the rebar can be obtained. In this case, the simulation can be modelled all corrosion data in the same way as the real structure. All initial damage and local failure behavior can be simulated. Then, in this condition, the simulation will be very powerful technique to simulate the structure behavior and find the residual capacity precisely.

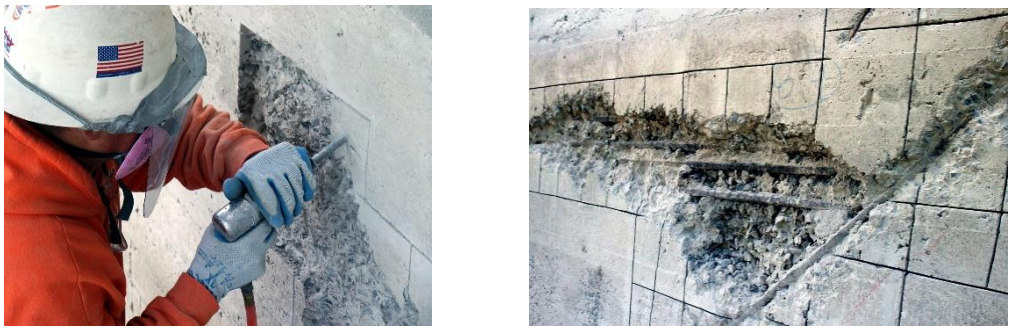

Fig. 6.1 Destructive method for investigate the rebar corrosion ration in real field.

b. Point data available

When the full-destructive method is not allowed, only some sample colleting can be performed, for example, the coring of steel sample. In this case, the corrosion pattern can be predicted by using the mathematic model. In 2016, there was a study of corrosion pattern prediction by using the Gumbel distribution model done by S. Lim et al. [1]. Location factor and scale factor of corrosion degree were investigated from rebar sample. Then, by using the Gumbel distribution, the corrosion percentage at different location along the rebar can be roughly predicted. By using this information, he performed corroded RC beams simulation comparing between the experiment result and the simulation that the corrosion along the rebar was treated as uniform and non-uniform pattern. The simulation results indicated that the simulation cases considering the nonuniformity of corrosion pattern shows a better prediction than the uniform corrosion pattern comparing with the experimental results.

In this case, the simulation still be a reliable tool for prediction of residual capacity and behavior of corroded RC structures.

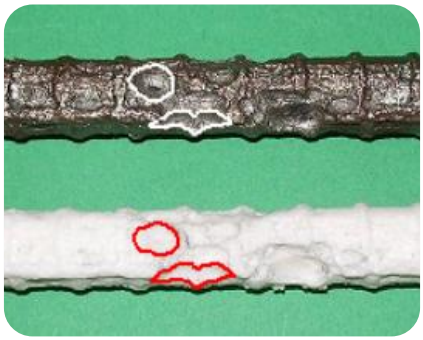

(a) Corroded rebar samples in real field

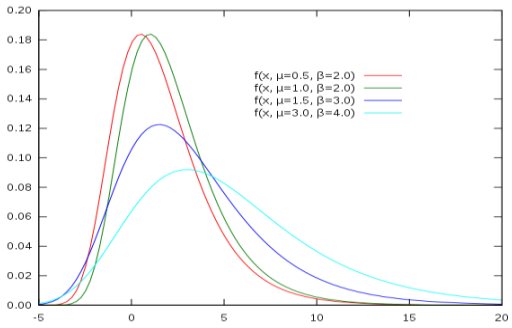

(b) Gumbel distribution theory

Fig 6.2 Example of data collection method in real field with semi-destructive method

c. Indirect measurement/ Non-destructive method

When any destructive method is not allowed. The only information available is the surface crack width from corrosion. In this case, it is still possible to estimate the corrosion percentage of the steel bar based on the crack width in formation.

For example, in 2017, Filipe et. al. had conducted the experiment to observe the relationship between the corrosion penetration depth and surface crack width from expansion damage as shown in Fig. 6.3. It is indicated that this relation is changing depending on the corrosion speed. Under high acceleration speed (given high electrical current), the corrosion product will form up in liquidity form and create less damage to surround concrete. Under low acceleration speed (given low electrical current), the corrosion product will form up more solid form and create high pressure to surround concrete. In this case, the surface crack width was large even small corrosion degree. Using this experimental data and considering the corrosion speed in reality which should be very slow, it could be considered the corrosion degree-crack width relationship in reality is same as the slowest case (lowest electrical current was giving to specimen) in his experiment. Hence, by this scheme, the corrosion percentage can be assumed from the surface crack width. However, the corrosion pattern predicted by this method still has low accuracy. Because the crack width is not proportionally change due to the corrosion at that location, but it is also affected by the adjacent corrosion.

Therefore, the accuracy of simulation under this condition may not precise in the current research level. Nevertheless, in the future, if the real field investigation technique is improved, such as the development of portable X-ray photogram machine for collecting rebar condition, or the relationship between surface crack width and corrosion percentage are will identified, at that time, this numerical model will be powerful tool for predicting the corroded structure behavior.

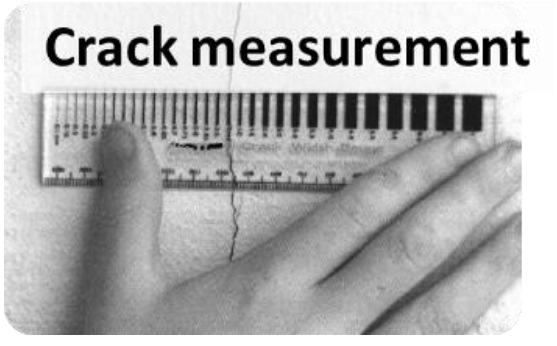

(a) Crack width measurement

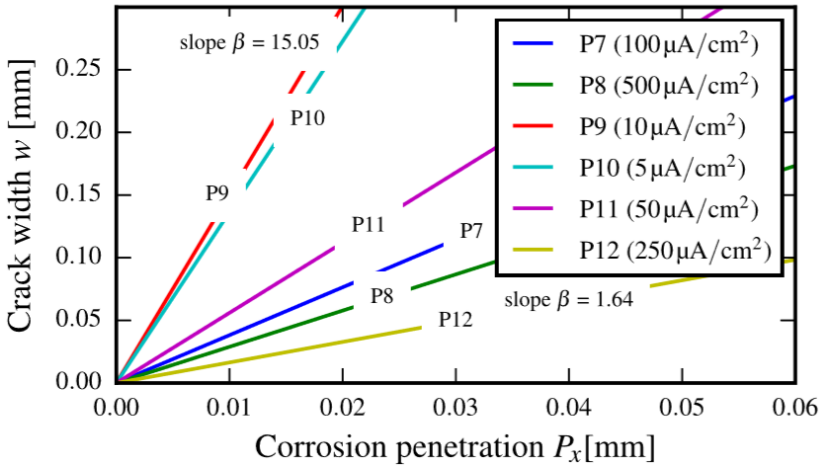

(b) Relationship between surface crack with and corrosion penetration, Filipe et. al. , 2017

Fig. 6.3 Non-destructive method for estimate the corrosion percentage from real corroded structure.